DESIGN AND INTRACELLULAR TRAFFICKING OF POLY(L-LYSINE)-GRAFTED-POLY(ETHYLENE GLYCOL) FIBERLESS ADENOVIRAL GENE DELIVERY VECTOR

By

YASMINE GABAL

Bachelor of Science in Pharmacy
Ain Shams University
Cairo, Egypt
2006

Master of Science in Pharmaceutics
Ain Shams University
Cairo, Egypt
2014

Submitted to the Faculty of the
Graduate College of the
Oklahoma State University
in partial fulfillment of
the requirements for
the Degree of
DOCTOR OF PHILOSOPHY
July 2020

DESIGN AND INTRACELLULAR TRAFFICKING OF POLY(L-LYSINE)-GRAFTED-POLY(ETHYLENE GLYCOL) FIBERLESS ADENOVIRAL GENE DELIVERY VECTOR

Dissertation Approved:

Dr. Joshua D. Ramsey

Dissertation Adviser

Dr. Heather Gappa-Fahlenkamp

Dr. Ashlee N. Ford Versypt

Dr. Ashish Ranjan

Dr. Francisco Ochoa Corona

ACKNOWLEDGEMENTS

I would like to express my deepest appreciation and gratitude to everyone who helped me accomplish this work. I would like to thank my advisor, Dr. Josh Ramsey, for his constructive mentoring, and continuous advice throughout the development of this work. I would like to thank Dr. Fahlenkamp, Dr. Ford Versypt, and Dr. Ranjan for serving on my committee, and Dr. Francisco Corona for the expertise he provided in the PCR part of this work.

Grateful thanks are extended to my lab mates and friends in the school of chemical engineering for their valuable help, support and encouragement.

I would like to offer the fruit of this work to the soul of my father who planted the seeds of loving science and would have been very proud (May Allah bless his soul). I would especially like to thank my beloved mother and brother for their continuous encouragement and support. A special thanks to my sister, Basma -in Arabic language it means smile- who always brought a smile on my face whenever I faced any problem throughout the whole work in this thesis. Finally, I would like to thank my husband and my lab mate, Momen Amer, for all his love and support. I am especially thankful to my children, Maryam and Yassin for all the patience and love they showed. A special debt of gratitude is gladly acknowledged to my family for their help in enduring all the hardships throughout this work, especially during this pandemic of COVID-19.

.

Name: YASMINE GABAL

Date of Degree: JULY 2020

Title of Study: DESIGN AND INTRACELLULAR TRAFFICKING OF POLY(L-LYSINE)-GRAFTED-POLY(ETHYLENE GLYCOL) FIBERLESS ADENOVIRAL GENE DELIVERY VECTOR

Major Field: CHEMICAL ENGINEERING

Abstract: The first gene therapy clinical trials were started nearly 30 years ago, but the field only now seems to be on the verge of widespread adoption. Safe and efficient gene delivery, however, is still a major obstacle and is often described as "the Achilles' heel of gene therapy." Adenovirus (Ad) is the most common viral vector in gene therapy clinical trial. Adenovirus fiber and capsid proteins, however, mediate an immunogenic response and relies on interaction of the virus with the coxsackie adenovirus receptor (CAR), which limits the ability of the virus to deliver genes into CAR-negative cells such as cancer cells. Our goal was to develop a hybrid vector that overcomes Ad drawbacks as well as understand how our hybrid vector compare to the native virus in intracellular trafficking. A fiberless adenovirus (FlAd) was used with a replacement for the removed fiber protein by poly-L-lysine copolymer grafted polyethylene glycol (PLL-g-PEG). A copolymer library was synthesized using varying molecular weights of PLL and PEG with different degrees of grafting. Hybrid vectors were formed by electrostatically associating PLL-g-PEG with FlAd at different ratios, where "design of experiments" was used to optimize the approach. Hybrid vectors were evaluated by their ability to infect both CAR-positive (HEK 293) and CAR-negative (NIH 3T3) cells. To guide further development of the hybrid vector, we investigated the mechanisms of intracellular trafficking by measuring transduction efficiency and cellular uptake in the presence of a panel of drug inhibitors of various cellular pathways. PLL-g-PEG-FlAd hybrid vectors were able to transduce CAR-positive HEK 293 cells and CAR-negative NIH 3T3 cells with a 3.5- and 10.2-fold increase compared to unmodified FlAd. Addition of the PLL-g-PEG copolymer restored 85% of the infectivity of Ad in HEK 293 cells that was lost as a result of removing the fiber. In addition, hybrid vector was non-cytotoxic on both cell types and showed good serum stability up to 40%. The production of inflammatory cytokines IL-6 and TNFα was also reduced by 70% and 50%, respectively. The removal of the fibers besides the surface modification with PLL-g-PEG copolymer have modified the intracellular trafficking of the hybrid vector to affect the efficiency of the expression of the targeted gene. This stepwise transition from viral to non-viral vectors will lead to novel vectors that are both safe and highly efficient.

TABLE OF CONTENTS

LIST OF TABLES

Table Page

LIST OF FIGURES

Figure Page

Figure Page

CHAPTER I

GENE THERAPY FROM CONCEPT TO MARKET: CURRENT TOOLS AND LIMITATIONS

The human genome contains ~20,000–25,000 genes encoding different proteins that drive every biological process necessary for life and death [1]. The Human Genome Project, an international scientific research project, advanced the understanding of the genetic code embedded in the DNA by identifying the genetic makeup and mapping the human DNA [2, 3]. Any abnormalities in the genome can lead to genetic malfunctions that are translated to altered proteins which cause the diseases. Gene therapy is an experimental technique that delivers genes into a patient's cells to either replace a mutated gene with a healthy copy of the gene, or inactivates, "knocks out," a mutated gene that is functioning improperly, or introduces a new gene into the body to help fight a disease. The FDA defines gene therapy as products that mediate their effects by transcription and/or translation of transferred genetic material, and/or by integrating into the host genome and that are administered as nucleic acids, plasmids, viruses, or genetically engineered microorganisms [4].

1.1 TYPES OF GENE THERAPY

Depending upon the type of disease, the therapeutic gene, and the gene delivery vector, gene therapy can be *in vivo* or *ex vivo* (Figure 1.1). An *in vivo* gene therapy involves the administration of the therapeutic gene into the patient with the help of a delivery system that is used for all patients with a similar diagnosis. *In vivo* gene therapy, however, usually causes

a wide distribution of vectors to undesired tissues and leads to complications [5]. *In vivo* gene therapy also requires vectors that can maneuver through the patient's body to deliver the therapeutic gene to a specific tissue. Gene delivery vectors have to overcome tissue matrices, avoid enzymatic degradation, and evade inactivation by the immune system to effectively transfer the gene into the desired cell [6]. *Ex vivo* gene therapy, in contrast, involves the administration of treated cells originally extracted from a patient. The cells then introduce the desired therapeutic change in the body of the patient. This method is invasive and requires patient-specific tailoring, hence incurring high manufacturing costs and quality-control difficulties. Having all these principles in mind, solving the technical challenges has been a priority to put gene therapy into daily practice.

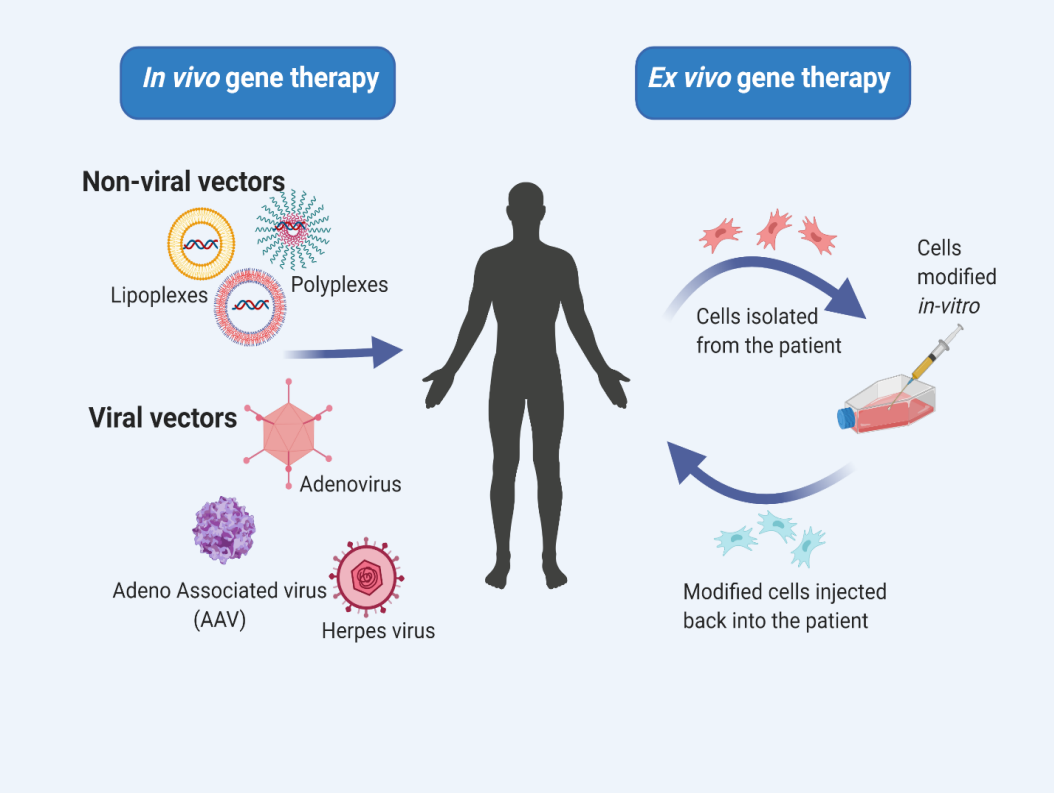

Figure 1.1: Schematic diagram of *in vivo* and *ex vivo* gene therapy. *In vivo* gene therapy involves the administration of the gene delivery vector that contains the therapeutic gene. *Ex vivo* gene therapy involves the use of cells extracted from the patient to be engineered in the lab and delivered back to the patient to provide the desired therapeutic change.

1.2 FIRST STEPS OF GENE THERAPY

Gene therapy was conceptualized in 1970 when Stanfield Rogers proposed the use of "good" DNA to replace defective DNA as a treatment for inherited diseases [7]. Despite the idea having been introduced, the first gene therapy procedure did not occur until 1990 on patients suffering from ADA-SCID, or “Bubble Boy Disease”. Adenosine deaminase (ADA) deficiency is an inherited disorder that damages the immune system and causes severe combined immunodeficiency (SCID) [8, 9].

Two ADA-SCID patients were treated with white blood cells taken from their own blood and modified *ex vivo* to express the normal gene. The introduction of the correct genes showed vast improvement to the point of having normal immune systems [10]. One patient, Ashanti DeSilva, exhibited a good response, whereas the response in the second patient was far less (Blaese et al., 1995). However, there was a debate about the effect of DeSilva’s gene therapy as she still received simultaneously enzyme replacement therapy alongside with the gene therapy. This gene therapy clinical trial was not curative, but an effective treatment that did open the door for further successful trials that have cured patients of several diseases. Several gene therapy clinical trials followed, but in some studies, patients who received the treatment developed leukemia which raised a safety concern [11]. Gene therapy thrived until the tragic death of Jesse Gelsinger [12]. In 1999, the worst-case scenario for gene therapy happened, when 18-year old Jesse Gelsinger took part in a gene therapy clinical trial at the University of Pennsylvania. He suffered from a deficiency of ornithine transcarbamylase (OTC), a liver enzyme that is required for the removal of excess nitrogen from amino acids and proteins. Gelsinger's death was attributed to his body's inflammatory immune response after a high dose of adenoviral vector injection [13]. In a flash, the field of gene therapy collapsed, and research became more oriented to achieve an efficacious, yet safe gene delivery system.

1.3 CURRENT POSITION OF GENE THERAPY

Several milestones have marked the field of gene therapy as shown in Figure 1.2. To date, a steady-state increase in the number of gene therapy clinical trials has been achieved with more than 2600 clinical trials completed.

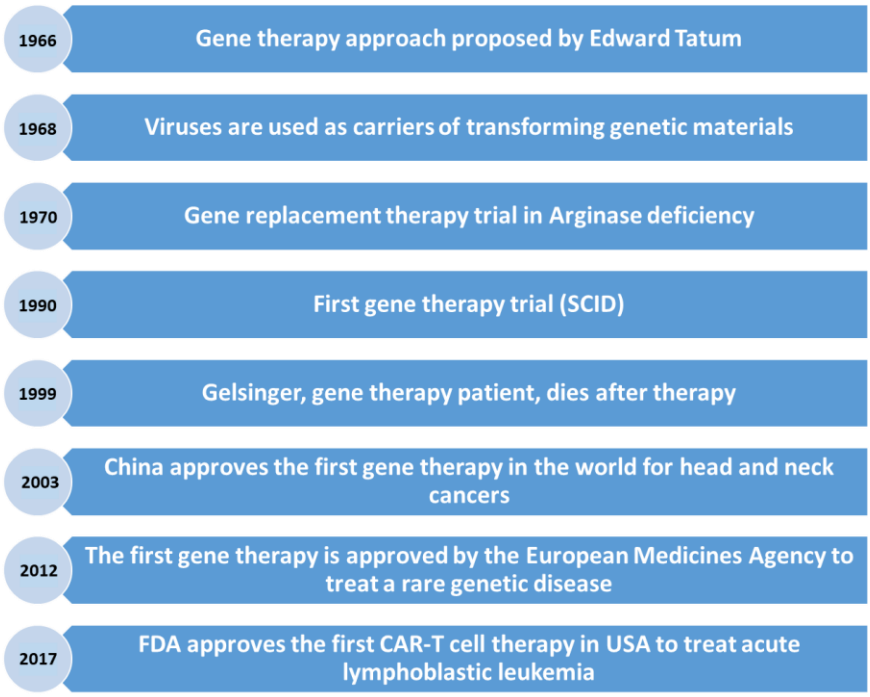

Figure 1.2: Milestones in gene therapy.

Gene therapy extended from treating inherited diseases such as muscular dystrophy [14] and cystic fibrosis [15] to treating acquired diseases such as cancer [16], cardiovascular diseases [17], Parkinson's disease, and Alzheimer's disease [18-21]. The ability of gene therapy to treat a wide variety of diseases is owed to the fact that gene therapy targets the underlying cause of the disease through long-lasting production of the desired therapeutic protein at the fixed area of the defect [22]. Thus, gene therapy provides a one-time treatment option for a complete cure as well as disease prevention. To date, the majority (76.1%) of gene therapy clinical trials have addressed cancer (65.0%), but the greatest success was for the inherited monogenic diseases (11.1%). Figure 1.3 shows a distribution of the indications addressed by gene therapy clinical trials [23].

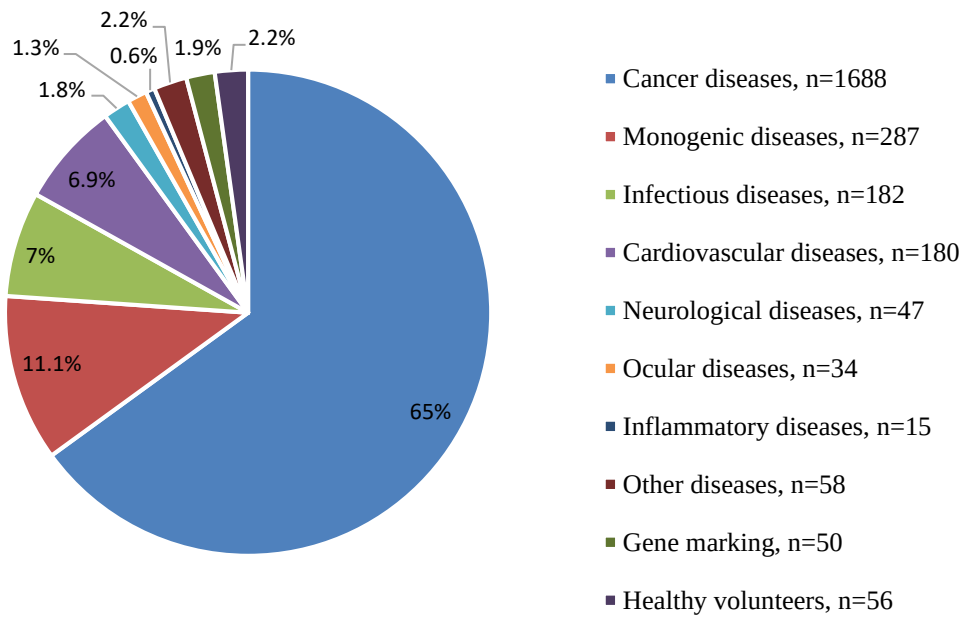

Figure 1.3: Indications addressed by gene therapy clinical trials.

Over the last two decades, gene therapy has made tremendous progress as it has moved to the market as shown in Figure 1.4. The first commercial gene therapy product was approved by China in 2004. Gendicine™ is an adenoviral vector, wherein the E1 gene is replaced with a human p53 cDNA, to treat head and neck squamous cell carcinoma [24]. Soon after approval, debates were raised against the efficacy of the treatment [25]. Despite the debates, China approved Oncorine™ two years later to be used in combination with chemotherapy for the treatment of late-stage refractory nasopharyngeal cancer. In 2004, Ark therapeutics in Europe manufactured Cerepro® to enter clinical trials as an adenoviral vector for the treatment of malignant brain tumors [26]. Cerepro® became the first adenoviral vector that has completed a phase III clinical trial. The first commercial gene therapy product (Glybera), was approved by the European Medicines Agency (EMA) in 2012 [26]. Glybera is an adeno-associated viral vector engineered to express lipoprotein lipase in the muscle tissue for the treatment of severe lipoprotein lipase deficiency (LPLD). However, only one or two people in every one million are estimated to carry LPLD, and despite Glybera's demonstrated potential in curing LPLD, it was

withdrawn from the market due to low patient demand. Another retrovirus-based drug, Strimvelis™, was approved later in 2016 to treat, ADA-SCID, or Bubble Boy Syndrome. In August 2017, the USA market launched the FDA approved Kymriah™ as the first CAR-T cell therapy product to treat acute lymphoblastic leukemia[27] . Soon after, Yescarta™ and Luxturna were granted by the FDA in October and December, respectively. Yescarta™ is another retrovirus-based CAR-T cell immunotherapy[28] , while Luxturna is the first adeno-associated virus (AAV) based gene delivery product to treat X-linked inherited retinal dystrophy that causes night blindness [29]. Finally, Zolgensma™ is the most recent gene therapy approved by the FDA on May 24, 2019 [30]. Zolgensma™ is an AAV based gene delivery product intended for use in children less than 2 years old with spinal muscular atrophy (SMA).

Product	Gendicine	Oncorine	Glybera	Zalmoxis	Strimvelis	Kymriah	Yescarta	Luxturna	Zolgensma
Vector	Adenovirus	Oncolytic Adenovirus	AAV1	Retrovirus	Ex vivo stem cell	CAR-T	T-cell	AAV-1	AAV9
Approving Country/ agency	China	China	EMA	EMA	EMA	FDA	FDA	FDA	FDA
Disease treated	Head and neck cancer	Late stage refractory nasophar-yngeal cancer	Lipoproti-ein lipase deficiency (LPLD)	Add-on treatment haematopoie tic stem cell transplant	ADA-SCID	B-cell acute lymphoblas -tic leukemia	large B-cell lymphoma	Retinal dystrophy	Spinal muscular atrophy
Year	2003	2005	2012	2016	2016	2017	2017	2019	2019

Figure 3.4: Gene therapy drugs in the pharmaceutical market and a timeline of their approval.

Gene therapy is a rapidly growing field, where scientists have only scratched the surface of its potential. As mentioned elsewhere, the more that is discovered about how to optimize gene delivery vectors, the closer this field gets to delivering wide scale solutions to modern medicine [31]. The future of gene therapy moves toward engineering safer and more efficient vectors,

combining multiple existing strategies such as viral vectors with genetic and chemical engineering techniques. To achieve these goals, understanding of the physicochemical characteristics as well as the trafficking of the designed gene delivery are necessary.

1.4 GENE THERAPY CHALLENGES

Ethical concepts

All cells in the human are potential targets for gene therapy. However, gene therapy can be divided into two major categories depending on the target cell: ***somatic cell*** gene therapy (most cells of the body) or ***germline*** gene therapy (eggs or sperm). To date, somatic cell gene therapy to treat different diseases undergoes acceptable clinical trials. However, ethical concerns limit the feasibility of germline gene therapy as the genetic change can be used for trait enhancement of off springs. There is a public debate from the fields of biology, government, law, medicine, philosophy, politics, and religion, each bringing different views to the discussion.

Extracellular and Intracellular barriers

Regardless of the method of its administration *in vivo* (e.g., by inhalation, intramuscular injection, intravascular injection, etc), the gene delivery vector will face extracellular and intracellular barriers before it delivers its cargo inside the target cell nucleus.

Extracellular barriers

Multiple barriers exist within the extracellular milieu, which can result in rapid clearance and/or degradation of the vector before it ever reaches the target cells. These barriers include enzymatic degradation and serum protein interaction. Intravenously delivered naked DNA has a very short half-life within serum (1.2–21 minutes) [32]. This is believed to be the result of both endo- and exo-nuclease activity in the plasma. Different strategies have been adopted to protect the DNA from enzymatic degradation like coating with cationic lipids and polymers as well as coating with a hydrophilic polymer like polyethylene glycol (PEG) to enhance the stability of DNA [33]. After evading nucleases, the gene delivery vector must resist undesired interactions

with serum proteins. Negatively charged serum proteins form aggregates with cationic vectors which results in their rapid removal from the circulation.

Gene delivery vectors also encounter different blood cells, including erythrocytes, leukocytes, macrophages, and platelets. Cells have a negative surface charge which allows for electrostatic interactions with cationic vectors [34]. Interaction with erythrocytes leads to haemagglutination and it speeds up the removal of the vectors via the reticuloendothelial system (RES). The gene delivery vector is also engulfed with macrophages before it can transfect any other cell type [35].

Another extracellular barrier to consider is the activation of both the innate and adaptive immune responses. After systemic administration of either viral or non-viral vectors, the body develops an inflammatory response leading to the release of multiple cytokines that clears the vector from the circulation [36]. The presence of preexisting neutralizing antibodies (NAbs) in the human population from earlier natural infections also reduces the efficacy of viral vectors [37]. A common approach to reducing both innate and adaptive immune responses to viral vectors is to coat the virus surface with PEG. Coating with PEG reduces the clearance of the virus from circulation and hence improves the efficiency of the treatment [38, 39]

Intracellular barriers

Once the gene delivery vehicle has reached a cell, it then encounters multiple intracellular barriers. First, the vector must pass the plasma membrane and be endocytosed. Naked DNA does not associate efficiently with the plasma membrane due to the negative charge density on both the DNA and the cell surface. Different delivery vectors have been developed to help circumvent this problem.

Gene delivery vectors then moves through the cytoplasm to reach the nucleus, where they have to escape degradation by the endolysosomal network and the harsh pH conditions inside the lysosomes. There are several mechanisms employed to increase the likelihood of endosomal escape including membrane fusion, i.e. proton-sponge effect and incorporation of fusogenic and

pore-forming peptides. Lipoplexes escape the endosome through a fusion of the liposome with the endosomal membrane [40], while the proton sponge effect helps polyplexes containing polyethyleneimine (PEI) to escape endosomes [41].

Once the vector has successfully been released, it moves through the cytoplasm to reach where gene expression occurs. This step represents another significant barrier to gene delivery. First, the cytoplasm contains nucleases that will degrade free DNA, whether this DNA is delivered naked or dissociated from the vector before nuclear entry [6]. Additionally, the cytoplasm itself poses a diffusional barrier, being a viscous environment crowded with molecules, which results in decreased mobility of macromolecules [42]. Thus, the vectors must translocate through the cytoplasm by binding to the microtubule network to release the DNA near the nucleus.

The size of the DNA is a determining factor for nuclear transport through the nuclear membrane. Only molecules less than 9 nm in diameter successfully diffuse through the membrane, while larger molecules need active transport by nuclear localization signal peptides [43]. Viral vectors have inherent properties that allow them to utilize the nuclear import facilities of the cell. In contrast, non-viral vectors like lipids and polymers do not have that ability and they rely upon cell division. During the cellular division, the nuclear membrane of the cell breaks down thereby giving a chance to the therapeutic gene for nuclear entry. Performing transfection studies immediately before cell division increases the gene expression by 30 to 500-fold compared to the transfection studies at the beginning of the cell cycle [44].

Although complex formation between DNA and gene delivery vectors protects the gene from degradative enzymes inside the cell, this complexation prevents transcriptional protein binding to therapeutic genes [45]. For gene expression inside the cell, binding of a therapeutic gene with transcriptional proteins is the initial step. Therefore, the gene delivery vector should be designed to incorporate the balance between enzymatic degradation and gene release. Earlier studies have shown that the addition of PEG or reduction of polymer molecular mass can reduce

the positive charge of cationic polymer and thereby reducing the binding strength and increasing gene expression [46]. Finally, even though the intracellular trafficking poses as a significant barrier to gene transfer, many techniques for overcoming this problem are being revealed.

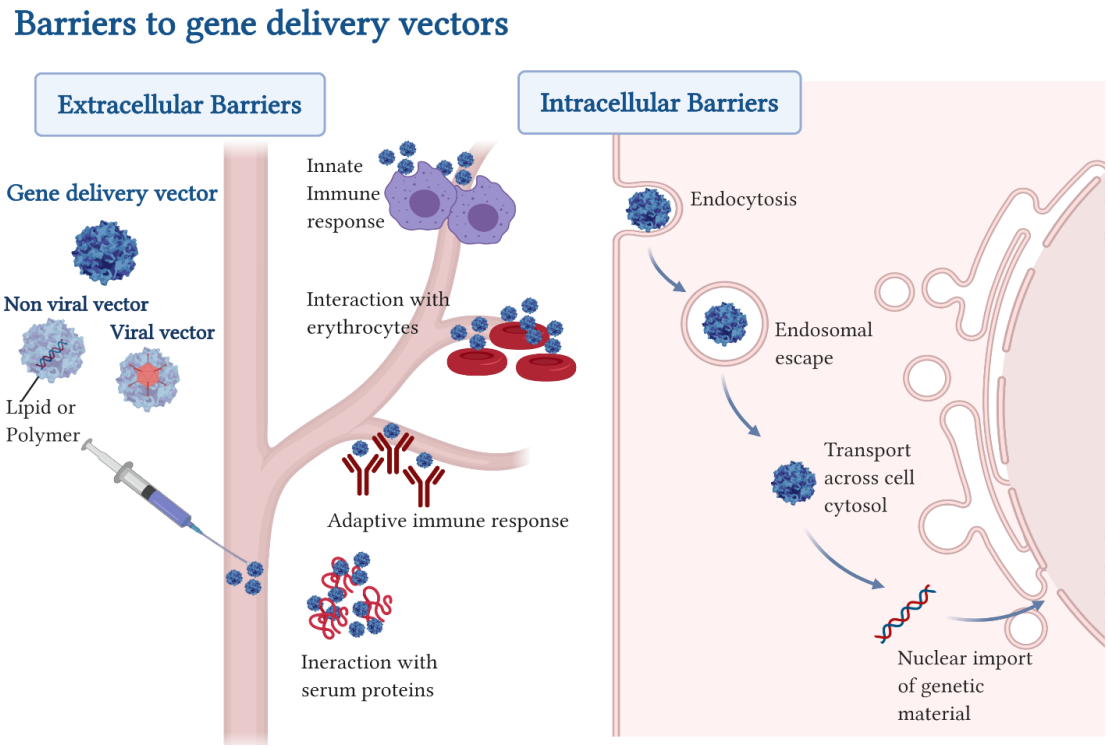

Figure 4.5: Schematic diagram of barriers facing gene delivery vector. Extracellular barriers are encountered after systemic administration of the vector, including interaction with serum proteins and erythrocytes, innate immune response, and adaptive immune response. Intracellular barriers start by facing the cell membrane where the vectors must bind to cellular components that induce endocytosis. After entering the cell, the vector must escape the endosome and release the genetic material close to the nucleus. The genetic material is then taken up by the nucleus via the nuclear pore.

1.5 GENE DELIVERY VECTORS

For successful gene therapy, a safe and efficient delivery vehicle that can carry a gene to the desired cell has to be developed. Ideally, gene delivery vectors have to selectively deliver the genetic material to the target cells, be immunologically inert, and have a large capacity to carry large-sized genetic materials. Besides, gene delivery vectors should not interfere with the genes in the host cell since unsought gene integration to the host genome might result in mutagenesis. As

mention before, the gene delivery vector must overcome all the extracellular and intracellular barriers before delivering its cargo inside the nucleus to achieve the required therapeutic action. Developing an ideal gene delivery vector meeting all these conditions is very difficult and is considered the 'Achilles heel' of gene therapy [18].

Gene delivery vectors are generally classified into viral and non-viral vectors. A variety of different vectors and delivery techniques has been applied in gene therapy trials as shown in Figure 1.6. Although non-viral approaches are becoming more common, viral vectors are still far more popular, having been used in approximately two-thirds of the trials performed to date [23].

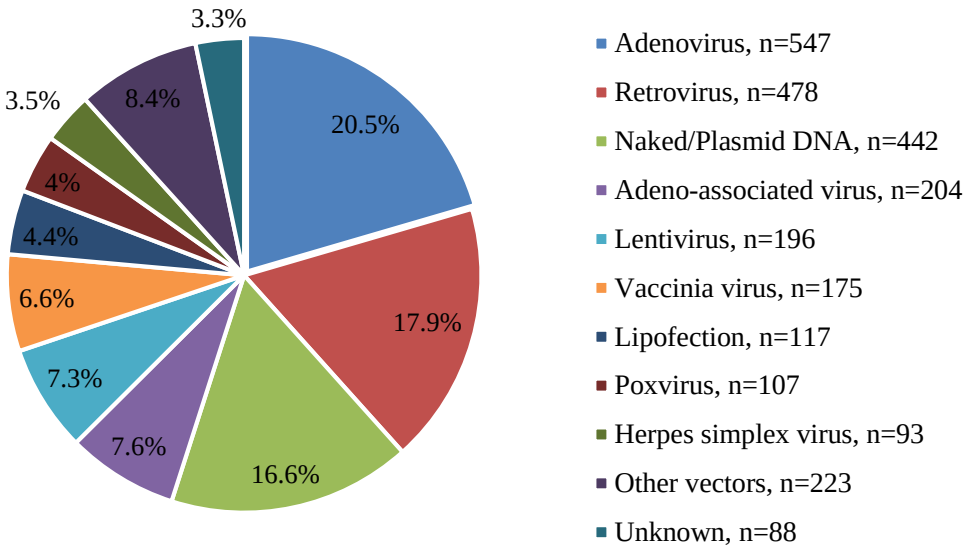

Figure 5.6: Vectors used in gene therapy clinical trials

Viral gene delivery vectors

Viral gene delivery systems are based on the natural ability of the virus to hijack the host cell and replicate their own genetic materials inside the cell. Since 1966 when Edward Tatum initially proposed to repurpose viruses for therapeutic gene delivery, gene therapy has come a long way from the construction of many types of viral vectors to their use in more than 3,000 clinical trials to date [4, 47]. Viruses used for gene delivery systems include retrovirus, adenovirus, adeno-associated viruses, lentivirus, poxvirus, and herpes simplex virus as shown in Figure 1.6 [48]. All viral vector genomes should be modified by deleting some areas of their

genomes to render them replication-deficient for a safe gene delivery vector and to free up some space for the desired transgene to be incorporated. Table 1.1 shows the different characteristics, advantages, and disadvantages of the most commonly used viral gene delivery vectors. Viral vectors exhibit high transduction efficiency to different cell types while providing long term gene expression. However, they possess some drawbacks such as immunogenicity, oncogenicity, pathogenicity, natural tropism, and high cost of production and purification [49].

Table 5.1: The properties of different types of viral vectors.

Viral vector	***Adenovirus***	***Retrovirus***	***Lentivirus***	***Adeno Associated virus (AAV)***	***Herpes virus***
Viral genome	DNA	RNA	RNA	DNA	DNA
Cell division requirement	No	Yes	G1 phase	No	No
Immune response	Extensive	Few	Few	Minimal or No	Extensive
Genome integration	No	Yes	Yes	No	No
DNA payload	8-30 kb	8 kb	8 kb	4.5 kb	>30 kb
Long-term expression	Transient	Long-lasting	Long-lasting	Potential long-lasting	Potential long-lasting
Advantages	Highly efficient in transducing cells. Non-pathogenic and non-oncogenic.	Persistent gene transfer in dividing cells.	Persistent gene transfer in non-dividing cells	Few inflammatory responses. Non-pathogenic.	Infects dividing and nondividing cells, the virus remains latent in neurons.
Drawbacks	Immuno-genicity, tropism, transient gene expression	Infects dividing cells only, a potential latent disease with malignancy or immune deficiency.	Direct transduction is more sensitive to tissue barriers, limited expression of the transgene.	Low packaging capacity, labor-intensive large-scale production	Vector targeting is complex since the mechanism involves multiple virus proteins, pathogenic, cytotoxic.

Non-viral gene delivery vectors

Safety, toxicity, and immunogenicity concerns along with the relatively small capacity for the therapeutic DNA of viral vectors have prompted the development of synthetic vectors not based on viral systems. Non-viral gene delivery vector uses “naked” DNA or plasmid DNA which when injected directly into certain tissues produces significant levels of gene expression, but lower than those achieved with viral vectors. Despite the safety and simplicity of large-scale production of non-viral vectors, low levels of transfection and transient gene expression are major limitations to their use. Treating diseases requires a continued and high-level of gene expression, which makes viral vectors better candidates for delivering the therapeutic genes.

Importantly, the efficiency of naked DNA delivery can be improved dramatically when combined with other physical or chemical modifications. Physical vectors include gene gun, electroporation, particle bombardment, ultrasound utilization, and magnetofection, while chemical ones include cationic polymers and lipids [48]. Cationic polymers or lipids can form complexes by binding to the negatively charged DNA to form either polyplexes or lipoplexes, respectively [50]. As shown in Figure 1.6, naked DNA remains the most popular non-viral vector used in clinical trials, followed by lipofection, which involves cationic lipid/DNA complexes. Table 1.2 describes different examples of non-viral gene delivery vectors, their advantages, and disadvantages.

Table 5.2: Summary of advantages and disadvantages of non-viral vectors.

Non-viral vector		***Advantages***	***Disadvantages***
Lipids	***DOTAP***	Condense DNA efficiently, commercially available	Low efficiency, toxic
	DOTMA	Condense DNA efficiently, commercially available, biodegradable	Low efficiency
	Helper lipids (cholesterol, DOPE, …)	Promote endosomal escape, commercially available	Doesn't condense DNA
Polymers	***PEI***	Excellent transfection efficiency	Toxic, limited efficiency
	PLL	Biocompatible, biodegradable, Efficient in condensing DNA	Low proton sponge, low efficiency
	Polysaccharides (Chitosan, Dextran, ..)	Biocompatible, biodegradable, nontoxic,	Poor endosomal escape, low efficiency
	Dendrimers (PMAM, PPI, ...)	Higher generation show good transfection efficiency	Non-biodegradable, higher generation are cytotoxic
Peptides	***CPP***	Enhance cellular uptake and endosomal escape	Low efficacy
	RGD	Promote targeting	Low efficacy
	NLS	Promote nuclear import	Low efficacy, complex dissociation before nuclear import

1.6 ADENOVIRUS

Adenovirus (Ad) was the first viral vector developed for gene therapy and was approved for clinical trials in 1990. Ad was isolated from human cultured adenoid tissue for the first time in 1953, hence the term adenovirus [51]. Since then, 57 adenovirus serotypes have been isolated and classified into seven distinct subgroups (A to G) based on their immunological properties [52, 53]. Ads have been associated with different pathophysiology, ranging from gastrointestinal to ocular to respiratory tract infections. Ad is a non-enveloped linear double-stranded DNA virus (26 – 45 kbp), with an approximate diameter of 90-100 nm. The estimated mass of the Ad particle is at least 150 x 10^6 Da, of which 22.6 x 10^6 Da are DNA [54]. In 1959, the negatively stained EM pictures first revealed the icosahedral shape of the virus with long fibers extending from each of the 12 vertices [55, 56]. Ad is composed of eleven well-identified structural proteins, three of which are major proteins: hexons, pentons, and fibers (Figure 1.7A) [57].

Hexon proteins are arranged in trimers and present in 240 copies that form the 20 faces and 30 edges of the icosahedral capsid. Penton bases are present in 12 copies located at each apex. Each penton capsomere is made up of a fiber, a homotrimer protein attached to a pentameric protein, the penton base, that closes up the vertices of the capsid [58]. The adenovirus fiber protein is composed of three domains: the tail, shaft, and knob (Figure 1.7B) [59]. The first 17 residues from the amino (N)-terminus forms the tail and non-covalently attach the fiber to the capsid penton base. The shaft consists of 22 structural repeats downstream from the tail. The remaining carboxy (C)-terminal segment folds into the globular knob containing the receptor-binding domain [60].

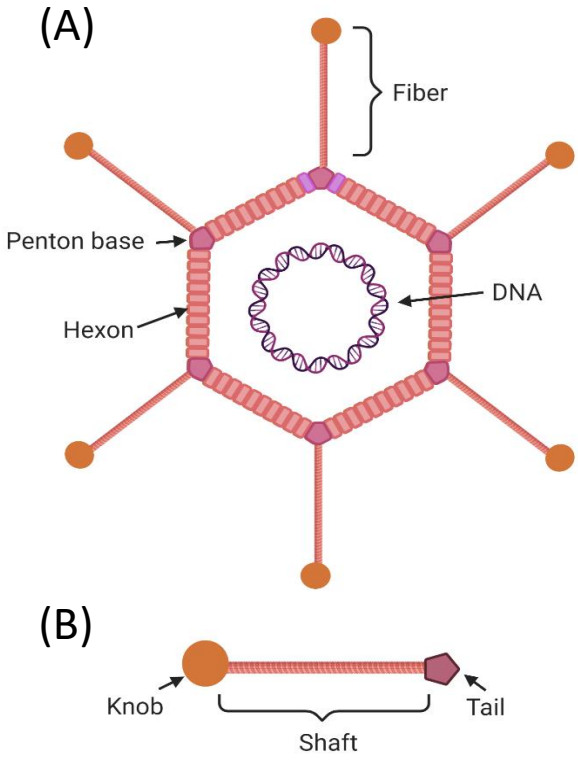

Figure 1.7: A schematic depiction of Ad structure enclosing double stranded DNA. (A) The icosahedral Ad capsid is composed of hexon proteins and penton bases from which fiber protein emanate. (B) The fiber protein incorporated into each of the 12 vertices of Ad capsid is a homo-trimeric molecule, which consists of three distinct structural domains: the tail, the shaft, and the knob.

Ad infection is initiated by high-affinity binding (Kd = 1.7 nM) of the fiber knob to a cellular receptor known as Coxsackievirus-Adenovirus Receptor (CAR) [61, 62]. This interaction docks the virus to the cell allowing secondary binding of the penton base to αv integrins, which triggers the receptor-mediated endocytosis of the whole virus [62].

1.7 ADENOVIRUS AS GENE DELIVERY VECTOR

Adenoviruses have several features that make them among the most widely used vectors for gene therapy, where they account for 20.5 % of all ongoing gene therapy clinical trials [23]. First, Ad vectors can carry relatively large DNA payload (up to 35 kb), transduce a broad range of human cells including dividing and non-dividing cells. They are known for their high efficiency of transduction and their high levels of gene expression (though transient). Second, Ads have low pathogenicity in humans, they cause few and only mild symptoms associated with the common cold. Third, Ad vectors do not insert their genome into the host nucleus but store it as an episome. Therefore, there is a low probability of oncogenicity, disturbance of vital cellular genes or processes. Fourth, Ads are abundant in several serotypes, and most adults have been exposed to the commonly used Ad serotypes in gene therapy (serotypes 2 and 5). Fifth, Ad vectors are easy to propagate and purify at high titers, also they are relatively easy to manipulate using recombinant DNA techniques. The vectors, however, have certain drawbacks which limit their use as a safe and efficient gene delivery vector. These include the inflammatory response, pre-existing immunity in humans, liver and spleen sequestrations as well as the virus promiscuous tropism.

After intravenous injection, Ad vectors induce an innate immune response that is maximal by 6 hours. This immune response results in inflammation of the transduced tissues and efficient clearance of the administered vectors. The inflammatory response is mediated by the virus fiber, capsid, and DNA, independent of viral gene transcription [63, 64]. Phagocytic antigen-presenting cells such as macrophages and dendritic cells take up the virus particles

through scavenger receptors [65]. Inside the cell, the virus is sensed through various intracellular molecular sensors such as Toll-like receptors (TLRs) [66]. Several cytokines are then released like tumor necrosis factor α (TNF-α), IL-6, IL-1ß, interferon γ (IFN-γ), and IL-12 and chemokines macrophage inflammatory protein (MIP)-2, IFN-γ-inducible protein 10 (IP-10), and RANTES [67, 68]. The infected cells are specifically destroyed via the formed cytotoxic T lymphocytes (CTL) [69]. After the fatal incident in the clinical trial of Jesse Gelsinger [42], it became evident that the innate immune system is highly activated by intravascular administration of high doses of Ad vectors [43]. This tragedy halted all gene therapy trials in the USA for six years [70, 71]. Subsequent animal experiments were able to reproduce the events, where an inflammatory response was lethal to mice at a dose of 10^{10} virus particles (vp) per mouse; and to large animal models at high doses, such as $>10^{13}$ vp per kg [72]. High doses of adenoviral vectors were reported to cause hepatotoxicity [73] and acute inflammatory response in addition to a reduction in gene delivery efficiency [74]. The induction of innate immune responses is critical in adenoviral vector-based strategies. To allow efficient gene delivery, the Ad vector should have a minimal innate immune response. Ad vectors, however, could benefit from the virus's intrinsic property of innate immune response to allow efficient activation of transgene-specific adaptive immune responses to be used in vaccine delivery.

The adaptive immune response to adenoviruses is another obstacle in Ad vector development as a gene delivery vector. An estimated 80% of the human population have pre-existing immunity to human adenovirus serotype 5 [37]. Even if they were not exposed before to Ad and do not possess neutralizing antibodies, they will develop resistance against reinfection if exposed to an Ad vector at a high concentration [75]. Ad surface antigens such as hexon, penton, and fiber induce the production of neutralizing antibodies [76]. These neutralizing Abs recognize the virus leading to rapid clearance from the circulation which would limit the number of administrations that can be done and reduce the efficiency of transgene expression. Many approaches, for example, development of alternative Ad serotypes, varying immunization routes,

and using prime-boost regimens are in the pre-clinical or clinical stages of development to avoid pre-existing immunities against adenoviruses [37]. From a general health perspective, it is advantageous to have long-term immunity against adenovirus infection, but from a gene delivery standpoint, the innate and adaptive immune responses to the virus limit the efficacy of an adenovirus vector.

CAR is a 46-kDa single transmembrane protein that is widely spread in a range of tissues including the brain, liver, heart, lungs, kidneys, and specifically, localizes with αvß3 and αvß5 in cardiomyocytes (Figure 1.8) [61, 77]. CAR acts as a pathfinder protein, directing organ formation during embryogenesis and re-expressing this embryonic pattern after cytopathic damage [78]. In cultured cells, CAR induces the formation of cell aggregates and accumulates at cell-cell contacts [79]. Some cells such as primary and cancer cells do not express CAR on their surface, and thus are refractory to transduction by CAR-binding Ad vectors [80]. The dependence of Ad on CAR for binding to cells to be endocytosed creates the problem of promiscuous tropism. This highlights the need for Ad vectors with CAR-independent internalization for cancer gene therapy. Furthermore, nonspecific binding between motifs present on the virus and proteins on the cell membrane can induce promiscuous tropism. For example, RGD motif on the penton base of the virus binds to αv-integrin receptors [62], while KKTK motifs on the fiber protein bind to heparan sulfate proteoglycans, leading to a wide tropism [81, 82]. The biodistribution of Ad vector does not only depend on the receptor usage as anticipated by *in vitro* experiments. After systemic administration, Ad vectors are rapidly cleared from the bloodstreams and most of the viral dose is sequestered in the liver or phagocytosed by macrophages. This markedly reduces the therapeutic gene transduction and displays severe hepatotoxicity. This hepatic tropism is due to binding of blood coagulation factor X (FX) to the hypervariable region (HPV) of Ad hexon subunit, followed by the interaction of the Ad-FX complexes to heparan sulfate proteoglycan (HSPG) molecules which are present in high concentrations at the surface of Kupffer cells in the liver [83]. Furthermore, Ad fiber protein binds to erythrocytes expressing CAR. This traps the virus in

the blood circulation, thereby reducing liver infection [84]. Although decreasing hepatic tropism is desirable, binding the virus to RBCs leads to haemagglutination and affects the bio-distribution and specific targeting to the diseased cell.

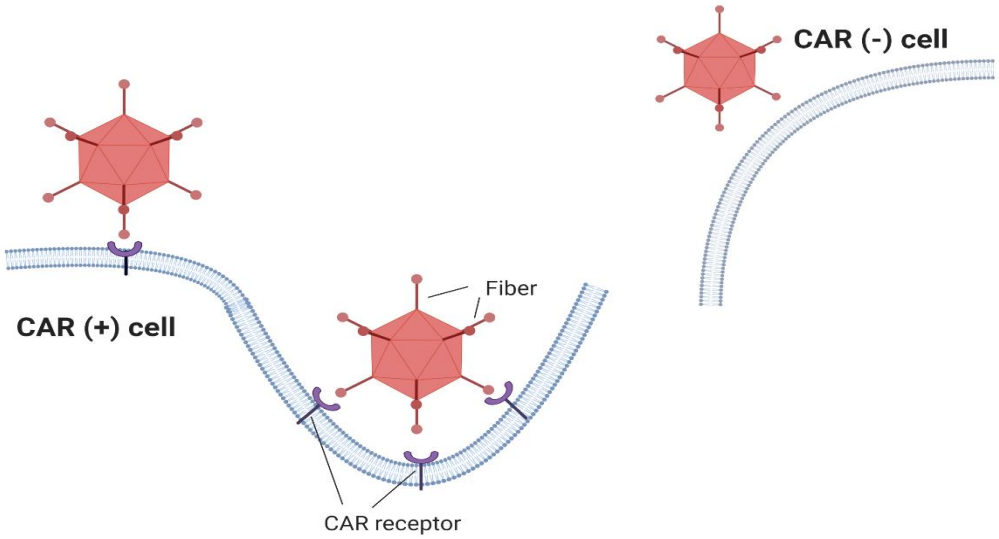

Figure 1.8: Promiscuous tropism of Adenovirus as CAR is widely spread in the body cells. A) Ad binds to CAR-positive cells via interaction between the knob of Ad fiber and CAR. B) Ad cannot bind to cells that lack CAR (CAR-negative cells) like cancer cells.

There has been a rapid expansion in the use of adenoviral vectors for *in vitro* and *in vivo* gene delivery [85]. Ad vectors have been used to treat monogenic diseases since 1992 when the first *in vivo* application for genetic therapy was reported. The case involved the expression of alpha-1 antitrypsin cDNA within hepatocytes of a patient with alpha-1 antitrypsin deficiency [86]. This was followed by two unsuccessful treatments, one was an ornithine-transcarbamylase deficiency in 1999 [13], and the other was an X-linked severe combined immunodeficiency in 2002 [87]. Over the next decade, safety concerns were raised against the application of viral vectors in humans and lead to a significant decline in studies [88]. Much of the research focus in that time then shifted toward developing less immunogenic viral vectors and AAV and lentiviral vectors emerged [89].

Despite these first impediments, Ads have returned to the light of human gene therapy in recent years being the most commonly studied viral vectors among clinical trials [23]. Ad vectors are now used for 1) gene therapy [90, 91]; 2) anticancer therapies, for example oncolytic Adenovirus [92], 3) vaccine therapy, for example vaccines against tuberculosis [93], HIV [94], malaria [95], influenza [96], and Ebola [97]. Recently Ad vectors have been used to effectively deliver engineered CRISPR/Cas9 systems to targeted cells and/or tissues for efficient genome editing, which cannot be effectively accomplished by other viral systems [98].

1.8 METHODS TO OVERCOME DRAWBACKS ASSOCIATED WITH ADENOVIRUS

Genetic modification of Adenovirus

The adenovirus problems can be addressed by modifying the virus either genetically or chemically. Ad genome is organized into early (E1, E2a, E2b, E3, and E4), intermediate (IVA2 and IX), and late genes (L1, L2, L3, L4, and L5) according to the expression of genes during infection and multiplication. The genome of Ad has been engineered several times to develop safe and efficient vectors for gene therapy applications. The first-generation vectors had a partial deletion of E1 and E3 genes. E1 genes are necessary for activation of viral promoters, expression of both early and late genes, and encoding of oncogenic transforming functions of the virus. E3 gene encodes proteins that subvert the host's immune response and allows the persistence of infected cells. Therefore, deleting parts of E1 and E3 regions resulted in replication-deficient and non-oncogenic vectors. The deletion also allowed the insertion of approximately 5.1 kb of therapeutic genes without affecting viral titer and growth rate [99]. A human embryonic kidney-derived line, HEK 293 cell line, has been transformed by the adenovirus E1 region to be able to propagate the first-generation vectors [100]. These vectors, however, still showed a strong immune response and would be contaminated with the replication-competent virus [101]. Second-generation vectors were created by deleting E2A, E2B, and E4 from the genome of the first-generation Ad vectors to overcome their problems. These new vector constructs have decreased

toxicity and result in prolonged gene expression *in vivo* but their production has become complicated. The new vector constructs also did not prevent leaky expression of viral proteins and rapid loss of therapeutic gene expression, and thus were not widely used in gene therapy [102]. The third-generation vectors, known as gutless or helper-dependent Ad vectors, lack all viral genes except the packaging and ITR sequences. They have the highest capacity among all vectors due to their ability to carry therapeutic genes up to 37 kb in size. Third generation Ad vectors also have long-term transgene expression, less contaminated with replicating virus particles, and are less immunogenic than first- and second-generation vectors [103].

Genetic modifications of Ad have also addressed the tropism problem, evaded pre-existing immunity, and changed the biodistribution of Ad vectors after systemic application. Ad attaches to its target cell via the knob domain of the fiber which is structurally conserved between different Ad serotypes. In 1995, the first replacement of the fiber knob of Ad-5 with that of Ad-3 altered the viral tropism and enhanced the binding and entry especially into primary cells [104, 105]. In addition to the exchange of the fiber knob domain, genetic modifications included exchanging knob and shaft domains [106], varying the length of the fiber [107, 108], the formation of knobless fibers [109], and replacing equivalent domains from human Ad with others from animal Ad in a strategy known as " Xenotype switching" [110, 111]. These genetic modifications generated Ad chimeras with ablated natural tropism and specific cell transduction abilities. In addition to changing primary receptor binding, intracellular virus trafficking [112] and induction of immune responses [113] might be altered by fiber modification.

Genetic modification of Ad has also reduced the immunogenicity problem of the virus. Since the capsid protein hexon is the main antigenic component [114, 115], attempts have included hexon exchange or replacement of immunodominant hypervariable regions (HVRs) of Ad-5 with that of other serotypes [116]. Genetic manipulations of the fiber knob also generated Ad-5 vectors carrying the Ad-3 knob [117]. These modifications lead to successful evasion of neutralizing antibodies that recognize the parental vectors. Furthermore, the liver sequestration of

Ad was markedly decreased by the insertion of mutations in the FX-binding domain of HVR and its replacement with HVR of other serotypes [118, 119]. However, genetic capsid modifications are difficult to perform as they potentially interfere with correct folding of capsid proteins and/or particle assembly.

Chemical or Physical modification of Adenovirus

Although genetic modifications overcome the most relevant barriers to the clinical application of Ad-based therapies, the development of a production system for such vectors has been hampered by technical complexity and low titers. In contrast, chemical/physical modification is performed after the production and purification of the vectors. Therefore, high vector titers can be obtained as well as conventional producer cells can be used. Besides, chemical modification of the Ad capsid can be performed in a way that modifies thousands of amino acids on the capsid surface simultaneously [120].While Physical modification can be obtained by coating the Ad surface without chemical linking bonds. The primary purpose of chemical/physical modification is to shield the Ad capsid proteins (hexon, penton, and fiber) from unwanted interactions with the host cells, ablate Ad tropism while maintaining the infectivity of Ad. Surface modification of a viral vector leads us to the term hybrid viral vector. In this review, a hybrid vector is a gene delivery vector that combines the beneficial features of a viral vector and a non-viral vector. We will discuss hybrid vectors in the context of the chemical modifications of adenovirus, in which a biocompatible, and non-toxic material (polymer, lipid, etc.) binds with adenoviral vector to enhance its gene delivery properties.

Coating of Ad with polymers. Two kinds of strategies have been commonly used for surface modification of the Ad with polymers: covalent coating and noncovalent coating through electrostatic interactions. This surface modification facilitates the evasion of the host immune response and the ablation of the Ad tropism.

Covalent coating of the Ad with hydrophilic polymers. The Ad capsid has approximately 1800 exposed lysine residues located on the hexon, penton, and fiber proteins [121]. This allows covalent bonding between the polymers and the amine groups of the lysine residues on Ad surface [120]. Polyethylene glycol (PEG) and poly-N-(2-hydroxypropyl) methacrylamide (pHPMA) are representative polymers of chemical engineering to Ad vectors.

Polyethylene glycol (PEG). PEG is a hydrophilic neutrally charged biocompatible polymer [122] that is commonly used to reduce protein-protein interactions between therapeutic compounds and proteins *in vivo* [123]. Coating of Ad with PEG in a technique called "PEGylation" has been shown to prevent the undesirable interactions between the Ad and the host cell. PEGylation has helped Ad in evading the host immune response as well as ablating the Ad tropism. In 1999, O'Riordan et al. carried the first PEGylation of Ad which resulted in the escape of the PEGylated virus from the neutralizing antibodies (NABs) both *in vitro* and *in vivo* [39]. Later, Croyle et al. confirmed that PEG can shield the surface of Ad from NABs and evade the adaptive immune response [124, 125]. PEG can also attenuate the innate immune responses induced by Ad after systemic administration. Mok et al. first demonstrated that PEGylation of Ad reduced interaction with immune cells, such as macrophages [126]. Studies have shown that IL-6, IL-12, and TNF levels were significantly decreased after intravenous administration of PEGylated Ad vectors [127, 128]. Furthermore, PEGylation is a promising tool to address the Ad tropism problem. Ad depends on the specific receptor (CAR) for binding and internalization and has shown high liver tropism. Thus, for many cells types that lack Ad primary receptors, such as tumor cells, skeletal and smooth muscle cells, peripheral blood cells, ciliated airway epithelium cells, and hematopoietic stem cells [129], infection with Ad is difficult. PEGylation of Ad blocks CAR interactions and changes the vector particle diameter to avoid entrapment in liver fenestrations, allowing higher vector concentrations to reach the target cells. Although PEGylation is a practical approach to improve the efficacy and safety of Ad vectors for gene delivery, it has some drawbacks that should be noted. First, most of the experimental animals had

NABs against Ads, not against PEGylated Ads, thus the ability of PEGylated Ads to evade NABs needs to be further considered. Second, PEGylation can block the interaction with cells, blunting the cellular uptake, and transduction efficiency of Ad vectors. In this case, another approach should be adopted to enhance the cellular uptake of PEGylated Ad vectors.

Poly-N-(2-hydroxypropyl) methacrylamide (pHPMA). pHPMA is a hydrophilic polymer that has multiple amino-reactive groups, allowing approximately 10–15 points of attachment to the virus [130]. Thus, pHPMA forms polymer "stitches" that covers the Ad with a dense and stable coating [131]. pHPMA, also have adequate reactive sites for subsequent covalent attachment to other polymers without biofunctionalization like PEG. Inspired by these advantages of pHPMA, Fisher et al. modified the Ad with a multivalent reactive 16.5 kDa pHPMA [132]. In this study, modified pHPMA-Ad vectors evaded NABs by approximately 80% and ablated the CAR tropism of Ad in A549 (Ad-permissive human lung carcinoma cell line) *in vitro*. pHPMA-Ad vectors reduced liver transduction as well because the dense coverage of Ad blocked FX from binding to the Ad hexon . In summary, pHPMA-lation of Ad can blunt the interaction with the host proteins in a more effective way than PEGylation. However, this modification may result in undesired effects like the interference with regular capsid disassembly during gene delivery because of the multiple reactive sites of pHPMA that cross-link different Ad capsids together.

Non-covalent coating of Ad.

Cationic polymers. Different polymers have been utilized to noncovalently coat the Ad surface, including poly ethylenimine (PEI), poly-l-lysine (PLL), polyamidoamine dendrimer (PAMAM), poly amino ethers, and chitosan. Those polymers are cationic in nature and can form complexes with the negatively charged virus surface through electrostatic interactions. Because of its simplicity, safety, and the ability to maintain the virus infectivity [133], the non-covalent coating has been widely employed to modify Ad surface. Cationic polymers can change Ad tropism by blocking the receptor-mediated endocytosis and increasing the cellular uptake of the modified virus in CAR-deficient cells. PEI and PLL are the first cationic polymers to increase the

cellular uptake of Ad in cells refractory to infection such as ciliated airway epithelial cells, skeletal cells, and smooth muscle cells [73–76]. Although PLL and PEI are efficient transfection polymers, their toxicity is a significant limitation to their subsequent use. Thus, new polymers that demonstrate high infectivity and low toxicities have been developed including PLL-b-PEG [134], PEG-g-PEI [135], PEI-bile acid conjugated [136], EGDE-3,3′(aminoglycoside polymer) [137], and PNLG (methoxy polyethylene glycol-b-poly) [138]. Another advantage of cationic polymers is that they can block liver tropism *in vivo*, which allows the modified virus to reach the targeted cells in higher concentrations. Kim et al. showed that localization of Ad/PNLG complex in the liver was significantly reduced compared to the naked Ad [139]. Cationic polymers also reduce the host innate and adaptive immune response. This beneficial feature was observed when IL-6 levels decreased after the systemic administration of Ad/PNLG complexes [139]. Dodds et al. also reported that coating Ad with polycations led to partial protection of Ad against the neutralizing effect of Ad antiserum [140]. Other examples include PEI and APC, cationic polyethylene glycol derivatives, that tightly coat Ad, thus shielding the virus from NABs [141, 142]. In conclusion, cationic polymers can shield Ad to redirect Ad tropism, reduce liver accumulation, and enhance cellular uptake in CAR-negative cells. Besides, coating Ad with cationic polymers reduces the innate and adaptive immune response to Ad. However, careful design of physically modified Ad/polymer complexes should be implemented, due to the possible associated limitations including nonspecific uptake in cells, cytotoxicity of polymers, and serum instability of the Ad/polymer complexes leading to their rapid dissociation in blood.

Cationic lipids. Cationic lipids have been used to modify Ad including lipofection [143], DOPE (1,2-dioleoyl-*sn*-glycero-3-phosphoethanolamine), DOTMA (N-[1-(2,3-dioleyloxy)propyl]-N,N,N trimethylammonium chloride), DOTAP (1,2-bis(oleoyloxy)-3-(trimethylammonio) propane), and DC-Cholesterol (3β[N-(N′, N′-dimethylaminoethane)-carbamoyl] cholesterol). Cationic lipids are biodegradable, readily available commercially, and can be relatively easily modified for specific applications [1, 2, 8]. In aqueous media, cationic lipids are assembled into a bilayer vesicular-like structure called liposomes. Cationic liposomes can envelop Ad through electrostatic interaction with the negatively charged virus, and similarly can bind to the negatively charged cell surface to enhance their uptake [70]. Complexing adenovirus with cationic liposomes is effective in increasing adenoviral transgene expression particularly in CAR-deficient cells [144]. Liposome complexation also resulted in reduced immunogenicity of adenovirus [145, 146]. Our lab has previously produced Ad associated with PEGylated cationic liposomes composed of ternary lipids DOTAP**,** DOPE, and cholesterol that were able to infect cells in a receptor-independent manner and protect the virus from innate and humoral immune responses.

Cell-Penetrating Peptides. Cell-Penetrating Peptides (CPP) are short peptides, typically less than 30 amino acids, that can deliver cargo across the cell membrane of mammalian cells [147]. They are typically classified as either polycationic, amphipathic, or hydrophobic. CPPs have been used to facilitate the transport of different therapeutic agents into cells, including plasmid DNA, siRNA, therapeutic proteins, viruses, and other various nanoparticles [148]. Penetratin [149], Tat [150], and polyarginine [151] are polycationic cell-penetrating peptides enriched with arginine and lysine that have been successfully used to modify adenovirus to enhance its translocation into different cell types [152]. CPPs can be associated with the virus covalently via genetic modification of the capsid proteins or chemical conjugation or noncovalently based on electrostatic interactions to the surface of the virus particle [153]. Our lab has previously produced CPP-PEG-Ad where PEGylated Ad was conjugated to different kinds of

CPP: Penetratin, TAT, Pep1, polyarginine. Penetratin-PEG-Ad showed the highest transduction efficiency in CAR-negative cells compared to other CPP modified Ad vectors and was able to extend the potential gene therapy treatments to a much broader range of cell types[151].

1.9. HYPOTHESES AND OBJECTIVES OF PRESENT WORK

The motivation of the present work was to develop a hybrid gene delivery vector that combines a fiberless Adenovirus (FlAd) and synthetic materials that maintain the efficiency of the virus while avoiding its drawbacks.

The working hypothesis of this study is:

(i) *The function of fiber protein could be replaced by a PLL-g-PEG copolymer to augment the virus transduction efficiency and reduce its immune response.*

(ii) *PLL-g-PEG copolymer would modify the cellular trafficking of the hybrid fiberless adenovirus vectors to affect the efficiency of expression of the target gene.*

Our rationale for investigating FlAd and PLL-g-PEG copolymers for gene delivery was that FlAd will have advantages over native Ad (NtAd) such as a reduced immune response and independence on CAR binding for cell transduction. Further, the coating of the FlAd with the copolymer can shield the virus hexon protein from an immune response as well as increase the transduction efficiency of the virus in cells that are refractory to infection with NtAd.

The objectives of this study:

(i) *Investigate the effects of PLL-g-PEG copolymer on the physicochemical properties and the overall performance of the PLL-g-PEG-FlAd vector.*

(ii) *Compare the cellular trafficking of PLL-g-PEG-FlAd vectors to the native adenovirus and determine the limiting steps of the pathway.*

Outline of this study:

Chapter 2:

Investigation of the effects of PLL-g-PEG copolymer on the physicochemical properties and the overall performance of the PLL-g-PEG-FlAd vector will be studied as follow:

- Preparation of PLL-g-PEG-FlAd hybrid vector via electrostatic association between FlAd and PLL-g-PEG at various formulation factors (PLL Mwt, PEG Mwt, Degree of PEGylation, PLL-g-PEG amount (μg)/10^6 FlAd particles).
- Studying the effect of these factors on the physicochemical properties as particle size, zeta potential as well as on the transduction efficiency in CAR-positive (HEK 293) and CAR-negative (NIH 3T3) cells.
- Optimization of PLL-g-PEG-FlAd using response surface method (RSM) to achieve highest transduction efficiency in CAR-positive (HEK 293) and CAR-negative (NIH 3T3) cells.

Chapter 3:

Investigation of optimized hybrid vectors on the overall performance of the PLL-g-PEG-FlAd vector will be studied in terms of:

- Cytotoxicity on CAR-positive (HEK 293) and CAR-negative (NIH 3T3) cells.
- Innate immune response via measurement of levels of proinflammatory cytokines produced from macrophages.
- Serum stability when subjecting hybrid vectors up to 50% serum.
- Transduction efficiency in different CAR-negative and low cells like CHO and MCF-7 cells, respectively.

Chapter 4:

Comparison of the cellular trafficking of PLL-g-PEG-FlAd vectors to the native adenovirus in both CAR-positive (HEK 293) and CAR-negative (NIH 3T3) cells will be achieved as follow:

- Determination of the binding and internalization levels of hybrid vectors.
- Investigation of the attachment of hybrid vectors to heparin sulfate proteoglycan receptors (HSPGs).
- Determination of endocytic pathway for internalization of hybrid vectors.
- Determination of effect of pH on endosomal escape of hybrid vectors.
- Determination of cytosolic transport pathway of hybrid vectors.

The broader impact of the project is its culmination in an improved gene delivery vector that would be a potential step in the top-down approach which fully replaces a viral vector with a synthetic one, possessing the same advantages but not the disadvantages of a virus. This project would also greatly impact society by transitioning gene therapy from a fringe medical treatment to common practice. Finally, no boundaries limit a discovery; every bump in the investigation path can be an inspiration and source of energy to advance research, a never-ending learning process.

CHAPTER II

DESIGN OF HYBRID PLL-G-PEG FIBERLESS ADENOVIRAL GENE DELIVERY VECTORS

2.1 INTRODUCTION

Several challenges need to be addressed when developing a gene delivery vector for an efficient and safe delivery of genes for any clinical application. Viral vectors account for nearly two-thirds of the gene therapy clinical trials [23]. Ads are among the most popular viruses used for gene therapy (20.5% of all trials) with Ad serotype 5 being the most commonly used serotype. Ad vectors can carry large DNA payloads, transduce both dividing and non-dividing cells with high levels of gene expression (though transient) [89, 154-156]. However, the vectors exhibit some drawbacks like immunogenicity and wide tropism which causes difficulty in cell-specific targeting [37, 72, 129]. The dependence of the virus on binding to the cell surface receptor Coxsackie Adenovirus receptor (CAR) for attachment and internalization leads to the wide tropism of the Ad vectors [157]. Most cancer cell [80, 158, 159], ciliated airway epithelium [160], smooth muscle cells [161], skeletal muscle cells, peripheral blood cells, dendritic cells, and hematopoietic stem cells [162] exhibit low levels of CAR and thus are refractory to Ad vector transduction. The immune response against the virus capsid and fiber proteins prevents the vector from transducing the target cells [163]. Further, pre-existing neutralizing antibodies against Ad would require frequent and high doses of the vector to be administrated to deliver the desired therapeutic response. Nonetheless, high doses of Ad vectors can cause hepatotoxicity and severe

inflammatory response [73, 74].

One promising vector design strategy is to engineer adenoviruses with enhanced gene delivery properties. Ads have been genetically modified to reduce immunogenicity and undesired tropism of the virus, enhance gene transfer efficiency, and provide targeted delivery [109, 164-169]. Replacing the knob of Ad serotype 5 with other serotypes ablated or altered the virus tropism [170]. For example, transduction levels of primary melanoma cells with Ad-5 with a knob of Ad-3 increased up to three folds when compared to Ad-5 control [171]. A novel tropism towards pancreatic cancer cells was also displayed upon replacing the fiber of Ad-5 with the fiber of Ad-16 or Ad-50 [172]. Furthermore, switching the Ad-5 hypervariable regions (HRVs) with those of Ad-48 plus exchanging the fiber knob with that of chimpanzee SAd-25 resulted in almost complete evasion of the neutralizing antibodies both *in vitro* and *in vivo* [114]. Studies have also shown that exchanging the hexon HRVs of Ad-5 by those of Ad-48 ablated hepatocyte transduction *in vitro* and reduced liver transduction *in vivo* [173] .

An alternative solution involves the design of a hybrid viral vector consisting of a viral vector complexed with biomaterials that exhibits the benefits of the parental virus but are safer, more efficient, and less expensive. Cationic polymers [174, 175] or lipids [176, 177], are safe and robust biomaterials that were previously combined with DNA to form a non-viral vector capable of gene delivery. Cationic polymers include poly-L-lysine (PLL) [178, 179], polyethyleneimine (PEI) [180], chitosan [181, 182] and poly-N-(2-hydroxypropyl) methacrylamide (pHPMA) [183], as well as a variety of materials specifically designed for gene delivery. Non-viral vectors must efficiently deliver DNA into the nucleus of the targeted cell and circumvent the intracellular barriers including endocytosis, endosomal escape, and transport through the cytoplasm and across the nuclear membrane. Synthetic materials are generally less efficient than viruses in overcoming one or more of the intracellular barriers, which makes non-viral vectors less clinically relevant.

In this chapter, we construct a hybrid vector in which the fiber part of adenovirus is removed, and its function is replaced with a synthetic material. Our lab has previously

constructed an adenovirus that lacks the fiber protein forming a fiberless adenovirus (FlAd) [184]. The fiber protein, specifically the knob, is essential for binding the virus to the Coxsackie adenovirus receptor (CAR) and is thus a major detriment of viral tropism [185]. After systemic administration of the virus, the fiber protein plays a role in the high transduction levels in the liver and the spleen as well as the innate immune response [186, 187]. Therefore, fiber truncation would reduce both the tropism and the immunogenic response problems. However, this fiber removal would result in a great reduction in the virus transduction efficiency (TE) due to the inability of the virus to attach to the CAR and induce internalization. We hypothesize that the cellular entry functions of FlAd can be replaced through physical modification of the virus with the cationic PLL-g-PEG copolymer.

PLL is one of the first cationic polymers employed for gene delivery [179]. PLL is a linear polypeptide with the amino acid lysine as the repeat unit; thus, possesses a biodegradable nature. Upon complexing PLL with Ad, the formed PLL-Ad vector lead to an increase in the virus uptake and the transgene expression in cells compared to cells treated with Ad alone [188]. However, PLL-Ad vectors are rapidly bound to plasma proteins and are cleared from the circulation [189]. Besides, PLL elicits undesirable cytotoxicity at high concentrations which hampers its application [190]. One popular modification that can increase both the transfection ability and the circulation half-life of PLL-Ad vectors is coating the vector with polyethylene glycol (PEG) [191, 192]. PEG is a hydrophilic polymer that reduces the protein-protein interactions between therapeutics, proteins, and cells *in vivo*. PEGylation of Ad vectors decreases recognition by neutralizing antibodies and reduces the innate immune response to the virus [193, 194]. Besides, PEGylation increases the vector circulation times and prolongs the transgene expression [124, 195]. However, PEGylation compromises the ability of the virus to interact with CAR, which reduces the transduction of Ad in cells [20]. This simultaneous ability to reduce immunogenicity and lower transduction efficiency in cells is known as the “PEG dilemma” [196].

Therefore, using PLL-g-PEG copolymer would be a good approach to gain the benefits of PEG while retaining the infectivity of the virus.

Based on this study, a PLL-g-PEG copolymer may be able to jointly eliminate the drawbacks addressed separately by each reagent. PLL-g-PEG-FlAd hybrid vector is expected to have improved transduction efficiency, and reduced immunogenicity. In this chapter, we report the formation of these hybrid vectors and investigate the variables that affect the physicochemical properties as well as the gene delivery efficiency such as PLL molecular weight, PEG molecular weight, Degree of PEGylation (DOP), and the ratio of PLL-g-PEG to the virus.

2.2 MATERIALS AND METHODS

Cell culture

Mouse fibroblast cell line (NIH 3T3), and human embryonic kidney cell line (HEK 293) were purchased from the American Type Culture Collection (ATCC) (Manassas, VA). The HEK 293 was cultured in Dulbecco's Modified Eagle Medium (DMEM) (Gibco-BRL, Grand Island, NY) supplemented with 10% fetal bovine serum (FBS) (Mediatech, Inc., Manassas, VA). The NIH 3T3 cells were cultured in DMEM with 10% calf serum (CS) (Mediatech, Inc., Manassas, VA). Cells were maintained in a humidified atmosphere at 37ºC and 5% CO2.

Adenovirus

Recombinant adenovirus type 5 (Ad) encoding lacZ reporter gene and lacking the E1 and E3 native genes was generated from the native adenoviral plasmid, pAdEasy-1 (Addgene plasmid 16400) and pShuttle-CMV-lacZ (Agilent, CA) [197, 198]. The virus was amplified in HEK 293 cells and purified using ion-exchange chromatography in a Vivapure Adenopack purification kit following the manufacturer’s protocol (Sartorius Stedim, CO). Ad was concentrated and stored in phosphate-buffered saline (PBS), pH 7.4. The number of virus particles (vp) was determined by measuring UV absorbance at 260 nm (1 U $\approx 10^{12}$ virus particles/ml) [198].

Fiberless Adenovirus generation

A Fiberless Ad serotype 5 plasmid (pAd5-FLAd) was generated using homologous recombination to remove the fiber gene from the native Ad plasmid (pAdEasy-1) [184]. Since the removal of the fiber severely reduced the infectivity of the virus, amplification of FlAd is required in 633 cell line that stably expresses fiber protein. Transfection of 633 cells with pAd5-FlAd produced a virus with fiber protein but lacking the fiber gene. Passaging the virus on 633 cells enriched the virus titer. The enriched virus was then used to produce FlAd through a final passage on HEK 293 cells. The virus was collected and purified using the Vivapure Adenopack purification kit following the manufacturer's protocol (Sartorius Stedim Arvada, CO). The virus was quantified by measuring the absorbance of the viral DNA at a wavelength of 260 nm (1 U ≈ 10^{12} virus particles/ml).

FlAd is unable to infect cells since it lacks the fiber protein. While generally the virus is referred to as infectious particles, it is better to think about the particles as being potentially infectious. Not all NtAd or FlAd particles, however, are infectious or potentially infectious. Mittereder et al. showed that only about 5% of adenovirus particles are infectious [199]. The other 95% of the virus particles are thought to be inactive due to harsh conditions the viral particles go through during the purification steps. An assumption made in the present study was that only 5% of FlAd is potentially infectious.

PLL-g-PEG copolymer synthesis

PLL-g-PEG was synthesized via reacting the primary amines (-NH2) on the lysine chains of PLL-HBr (Sigma, Aldrich) with the succinimidyl ester group on the mPEG-NHS (Creative PEGworks, NC). Various masses of mPEG-NHS (0.5, 2, and 5 kDa) were added to 15 mg of PLL-HBr (1–5, 4–15, 15–30, and 30–70 kDa) dissolved in 200 μL of phosphate buffered saline (PBS) to create a library of PLL-g-PEG as shown in Table 2.1. For 5%, 10% and 25% grafting ratio, (3, 10, and 14 mg), (6, 21, and 51 mg), and (14, 51, and 128 mg) of PEG 0.5, 2 and 5 kDa were added to the dissolved PLL, respectively. The mixtures were allowed to react for 2 hours

before being washed with ultrapure water in a 10 kDa centrifugal concentrator. After 3 washes, each grafted copolymer was lyophilized and stored at -20°C.

The grafting ratio of each PLL-g-PEG was determined using proton nuclear magnetic resonance spectroscopy (1H NMR). Lyophilized polymer was dissolved in D_2O, and 1H NMR spectroscopy was performed using a Bruker Avance INOVA 400 MHz spectrometer. The grafting ratio, or PEG chains per PLL chain, was determined by integrating the PLL and PEG peaks at 4.3 ppm and 3.7 ppm, respectively (Appendix I).

Formation of PLL-g-PEG-FlAd vector

PLL-g-PEG-FlAd vectors were prepared through electrostatic attraction between the positively charged copolymer and the negatively charged FlAd. PLL-g-PEG was dissolved in PBS, pH 7.4, followed by filtration through a 0.2 μm syringe filter. The required volume of the virus (according to the MOI used) was added dropwise to the copolymer to achieve a final concentration of 0.001 to 1 μg PLL-g-PEG/10^6 vp. Subsequently, the solution was mixed by gentle aspiration with the pipet tip and allowed to incubate for 10–30 min at room temperature before further use.

Transduction efficiency studies

The transduction efficiency of NtAd, FlAd, and PLL-g-PEG-FlAd vectors was studied on HEK 293 and NIH 3T3 cells. Cells were seeded for 24 hours before infection at 5×10^4 cells per well in 24 well plates. The cell culture medium was replaced with serum-free DMEM at 50% of the typical well culture volume (for example, 0.25 ml in a 24-well plate). The cells were then infected with the virus or hybrid viral vector using a MOI of 100 for HEK 293 cells and 250 for NIH 3T3 cells. Four hours later, the medium was replaced with fresh cell culture medium (containing serum), and cells were incubated for 48 hours. LacZ expression was quantified using the chemiluminescence based Beta-Glo assay (Promega Inc., Madison, WI). The reporter gene expression was measured in terms of relative light units (RLU) with a Lumat LB9507

luminometer (EG&G, Berthold, Bundoora, Australia). The gene expression was then normalized to total cellular protein determined using the bicinchoninic acid assay (BCA assay) (Pierce, Rockford, IL) to account for different cell densities at the time of reporter gene measurement.

Negative stain Transmission Electron Microscopy

For NtAd, FlAd and PLL-g-PEG-FlAd samples, each sample was placed on a copper grid and incubated for 2 minutes. Excess sample was wicked off the grid using a filter paper. A drop of 2% uranyl acetate stain was added and let sit for one minute. Excess stain was again wicked off using filter paper and the grid was dried for 15 minutes before viewing with JEOL JEM 2100 Transmission Electron Microscope.

Size and zeta potential measurements

NtAd, FlAd and PLL-g-PEG-FlAd samples were prepared as described above and diluted to a concentration of 10^6 vp/ml and the effective hydrodynamic diameter was measured using a ZetaPALS particle size analyzer (Brookhaven Instrument, Inc., Holtsville, NY). The measurements were performed in triplicate with 10 repeated measurements at 10-second intervals for each sample. Zeta potential was also measured for vectors diluted to a concentration of 10^9 vp/ml and measured in triplicate with 10 repeated measurements per sample.

Statistical analysis Design of Experiment (DOE)

D-optimal experimental design, one of the response surface model (RSM) design tools, was used to evaluate the effect of the independent variables on the transduction efficiency (TE) of PLL-g-PEG-FlAd vectors in CAR-positive (HEK 293) and CAR-negative (NIH 3T3) cells. The independent variables (factors) were the ratio of PLL-g-PEG to FlAd, degree of PEGylation, molecular weight (Mwt) of PLL and PEG, which were indicated by (a), (b), (c), and (d) respectively. Two dependent variables (responses) were the transduction efficiency (TE) of PLL-g-PEG-FlAd vectors in CAR-positive (HEK 293) and CAR-negative (NIH 3T3) cells. Table 2.2 summarizes all the factors and responses with their ranges. The range of the factors was chosen in accordance with the results of screening preparatory experiments.

A total number of 37 experimental runs with three replications of the central point were suggested by the software, as shown in Table 2.3. The experimental runs and data analysis were performed using Design Expert® v. 12 (Design Expert® Software, MN) to generate three-dimension (3D) surface plots for each response.

Check points analysis and model validation

Check point analysis was carried out to establish the model prediction performance. Three check points were chosen around the optimal area of the design space. Actual values were obtained from lab experiments that were performed in triplicates. Predicted values were obtained from the point prediction of the Design Expert® v.12 software. Predicted and actual values were compared to determine the percentage bias between the experimental values and the behavior described by the model. The percentage bias was calculated from the following equation [200]:

$$\text{Bias \%} = \frac{Predicted\ value - Actual\ value}{Actual\ value} \times 100$$

2.3 RESULTS

PLL-g-PEG-FlAd vector formation

PEG grafted PLL copolymer was synthesized by conjugating NHS-activated mPEG to ε-amine groups on the PLL, as shown in Figure 2.1. In this study, a library of PLL-g- PEG copolymers was synthesized with different molecular weights of PLL (1–5, 4–15, 15–30, and 30–70 kDa), PEG (0.5, 2, and 5 kDa) and different degrees of PEGylation (DOP) (5, 10, and 25%) as listed in Table 2.1. The degree of PEGylation on the PLL backbone was calculated from 1H NMR spectra analysis (data not shown), based on the relative integration ratio of a single –CH2– proton peak in PEG (s, 3.7–3.8 ppm) and multiple –CH– proton peaks in PLL (m, 4.3–4.4 ppm).

Figure 2.1: Structure of PLL-g-PEG grafted copolymer synthesized by interaction of PLL-HBr (Poly-l-lysine hydrobromide) and mPEG-NHS (methoxy-PEG-N-hydroxysuccinimide).

Table 2.1: Composition of synthesized PLL-g-PEG copolymers.

PLL Mwt (kDa)	*Degree of PEGylation (DOP)*	*PEG Mwt (kDa)*		
		0.5	***2***	***5***
1–5	***5%***	$PLL_{1\text{-}5}\text{-}g_{5\%}\text{-}PEG_{0.5}$	$PLL_{1\text{-}5}\text{-}g_{5\%}\text{-}PEG_{2}$	$PLL_{1\text{-}5}\text{-}g_{5\%}\text{-}PEG_{5}$
	10%	$PLL_{1\text{-}5}\text{-}g_{10\%}\text{-}PEG_{0.5}$	$PLL_{1\text{-}5}\text{-}g_{10\%}\text{-}PEG_{2}$	$PLL_{1\text{-}5}\text{-}g_{10\%}\text{-}PEG_{5}$
	25%	$PLL_{1\text{-}5}\text{-}g_{25\%}\text{-}PEG_{0.5}$	$PLL_{1\text{-}5}\text{-}g_{25\%}\text{-}PEG_{2}$	$PLL_{1\text{-}5}\text{-}g_{25\%}\text{-}PEG_{5}$
4–15	***5%***	$PLL_{4\text{-}5}\text{-}g_{5\%}\text{-}PEG_{0.5}$	$PLL_{4\text{-}5}\text{-}g_{5\%}\text{-}PEG_{2}$	$PLL_{4\text{-}5}\text{-}g_{5\%}\text{-}PEG_{5}$
	10%	$PLL_{4\text{-}5}\text{-}g_{10\%}\text{-}PEG_{0.5}$	$PLL_{4\text{-}5}\text{-}g_{10\%}\text{-}PEG_{2}$	$PLL_{4\text{-}5}\text{-}g_{10\%}\text{-}PEG_{5}$
	25%	$PLL_{4\text{-}5}\text{-}g_{25\%}\text{-}PEG_{0.5}$	$PLL_{4\text{-}5}\text{-}g_{25\%}\text{-}PEG_{2}$	$PLL_{4\text{-}5}\text{-}g_{25\%}\text{-}PEG_{5}$
15–30	***5%***	$PLL_{15\text{-}30}\text{-}g_{5\%}\text{-}PEG_{0.5}$	$PLL_{15\text{-}30}\text{-}g_{5\%}\text{-}PEG_{2}$	$PLL_{15\text{-}30}\text{-}g_{5\%}\text{-}PEG_{5}$
	10%	$PLL_{15\text{-}30}\text{-}g_{10\%}\text{-}PEG_{0.5}$	$PLL_{15\text{-}30}\text{-}g_{10\%}\text{-}PEG_{2}$	$PLL_{15\text{-}30}\text{-}g_{10\%}\text{-}PEG_{5}$
	25%	$PLL_{15\text{-}30}\text{-}g_{25\%}\text{-}PEG_{0.5}$	$PLL_{15\text{-}30}\text{-}g_{25\%}\text{-}PEG_{2}$	$PLL_{15\text{-}30}\text{-}g_{25\%}\text{-}PEG_{5}$
30–70	***5%***	$PLL_{30\text{-}70}\text{-}g_{5\%}\text{-}PEG_{0.5}$	$PLL_{30\text{-}70}\text{-}g_{5\%}\text{-}PEG_{2}$	$PLL_{30\text{-}70}\text{-}g_{5\%}\text{-}PEG_{5}$
	10%	$PLL_{30\text{-}70}\text{-}g_{10\%}\text{-}PEG_{0.5}$	$PLL_{30\text{-}70}\text{-}g_{10\%}\text{-}PEG_{2}$	$PLL_{30\text{-}70}\text{-}g_{10\%}\text{-}PEG_{5}$
	25%	$PLL_{30\text{-}70}\text{-}g_{25\%}\text{-}PEG_{0.5}$	$PLL_{30\text{-}70}\text{-}g_{25\%}\text{-}PEG_{2}$	$PLL_{30\text{-}70}\text{-}g_{25\%}\text{-}PEG_{5}$

PLL-g-PEG-FlAd vectors were formed via the electrostatic interaction between the positively charged cationic PLL-g-PEG copolymer and the negatively charged Ad surface as shown in Figure 2.2.

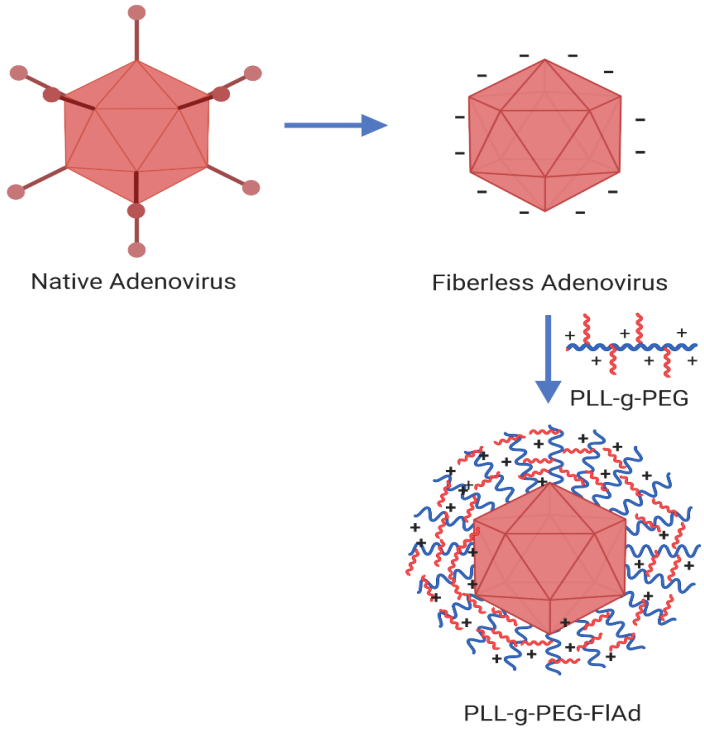

Figure 2.3: Schematic representation of FlAd coated with PLL-g-PEG, step 1: Formation of Fibereless Ad by genetic truncation of fiber proteins, step 2: Electrostatic attraction between negatively charged FlAd surface and positively charged PLL-g-PEG copolymer.

Transmission Electron Microscopy (TEM)

TEM was used to characterize the morphologies of PLL-g-PEG-FlAd vectors compared to FlAd (Figure 2.3). Photomicrographs of FlAd showed the hexon structure and the icosahedral shape of the viral particle compared to the roughly surface coated particles for PLL-g-PEG-FlAd vectors.

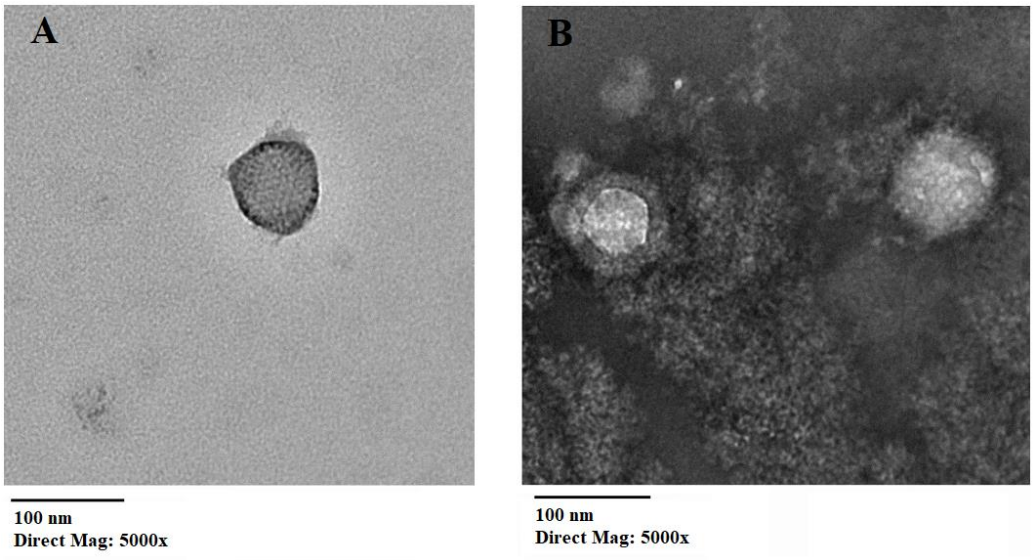

Figure 2.3: (A) Negative Stain TEM of FlAd alone, scale bar =100 nm. (B) Negative Stain Transmission Electron Microscopy of $PLL_{4\text{-}5}\text{-}g_{5\%}\text{-}PEG_5$ hybrid vector.

Transduction efficiency of PLL-g-PEG-FlAd

Transduction is a process by which DNA is introduced into a cell by a virus or a viral vector. FlAd had a packaging sequence encoding a reporter lac-Z gene. The efficiency of the virus in infecting the cells is measured by the level of the reporter gene expression which is called transduction efficiency (TE). Transduction efficiency of the PLL-g-PEG-FlAd vectors was compared to that of NtAd and FlAd in CAR-positive (HEK 293) and CAR-negative (NIH 3T3) cells. Several factors affected the transduction efficiency of hybrid vectors including multiplicity of infection (MOI), PLL Mwt, PEG Mwt, degree of PEGylation, and ratio of PLL-g-PEG to FlAd. Each factor was tested one at a time to determine the suitable levels that would lead to the best gene delivery.

Multiplicity of infection (MOI) effect on transduction efficiency by PLL-g-PEG-FlAd

The amount of virus particles added per cells for infection, the multiplicity of infection (MOI), is a critical factor in controlling TE. In order to optimize the transduction of PLL-g-PEG-FlAd vectors, we studied the effect of varying the MOI of hybrid vectors on HEK 293 and NIH 3T3 cells. The MOI was varied from 50 to 1000 virus particles per cells and the relative

increment in gene expression of the particles over FlAd was studied (Figure 2.4). In HEK 293 cells, the transduction efficiency of the hybrid vector increased with the increase in MOI, then transduction efficiency declined at 500 and 1000 (X-gal stained cells also confirmed the results, data not shown). In NIH 3T3, FlAd were not able to transduce the cells at sufficient levels at all MOIs, while hybrid vectors transduced the cells at MOI ≥ 250. PLL-g-PEG-FlAd vectors showed the maximum transduction efficiency in HEK 293 and NIH 3T3 cells at MOI of 100 and 250, respectively. These MOI values were selected to be used in further studies.

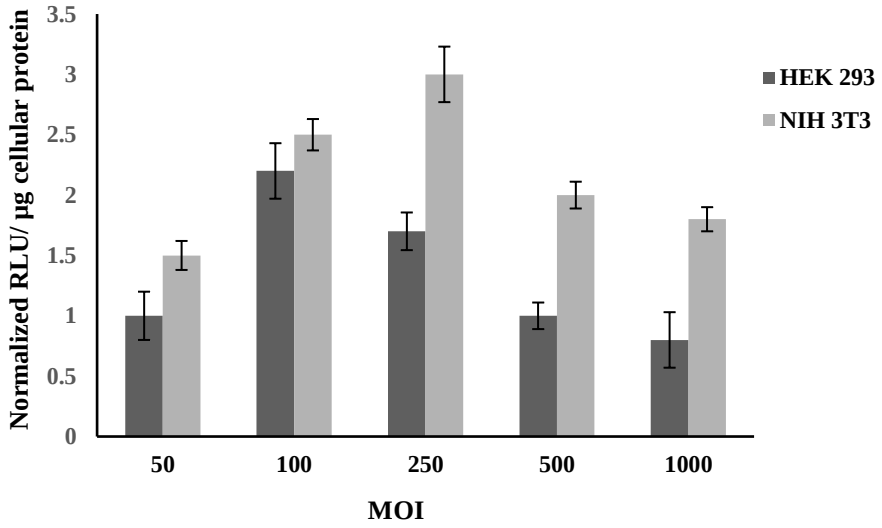

Figure 2.3: Effect of MOI on transduction efficiency of $PLL_{4\text{-}5}\text{-}g_{25\%}\text{-}PEG_5$ particles in HEK 293 and NIH 3T3 cells. The PLL-g-PEG-FlAd particles were formed at a ratio of 0.001 PLL-g-PEG µg/10^6 vp. The data points represent the mean ± standard deviation (n=3).

PLL molecular weight effect on transduction efficiency by PLL-g-PEG-FlAd

A wide range of PLL molecular weights (Mwts) from 1 to 70 kDa was tested to prepare PLL-g-PEG-FlAd vectors as shown in Figure 2.5. The transduction efficiency of the formed hybrid vectors decreased at PLL Mwt > 15-30 kDa. PLL of high Mwt (70 – 150 kDa) was excluded from further studies as the formed hybrid vectors did not transduce neither HEK 293 nor NIH 3T3 cells.

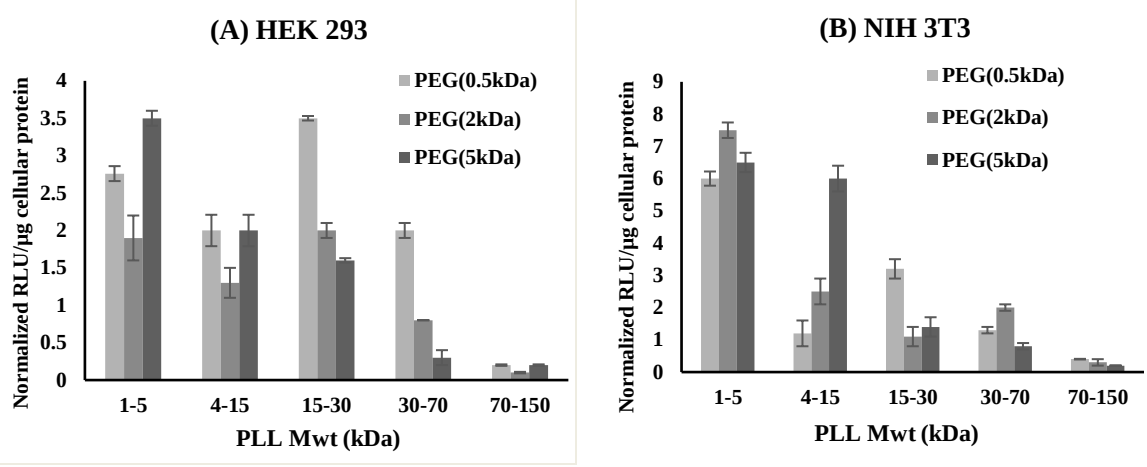

Figure 2.3: Effect of PLL molecular weight on transduction efficiency of PLL-g-PEG-FlAd particles in (A) HEK 293 and (B) NIH 3T3 cells. The PLL-g-PEG-FlAd particles were formed with PLL molecular weights of 1–5, 4–15, 15–30, 30–70, and 70–150 kDa. The molecular weight of PEG was held constant at 5 kDa PEG and 25% DOP and amount of PLL-g-PEG/ FlAd equal to 1 µg/10^6 vp. The data points represent the mean ± standard deviation (n=3).

PEG molecular weight effect on transduction efficiency by PLL-g-PEG-FlAd

Different molecular weights of PEG (0.5, 2 ,5, and 10) were used to prepare PLL-g-PEG-FlAd and the effect of variation of PEG Mwt on the transduction efficiency of hybrid vectors was also studied. High Mwt PEG (10 kDa) resulted in very poor transduction efficiency compared to other Mwts of PEG (Figure 2.6). This led us to exclude 10 kDa PEG from further studies.

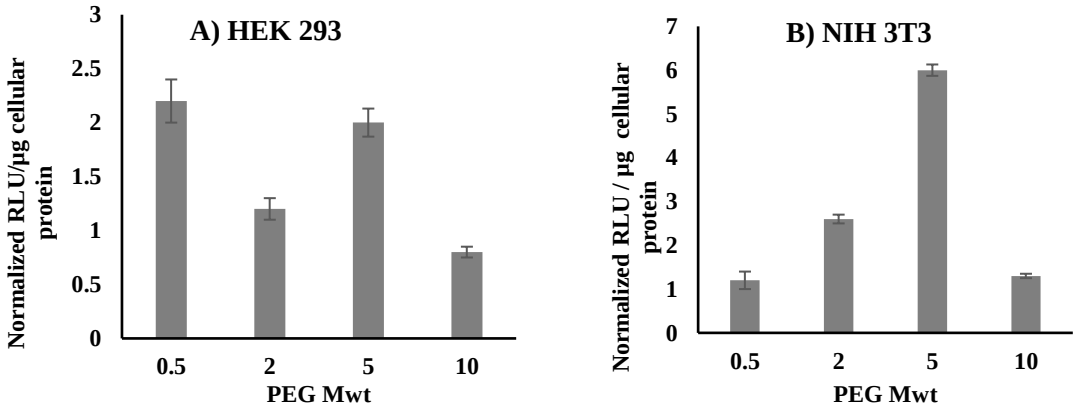

Figure 2.6: Effect of PEG molecular weight on transduction efficiency of PLL-g-PEG-FlAd particles in (A) HEK 293 and (B) NIH 3T3 cells. The PLL-g-PEG-FlAd particles were formed with PEG molecular weights of 0.5, 2, 5, and 10 kDa. The molecular weight of PLL was held constant at 4–15 kDa and DOP 25% and amount of PLL-g-PEG/ FlAd =1µg/10^6 vp. The data points represent the mean ± standard deviation (n=3).

Degree of PEGylation (DOP) effect on transduction efficiency by PLL-g-PEG-FlAd

The effect of different degrees of PEGylation (5, 10, 25, 30, and 40%) on the transduction efficiency of the prepared hybrid vectors is shown in Figure 2.7. The optimum range of DOP was 5–25%, while increasing the DOP to 30% and 40% led to a reduction in the transduction efficiency of hybrid vectors. Further experiments were conducted using PLL-g-PEG at DOP: 5, 10, and 25%.

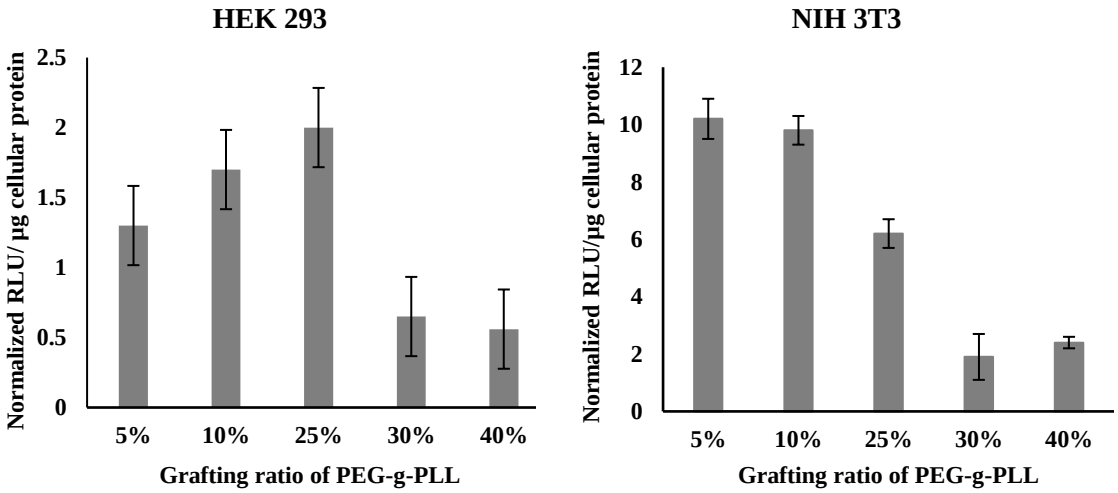

Figure 2.3: Effect of degree of PEGylation on transduction efficiency of PLL-g-PEG-FlAd particles in (A) CAR+ HEK-293 and (B) CAR– NIH 3T3 cells. The PLL-g-PEG-FlAd particles were formed with degree of PEGylations of 5, 10, 25, 30, and 40%. The molecular weight of PLL was held constant at 4–15 kDa and 5 kDa PEG and amount of PLL-g-PEG/ FlAd =1 µg/10^6 vp.

PLL-g-PEG/FlAd ratio effect on transduction efficiency by PLL-g-PEG-FlAd

A range of ratios of PLL-g-PEG to FlAd from 0.00001 to 10 µg PLL-g-PEG /10^6 vp was used to study their effect on the transduction efficiency. The hybrid vector ability in delivering genes started to increase at 0.001 PLL-g-PEG µg/10^6 vp. Afterwards, transduction efficiency decreased at concentrations higher than 1 µg /10^6 vp (Figure 2.8). The range of 0.001 to 1 PLL-g-PEG µg /10^6 vp was chosen to be used for next studies.

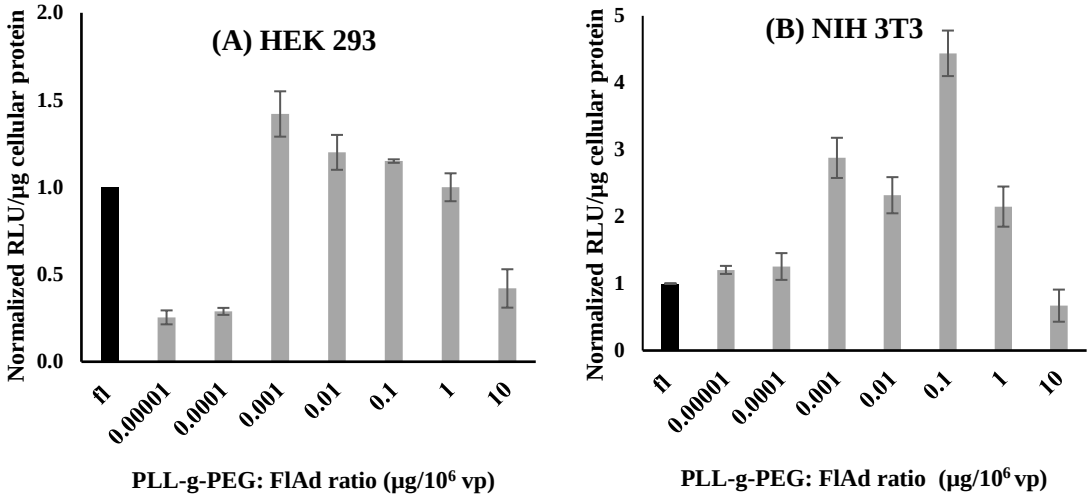

Figure 2.3: Effect of ratio of PLL-g-PEG/10^6 vp on transduction efficiency of PLL-g-PEG-FlAd particles in (A) CAR+ HEK 293 and (B) CAR– NIH 3T3 cells. The PLL-g-PEG-FlAd particles were formed with PLL 4–15 kDa, PEG 5 kDa and degree of PEGylation of 25%. The data points represent the mean ± standard deviation (n=3).

Particle size and zeta potential of PLL-g-PEG-FlAd

The particle size of NtAd, FlAd, and PLL-g-PEG-FlAd vectors were measured. The mean particle size of NtAd and FlAd, was 108 ±2.2 nm and 115 ±3.4 nm, respectively. Upon complexing FlAd with PLL-g-PEG, the particle size of the formed hybrid vector increased. The particle size of hybrid vectors varied according to the formulation parameters including PLL Mwt, DOP, and amount of PLL-g-PEG/ FlAd (Figure 2.9).

The particle size of hybrid vectors is directly proportional to the Mwt of the PLL used in the preparation of the vector. As PLL Mwt increased from 1–5 to 30–70 kDa, the particle size of the formed hybrid vectors increased from 259 to 570 nm at a concentration of 0.001 µg/10^6 vp, respectively. However, the particle size of hybrid vectors prepared with PLL (70 –150 kDa) exceeded 1 µm and this Mwt was excluded from further studies. Using higher concentrations of PLL-g-PEG/FLAd also led to the formation of larger sized particles. For example, hybrid vectors prepared with PLL-g-PEG at 0.001µg/10^6 vp had a particle size range of 270 to 984 nm which increased to 270 nm to >1 µm on increasing the ratio of PLL-g-PEG/FlAd to 1µg/10^6 vp.

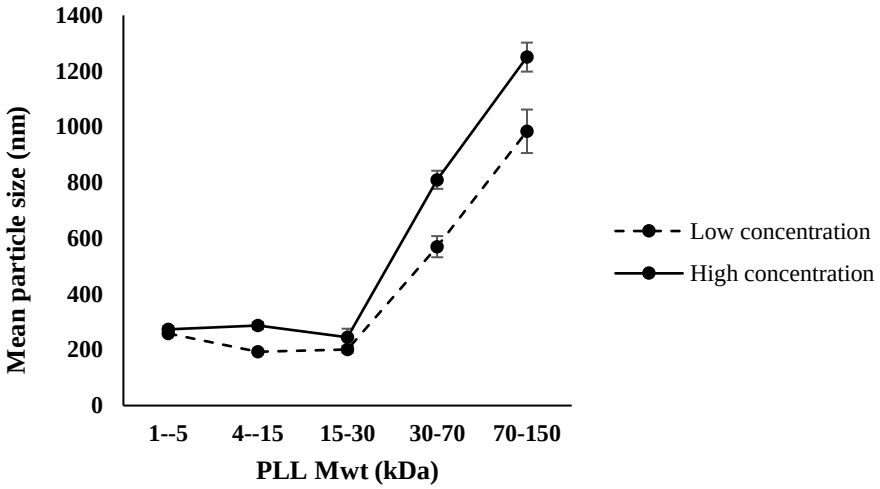

Figure 2.3: Mean particle size of PLL-g-PEG-FlAd formed with different PLL molecular weights of 1–5, 4–15, 15–30, 30–70, and 70–150 kDa, and 5kDa PEG at 25% DOP, at two concentrations: a) Low concentration = 0.001µg PLL-g-PEG /10^6 vp, b) High concentration = 1µg PLL-g-PEG /10^6 vp. Errors are standard deviations (n=3; 10 readings for every sample). The size of FlAd without addition of copolymers was 115 ± 3.4 nm.

The particle size of the formed hybrid vectors also changed as a function of degree of PEGylation of the copolymer used. As shown in Figure 2.10, the particle size of the vectors increased as the DOP increased. The particle size of the vectors was in the range of 139–259 nm when prepared with PLL-g-PEG at 5–25%. However, the particle size increased to a range of 260 – 335 nm at 30–40% DOP according to the PLL used. Therefore, further studies were conducted using 5 – 25% DOP.

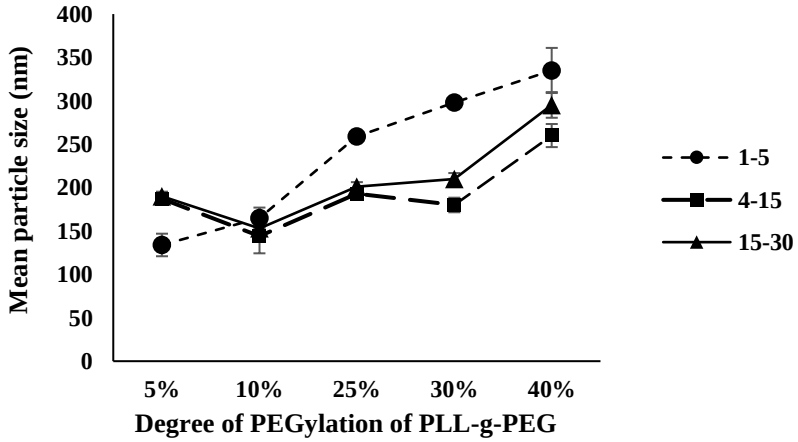

Figure 2.3: Effect of degree of PEGylation on mean particle size of PLL-g-PEG-FlAd particles. The particles were formed with PEG 5 kDa and amount of PLL-g-PEG/ FlAd equal to 0.001 µg/10^6 vp.

The zeta potential of NtAd, FlAd, and PLL-g-PEG-FlAd was also measured. NtAd and FlAd had a negative charge of -21.3 ± 0.5 and -17.7 ±1.5 mV, respectively. Upon complexing FlAd with PLL-g-PEG, the zeta potential showed a significantly higher positive charge with a range of +1.74 to +17.3 mV (Figure 2.11). The zeta potential was studied as a function of PLL Mwt, DOP, and concentration of PLL-g-PEG/FlAd as well. Both the increase in the Mwt of PLL and the concentration of PLL-g-PEG/FlAd resulted in an increase in the positive surface charge of hybrid vectors formed. For example, PLL-g-PEG-FlAd prepared with PLL (15–30 kDa) at 1 μg/10^6 vp showed the highest zeta potential with values of +17.3 and +9.5 mV at 5% and 25% DOP, respectively. The zeta potential of the formed hybrid vectors decreased upon increasing the DOP which can be correlated to the increase in the particle size of the hybrid vector as well.

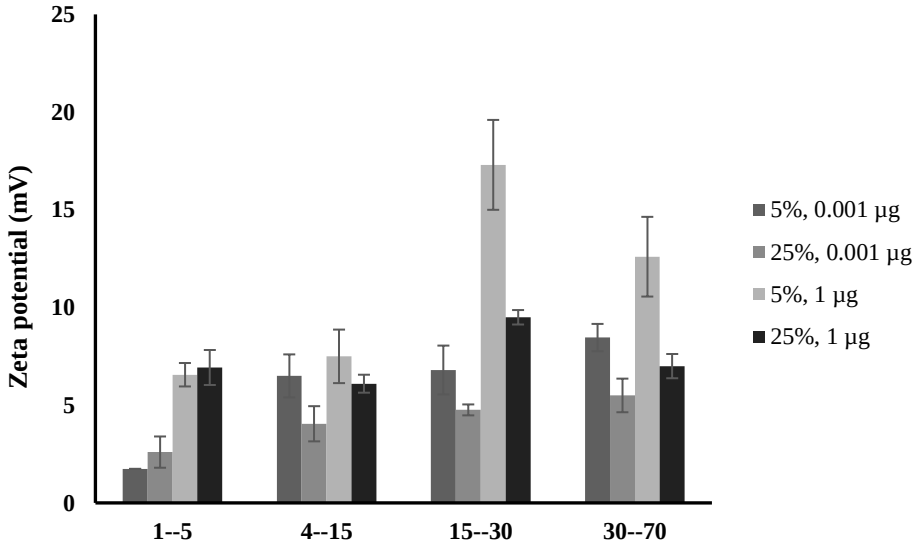

Figure 2.3: Zeta-potential of PLL-g-PEG-FlAd prepared with different PLL Mwt, PEG 5 kDa at DOP 5% and 25% and at concentration 0.001 and 1 µg PLL-g-PEG /10^6 vp.

Optimization of transduction efficiency of PLL-g-PEG-FlAd in CAR-Positive And CAR-Negative Cells Using Design Of Experiment (DOE):

The transduction efficiency of PLL-g-PEG-FlAd in CAR-positive and CAR-negative cells varied as a factor of PLL and PEG Mwt, degree of PEGylation (DOP) and ratio of PLL-g-PEG/FlAd. Hence, an optimization statistical model was required to achieve the maximum response (TE) in each cell type. Table 2.2 summarizes all the factors and responses with their ranges which were chosen in accordance with the results of preparatory experiments. A total number of 37 experimental runs were suggested by the software and are shown in Table 2.3. In CAR-positive (HEK 293) cells, the transduction efficiency of PLL-g-PEG-FlAd vectors varied from 0.1 to 3.5 folds compared to FlAd according to formulation parameters. In contrast, the transduction efficiency of PLL-g-PEG-FlAd vectors varied from 0.1 to 10.2 folds compared to FlAd in CAR-negative (NIH 3T3) cells according to formulation parameters.

Table 2.3: Factors and responses with their ranges.

Factor	***Name***	***Unit***	***Type***	***Range***		***Levels***
				Low	***High***	
A	PEG-g-PLL/Fl	µg/10^6vp	Numeric	0.0010	1.0000	
B	Degree of PEGylation (DOP)	%	Numeric	5%	25%	
C	PLL Mwt	kDa	Categoric	1–5	30–70	4
D	PEG Mwt	kDa	Categoric	0.5	5	3
Responses				***Minimum***	***Maximum***	
TE* in HEK 293				0.1	3.5	
TE* in NIH 3T3				0.35	10.2	

*TE: Transduction efficiency

Table 2.3: 37 experimental runs with three replications of the central point (n=3).

	Factor 1	*Factor 2*	*Factor 3*	*Factor 4*	*Response 1*	*Response 2*
Run	***A: PLL-PEG:Fl***	***B: PEG%***	***C: PLL***	***D: PEG***	***Transduction efficiency in HEK 293 cells***	***Transduction efficiency in NIH 3T3 cells***
1	0.001	5	15-30	5	0.14	4.2
2	0.001	25	4-15	5	1.3	2.9
3	1	25	4-15	0.5	2.2	1.2
4	0.001	25	1-5	5	0.8	1.1
5	1	5	15-30	2	0.12	0.8
6	1	5	4-15	5	1.2	10.2
7	0.1	10	4-15	2	1.2	2
8	1	25	15-30	0.5	3.5	3.6
9	0.001	5	1-5	2	0.4	0.35
10	1	10	15-30	5	0.61	2.5
11	1	25	15-30	0.5	3.5	3.4
12	0.1	5	30-70	5	0.8	0.95
13	0.001	10	15-30	2	1.6	1.4
14	0.001	25	1-5	0.5	0.5	0.7
15	1	5	4-15	2	0.4	3.3
16	1	5	30-70	0.5	0.1	0.89
17	0.1	25	30-70	2	0.12	0.92
18	0.1	10	1-5	5	1.5	1.8
19	0.001	5	30-70	2	1.2	1.2
20	1	5	30-70	5	0.1	0.65
21	0.001	5	15-30	5	0.14	4.2
22	0.001	5	4-15	0.5	0.2	1.6
23	1	10	30-70	2	0.2	1.6
24	0.1	25	15-30	5	0.7	1.2
25	1	10	1-5	0.5	1.4	4.3
26	1	25	30-70	5	0.3	0.61
27	0.001	5	4-15	0.5	0.2	2.3
28	1	5	1-5	5	3.2	3.9
29	1	25	1-5	2	1.9	8
30	1	25	4-15	0.5	2.2	1.2
31	0.001	25	30-70	5	0.1	0.4
32	0.01	10	30-70	0.5	2	1.6
33	1	5	1-5	2	1.1	2.5
34	0.001	25	15-30	2	2.1	2.1
35	1	25	4-15	2	1.2	2.5
36	0.1	5	15-30	0.5	0.5	5.6
37	0.1	5	15-30	0.5	0.1	5.5

The transduction efficiencies in CAR-positive (HEK 293) and CAR-negative (NIH 3T3) cell results were fitted to the quadratic model generated by the D-optimal design. The adequacy of each model was verified using ANOVA test. The P-values for the model was <0.0001. Table 2.4 shows a summary of the multiple regression analysis of the two generated quadratic models.

Table 2.3: Summary of the results of the regression analysis for the D-optimal design after fitting to the quadratic model.

Parameter	***Response 1:*** ***TE* in HEK-293 cells***	***Response 2:*** ***TE* in NIH-3T3 cells***
Significance	< 0.0001	< 0.0001
R-squared	0.9943	0.9950
Adjusted R-squared	0.9795	0.9807
Predicted R-squared	0.8929	0.7996
Adequate precision	28.5	35.7

*TE: Transduction efficiency

In CAR-positive model and according to the P-value of the coefficient estimate, the DOP and Mwt of PLL are highly significant in the model (P-value<0.0001), whereas the Mwt of PEG is less significant (P-value <0.001). The ratio of PLL-g-PEG/FlAd shows no significance effect in this model.

The transduction efficiency can be expressed as a function of ratio of PLL-g-PEG/FlAd (A), Degree of PEGylation (B), PLL Mwt (C), and PEG Mwt (D), levels of each factor are annotated as [1], [2] or [3] as shown in Equation (1):

Transduction efficiency in HEK 293 cells = +0.8080 +0.1000 A +0.4655 B +0.1619 C[1] +0.0391C[2] +0.1477 C[3] +0.1448 D[1] -0.2349 D[2] +0.2710 AB +0.7956 AC[1] -0.1474 AC[2] -0.1879 AC[3] -0.0399 AD[1] -0.1442 AD[2] -0.1879 BC[1] +0.0099 BC[2] +0.5202 BC[3] +0.5904 BD[1] -0.2538 BD[2] -0.6418 C[1]D[1] -0.3621 C[2]D[1] +0.4003 C[3]D[1] -0.2337 C[1]D[2] +0.0775 C[2]D[2] +0.3241 C[3]D[2] +0.7367 A^2 -0.4375 B^2…….Eq (1)

In CAR-negative model and according to the P-value of the coefficient estimate, the PLL-g-PEG/FlAd ratio, the Mwt of PLL, and the Mwt of PEG are highly significant in the model (P-value <0.0001), whereas the DOP is less significant (P-value <0.001).

The transduction efficiency can be expressed as a function of ratio of PLL-g-PEG to FlAd (A), Degree of PEGylation (B), PLL Mwt (C), and PEG Mwt (D), levels of each factor are annotated as [1], [2] or [3] which has been shown in Equation (2):

Sqrt(Transduction efficiency in NIH 3T3 cells)= +1.48 +0.2275 A-0.0943 B+0.1189 C[1] +0.2630 C[2] +0.0536 C[3] -0.0382 D[1] -0.1844 D[2] +0.1535 AB+0.4180 AC[1] +0.0614 AC[2] -0.2796 AC [3]+ 0.0058AD[1] +0.0570AD[2] +0.3561BC[1] -0.3160BC[2] -0.1095BC[3] -0.0393BD[1] +0.1448BD[2] -0.0782C[1]D[1] -0.5570C[2]D[1] +0.5755C[3]D[1] +0.1610C[1]D[2] -0.1374C[2]D[2] -0.3482C[3]D[2] +0.1855A^2-0.2407B^2 …….. Eq (2)

Figure 2.12 and Figure 2.13 demonstrate the 3D plots of D-optimal model in CAR-positive (HEK 293) cells and CAR-negative (NIH 3T3) cells. In HEK 293 model, the interaction between the ratio of PLL-g-PEG/FlAd and PLL Mwt (AC), and between PLL Mwt and PEG Mwt (CD) were significant with 15% and 19% contribution of the overall factors ($P<0.0001$). In NIH 3T3 model, the interaction between the ratio of PLL-g-PEG/FlAd and PLL Mwt (AC), and between PLL Mwt and PEG Mwt (CD) were significant with 30% and 12% contribution of the overall factors ($P<0.0001$). From the model plots, it can be inferred that there is an inverse relationship between the Mwt of PLL and the transduction efficiency in both cells at some concentrations and PEG Mwts. For example, hybrid vectors prepared with 30-70 kDa showed less than one-fold increase in transduction efficiency compared to those prepared with 1-5 kDa and 4-15 kDa vectors that showed 3.5- and 2-fold increase in transduction efficiency at 5 kDa PEG, 5% and 1 µg PLL-g-PEG/ 10^6 FlAd in HEK 293 cells. In NIH 3T3 cells, hybrid vectors prepared with 30-70 kDa showed less than one-fold increase in transduction efficiency compared to those prepared with 1-5 kDa and 4-15 kDa vectors that showed 4- and 10.2-fold increase in transduction efficiency at 5 kDa PEG, 5% and 1 µg PLL-g-PEG/ 10^6 FlAd.

HEK 293	D= 0.5 kDa	D= 2 kDa	D= 5 kDa
0.1 3.5 X1 = B X2 = A **Actual Factors** C = 1-5	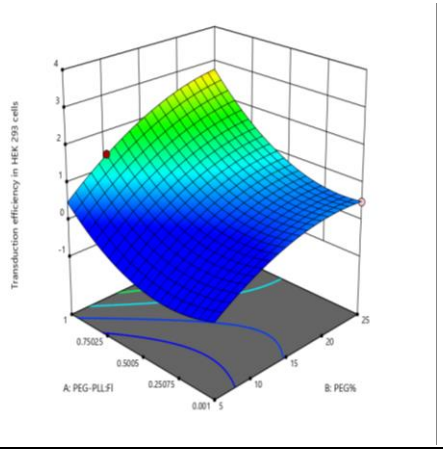	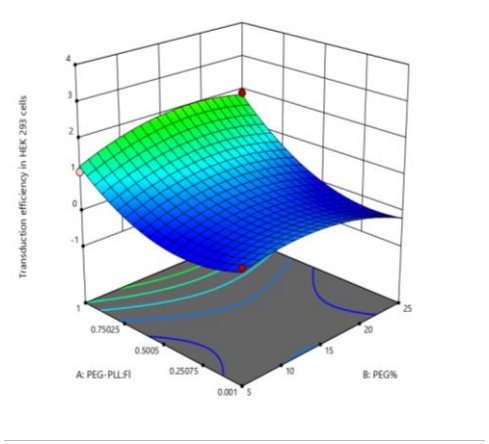	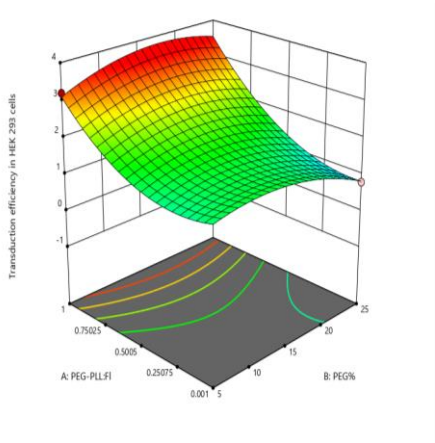
0.1 3.5 X1 = B X2 = A **Actual Factors** C = 4-15	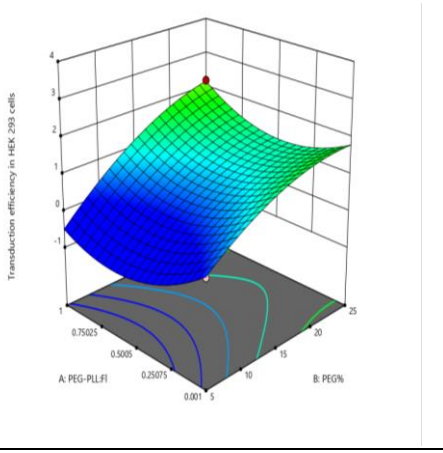	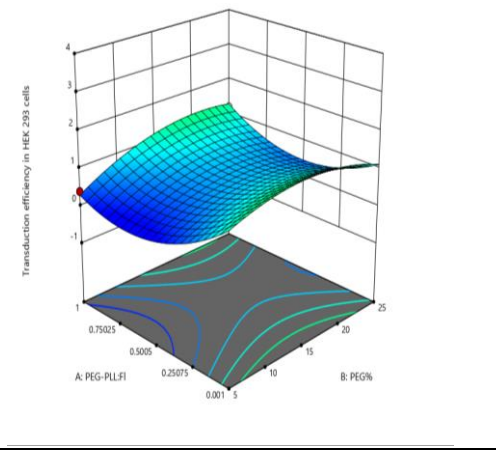	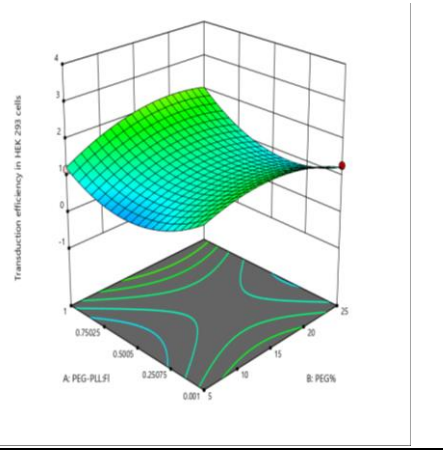

Figure 2.3: Three-dimensional surface plot of transduction efficiency in CAR-positive (HEK 293) cells.

HEK 293	D= 0.5 kDa	D= 2 kDa	D= 5 kDa
0.1 3.5 X1 = B X2 = A **Actual Factors** C = 15-30	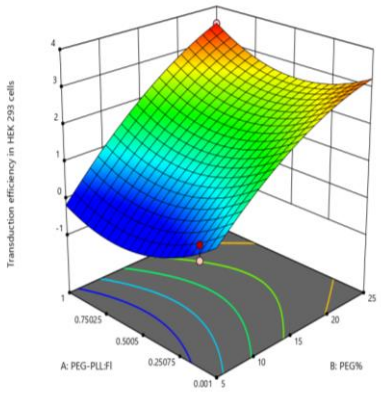	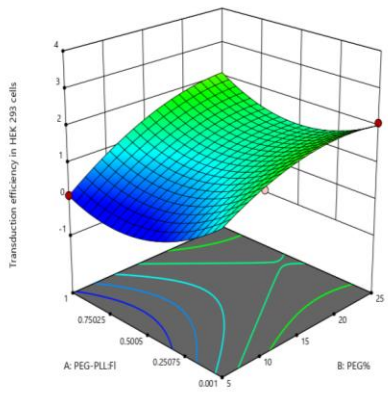	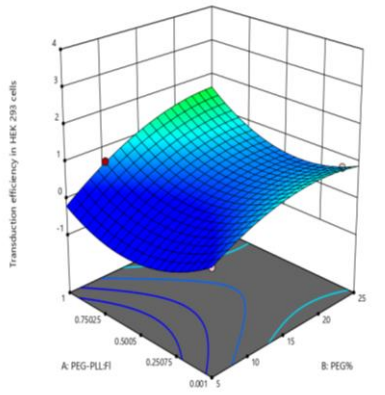
0.1 3.5 X1 = B X2 = A **Actual Factors** C = 30-70	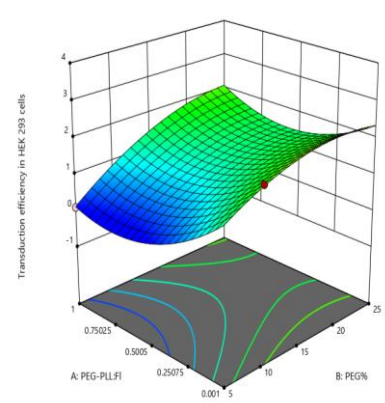	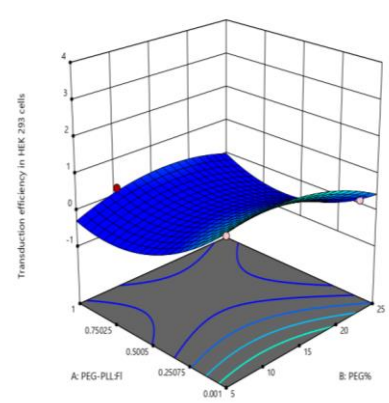	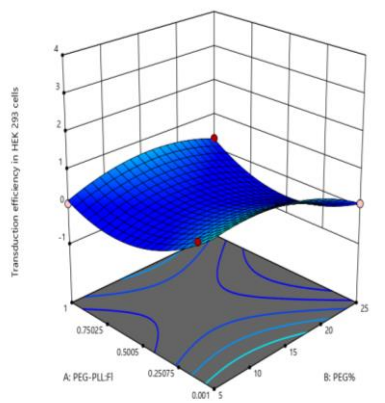

Figure 2.3: Continued.

NIH 3T3	D= 0.5 kDa	D= 2 kDa	D= 5 kDa
0.35 10.2 X1 = A X2 = B **Actual Factors** C = 1-5	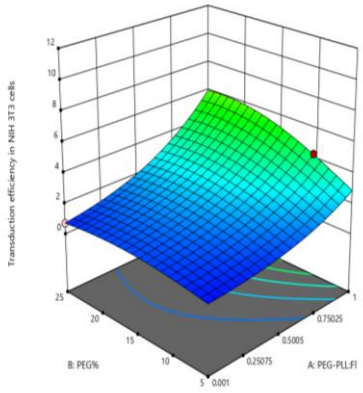	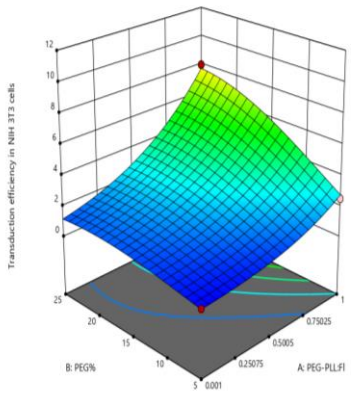	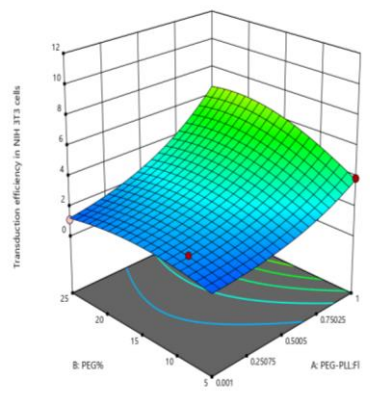
0.35 10.2 X1 = A X2 = B **Actual Factors** C = 4-15	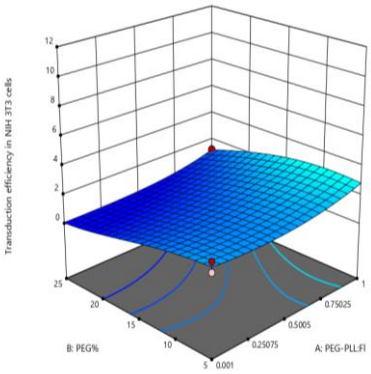	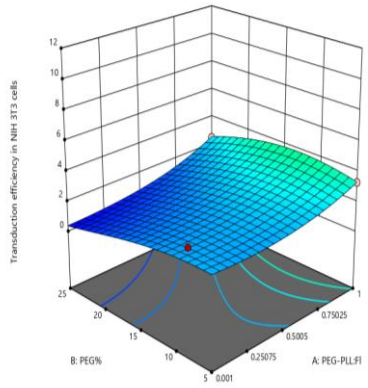	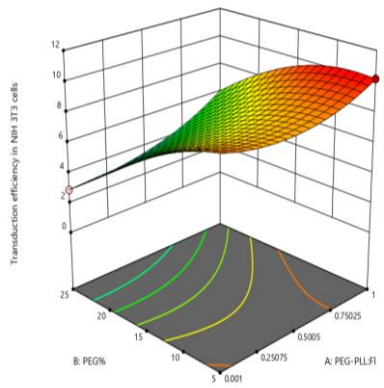

Figure 2.33: Three-dimensional surface plot of transduction efficiency in CAR-negative (NIH 3T3) cells.

NIH 3T3	D= 0.5 kDa	D= 2 kDa	D= 5 kDa
0.35 10.2 X1 = A X2 = B **Actual Factors** C = 15-30	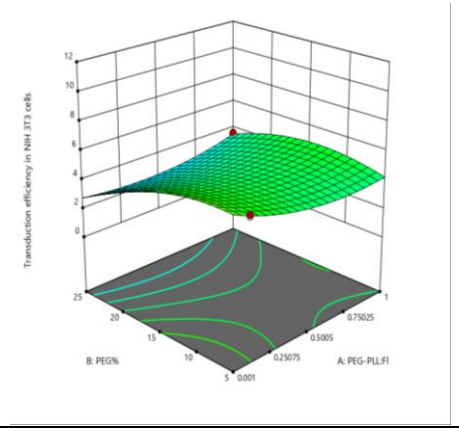	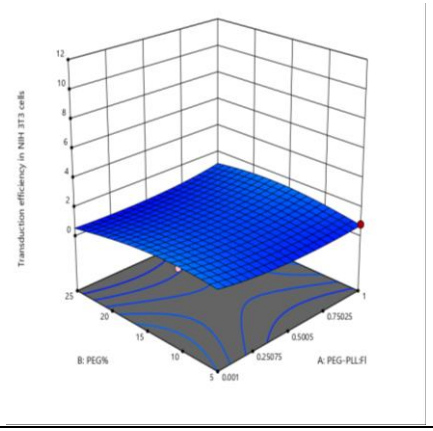	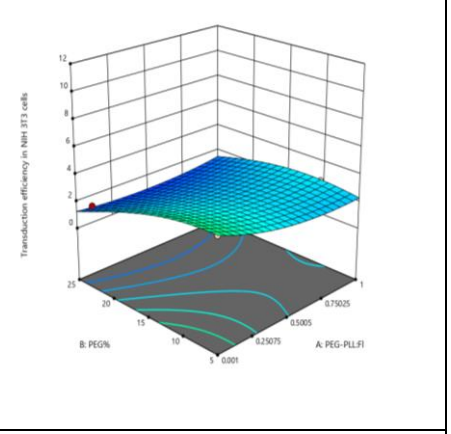
0.35 10.2 X1 = A X2 = B **Actual Factors** C = 30-70	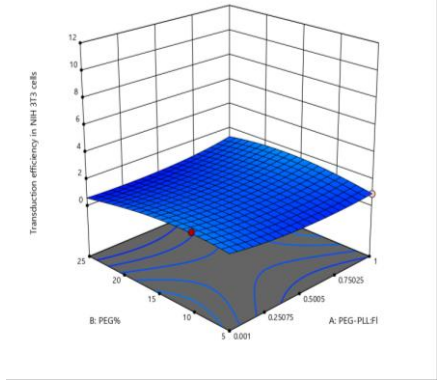	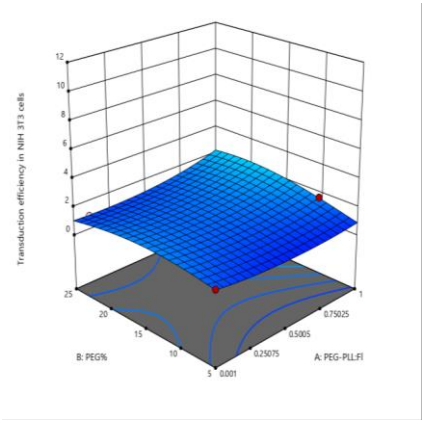	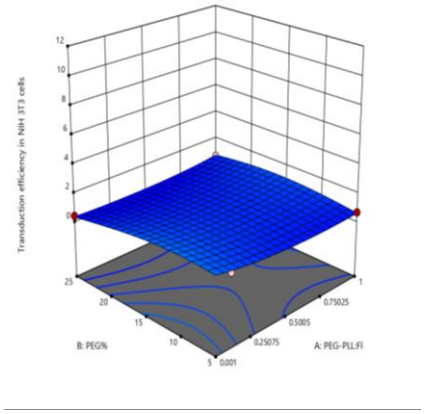

Figure 2.33: Continued.

Model validation and optimization

Model optimization

To obtain the optimized factors and levels required for maximum transduction efficiency in either cell line, the optimum point (goal) was set to maximum response. Figures 2.14 (A) and (B) show the desirability values for the various conditions in HEK 293 and NIH 3T3 cells, respectively. Based on HEK 293 model prediction, the optimum point will occur in PLL Mwt: 15–30 kDa, PEG Mwt: 0.5 kDa, degree of PEGylation: 25%, and PLL-g-PEG/ FlAd: 1 µg/10^6 vp, which will be designated $PLL_{15\text{-}30}\text{-}g_{0.5}\text{-}PEG_{25\%}$ (S_1) for further use in our study. Based on NIH 3T3 model prediction, the optimum point will occur in PLL Mwt: 4–15 kDa, PEG Mwt: 5 kDa, degree of PEGylation: 5%, and PLL-g-PEG/ FlAd: 1 µg/10^6 vp, which will be designated $PLL_{4\text{-}15}\text{-}g_5\text{-}PEG_{5\%}$ (S_2) for further use in our study.

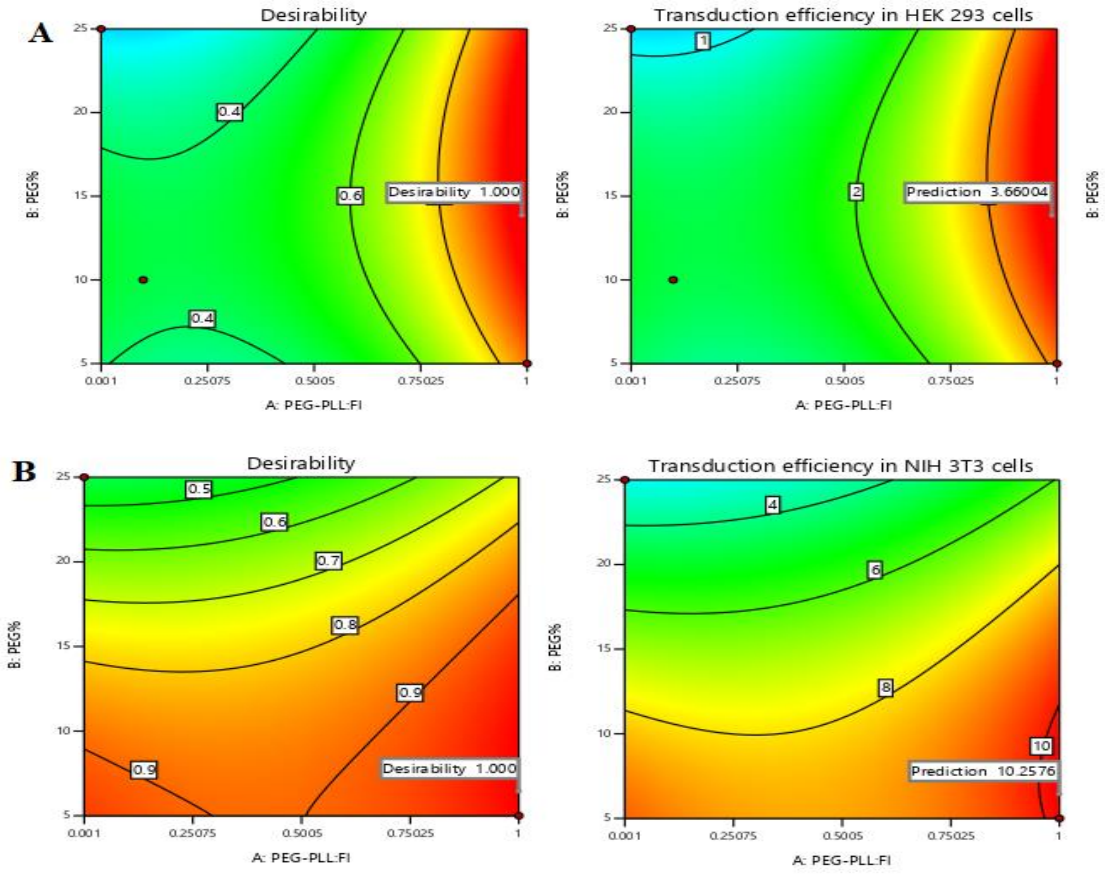

Figure 0.14: Contour plots of optimized PLL-g-PEG-FlAd vectors showing the highest desirability of transduction in A) HEK 293 and B) NIH 3T3 cells.

To sum up, transduction efficiency of NtAd, FlAd, and selected hybrid vectors are demonstrated in Figure 2.15. FlAd lost almost 75% of its ability to transduce CAR-positive (HEK 293) cells compared to NtAd. However, the selected hybrid vector S_1 restored 85% of the lost infectivity, where the transduction efficiency increased 3.5 folds compared to FlAd. In CAR-negative (NIH 3T3) cells, the transduction efficiency of NtAd and FlAd was almost negligible. However, the selected hybrid vector S_2 was able to transduce the cells with an efficiency 10.2 folds compared to FlAd.

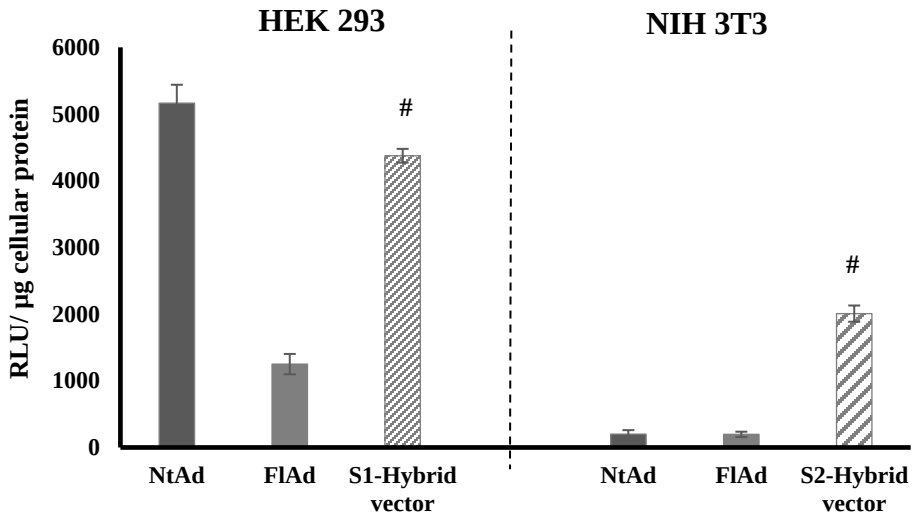

Figure 2.15: Transduction efficiency of NtAd, FlAd, and PLL-g-PEG-FlAd in HEK 293 and NIH 3T3 cells. $PLL_{15\text{-}30}\text{-}g_{25\%}\text{-}PEG_{0.5}$-FlAd ($S_1$), and $PLL_{4\text{-}15}$-g5%-PEG_5-FlAd (S_2) were used to transduce HEK 293 and NIH 3T3 cells at 1 µg PLL-g-PEG/10^6vp, respectively. X-axis is Relative Light Units (RLU) per µg total protein in cellular lysate. # $p<0.0001$ (values were compared to FlAd).

Model validation

In order to characterize an analytical method as robust, it must be able to predict responses with small differences from the experimental data. Thus, the validity of models was evaluated by experimentally preparing and characterizing the PLL-g-PEG-FlAd vectors in optimized points suggested by the model. Table 2.5 shows the results obtained of the three chosen random check points, together with their predicted values generated from the obtained equations

for the D-optimal quadratic models. There is a good agreement between the actual and predicted responses as seen in the low values of % bias in between.

Table 0.5: Check Point analysis results for responses.

	HEK 293 cells			***NIH 3T3 cells***		
Hybrid vector	***Actual TE***	***Predicted TE***	***%Bias***	***Actual TE***	***Predicted TE***	***%Bias***
P1[a]	7.7	7.9	2.5	1.84	1.9	3.2
P2[b]	1.34	1.3	3.1	1.3	1.1	18.2
P3[c]	1.84	1.6	15	8.3	7.3	13.7

[a] P1= PLL (1–5), PEG (2), 25%, 1µg/10^6 vp.
[b] P2 = PLL (15–30), PEG (2), 0%, 0.1 µg/10^6 vp.
[c] P3= PLL (4–15), PEG (5), 10%, 0.025 µg/10^6 vp.

Particle size and zeta potential of PLL-g-PEG-FlAd

Particle size and surface charge values of the selected PLL-g-PEG-FlAd vectors were measured by DLS and are listed in Table 2.6.

Table 0.6: Mean particle size of NtAd, FlAd, and PLL-g-PEG-FlAd vectors formed at parameters found to give optimum transduction efficiency.

Vector	**Mean particle size ± standard deviation (nm)**	**Zeta potential ± standard deviation (mV)**
NtAd	108 ± 2.2	-21.3 ± 0.5
FlAd	115 ± 3.4	-17.7 ±1.5
$PLL_{15\text{-}30}$-$g_{0.5}$-$PEG_{25\%}$ (S_1)	193 ± 3.9	11.2 ± 4.2
$PLL_{4\text{-}15}$-g_5-$PEG_{5\%}$ (S_2)	270 ± 6.4	7.5 ± 1.2

2.4 DISCUSSION

Adenoviral vectors have been widely used in gene therapy [23]. Despite having many benefits, Ad also has limitations [155]. Cellular uptake of Ad is dependent on the presence of CAR on the target cell surface because the fiber knob domain of the virus binds to this receptor. However, many cells including cancer cells have down regulated CAR which limits the ability of Ad-based vectors to infect those cells [158, 201, 202]. A promising strategy to overcome this obstacle is chemical or physical modification of the Ad surface with polymers to alter the native tropism of the virus [203]. In the present study, we used a fiberless Ad (FlAd) that was previously generated in our lab to overcome the native tropism problem [184]. However, fiber truncation

resulted in a reduction in the ability of the virus to enter CAR-positive or CAR-negative cells. To restore the transduction efficiency of the virus in a CAR-independent way, we constructed an FlAd hybrid vector, in which the negatively charged FlAd surface was physically coated with the cationic PLL-g-PEG copolymer via electrostatic interaction. PEG grafted PLL has been widely used for non-viral gene delivery [191, 204, 205] but have been of limited use with viral vectors and have not been comprehensively studied [134].

As measured by DLS, the increase in the particle size of PLL-g-PEG-FlAd relative to FlAd, indicated that FlAd was coated with PLL-g-PEG copolymer. Zeta potential is an important factor for the cellular uptake as well as the stability of the complex. The zeta potential of the FlAd was -17.7 ±1.5 mV, due to the negatively charged amino acids in the virus hexon proteins [134, 206, 207]. Upon complexing with copolymer, hybrid vectors showed a positive zeta potential. Formation of hybrid vectors was further verified by TEM microscopy as shown in Figure 2.3. TEM images of FlAd demonstrated the characteristic hexon structure and the icosahedral shape of the virus particle. In contrast, the hybrid vector had a rough surface structure with a coat of copolymer surrounding the virus particles. Particles that are formed by charge interactions with cationic polymers are prone to aggregation, leading to variability and instability. However, TEM imaging revealed that hybrid vectors retained their original shape with no aggregations. This might be due to the charge repulsion of the virus surface yielding a stable vector without significant aggregation. These data collectively demonstrate that the negatively charged FlAd was adequately complexed with the cationic PLL-g-PEG copolymer to form a stable hybrid adenoviral vector.

Transduction is a process by which DNA is introduced into a cell by a virus or a viral vector. The efficiency of the virus in infecting the cells is measured by the level of the reporter gene expression (lac-Z gene in the Ad we are using) which is called transduction efficiency (TE). The positive charge of the copolymer can enhance the virus gene transfer in a CAR-independent pathway. In this study, we demonstrated that PLL-g-PEG have replaced the function of the fiber

and have resulted in the formation of PLL-g-PEG- FlAd with an increased transduction efficiency in both CAR-positive and CAR-negative expressing cells.

The optimum MOI required to achieve a good transduction efficiency of hybrid vectors is important to be determined. Low MOI results in poor gene expression, whereas, high MOI often results in reduced cell viability. Also, MOI is cell specific and needs to be adjusted according to each cell type. As expected, the infectivity of the FlAd was low at smaller values of MOI and did not improve significantly even as the MOI was increased in both cell types. The infectivity of PLL-g-PEG-FlAd vectors was higher than FlAd at all MOIs tested suggesting that the vectors can effectively transduce the cells in a CAR-independent way. MOI of 100 and 250 infectious virus particles per cell showed the best transduction efficiency of hybrid vectors in HEK 293 and NIH 3T3 cells, respectively.

Formulation parameters including: PLL Mwt, PEG Mwt, degree of PEGylation and ratio of copolymer to virus, has been recognized as important factors that affect the physicochemical characteristics of the formed vectors and consequently their gene delivering efficiency [134, 136, 207]. Hence, a library of PLL-g-PEG copolymer with variation in PLL Mwt (1–5, 4–15, 15–30, 30–70, and 70–150 kDa), PEG Mwt (0.5, 2, 5, and 10 kDa), degree of PEGylation (5, 10, 25, 30, and 40%), was synthesized to prepare PLL-g-PEG-FlAd vectors to be used at 0.001–1 µg PLL-g-PEG /10^6 virus particles (vp).

Afterwards, the formulation parameters were varied one at a time to define the range of factors/levels that is required for an efficient gene delivery. The molecular weight of PLL affected the physicochemical characteristics and hence the gene delivery efficiency of the vectors. PLL-g-PEG-FlAd prepared with high Mwt PLL (70-15 kDa) showed a very poor transduction efficiency (Figure 2.5). High Mwt PLL induced crosslinking between the virus particles that resulted in the formation of large sized particles (>1µm) with reduced infectivity (Figure 2.9). Besides, cells infected with those vectors showed low cell viability owing to the cytotoxic

cationic nature of the polymer (Data not shown) [143]. Therefore, the 70-150 kDa PLL was excluded from further studies.

PEGylation is a popular modification that can reduce the cytotoxicity associated with PLL complexes, immunogenicity of the virus as well as increase the vector circulation times and prolong the transgene expression [124, 195]. However, PEGylation compromises the ability of the virus to interact with cell receptors, which reduces the transduction of Ad in cells [20]. Hence, PEG molecular weight and degree of PEGylation (DOP) must be balanced to gain the benefits while not sacrifice the TE. Hybrid vectors prepared with high Mwt PEG (10 kDa) showed the lowest transduction efficiencies among other vectors prepared with lower Mwts of PEG (Figure 2.6). This poor transduction efficiency is due to the increased shielding effect of the PEG molecules and the decreased accessibility of the positively charged PLL molecules to interact with the cell membrane for better binding and internalization. Zhang et al. have shown that the longer the PEG chain, the more PEG shielding effect and thus the lower the gene transfer efficiency [207]. The other important factor related to using PEG is the DOP of the copolymer. The lower number of PEG substitution on the PLL backbone (DOP) might be insufficient for the stabilization of the virus particles, whereas the higher number of PEG substitution could retard the internalization of the excessively PEGylated virus particles into the cells [134, 205]. Hybrid vectors showed high transduction efficiency up till 25% DOP, however, transduction efficiency dropped upon increasing the DOP to 30% and 40% (Figure 2.10). This might be attributed to three reasons. First, as the DOP increases, a transition of the PEG from the “mushroom” coil to the “brush” shape occurs [208]. As a result of the higher PEG shielding, fewer positive charges are exposed for electrostatic binding of the vector to the cells. Previous studies have explained that copolymers with few PEG blocks showed improved gene transfer efficiency compared to those with relatively more PEG blocks [205, 207]. Second, the brush-mushroom coil effect also resulted in the formation of larger particle size of PLL-g-PEG-FlAd vectors (Figure 2.10). For example, the particle size of vectors increased from 134 to 335 nm and from 190 to 295 nm upon

increasing the DOP from 5% to 40% when prepared with PLL (1–5) and (15–30 kDa), respectively. Third, the zeta potential values decreased upon increasing the DOP as demonstrated in Figure 2.11. The decrease in the surface charge of the vectors is directly correlated to the instability of the vectors as well as their tendency to aggregate and form larger sized particles [209]. This data collectively led us to exclude high Mwt PEG (10 kDa) and high DOP (30% and 40%) to complete our study.

The effect of PLL-g-PEG/FlAd ratio is the last factor studied. The transduction efficiency of hybrid vectors did not increase until the PLL-g-PEG/FlAd ratio reached 0.001 μg/10^6 vp. Very low ratios of PLL-g-PEG molecules to FlAd particles (0.0001 and 0.00001 μg/10^6 vp) were insufficient to coat the virus for better attachment and cellular internalization which might have led to the poor transduction efficiency observed. As the amount of PLL-g-PEG increased; the copolymer mediated better TE. However, an excess amount PLL-g-PEG/FlAd > 1 μg /10^6vp did not improve gene expression in both cell types. A high ratio of cationic copolymer to virus particle led to larger particle sized (Figure 2.9) and decreased surface charge vectors (Figure 2.11). Both effects might have prevented efficient viral infection [188]. Besides, high concentrations of cationic polymers are known to be toxic to cells [210]. Hence, a range of 0.001–1 μg /10^6 vp was used to prepare hybrid vectors for further studies.

We have covered a screening for the factors and ranges that affect the transduction efficiency in both CAR-positive and CAR-negative cells. In that step, we have used a one factor at a time (OFAT) experiment, where we varied one factor at a time to be able to conduct the study. OFAT experiments have been widely used for studying the factors affecting the gene delivery efficiency of different viral and non-viral vectors [38, 151, 211, 212]. Nevertheless, previous researchers have studied a limited number of factors with this kind of experiments. In contrast, Design of Experiments (DOE) statistical methodology permits the simultaneous evaluation of multiple factors effect on experimental performance and the analysis of their interactions in order to find their optimal combinations [213]. We have used DOE to facilitate the

exploration of that broader range of parameters combinations, which improved the prediction of the response. DOE has been primarily used in industry to optimize processes and maximize their robustness, but recently DOE has also been applied in biomedical research to different types of analyses, as determination of the best cell media composition and the optimization of cell transfection [214].

Two quadratic models were generated by the two investigated designs, one for CAR-positive (HEK 293) and the other for CAR-negative (NIH 3T3) cell. The transduction efficiency in each cell line (response) was fitted to the quadratic model and the adequacy of these models was verified using ANOVA test (Table 2.4). The R^2 values indicated that the model explained 99.4% and 99.5% of the variability of the transduction efficiency of PLL-g-PEG-FlAd vectors in HEK 293 and NIH 3T3 cells around the mean, respectively. Adequate precision measures the signal to noise ratio which is the range of a predicted response relative to its associated error. A ratio greater than 4 is desirable to qualify the model to be used to navigate the design space. The ratios were 25.7 and 35.7 for responses 1 and 2, respectively, indicating the adequacy of the two models in navigating hybrid vectors transduction efficiency space.

In order to characterize an analytical method as robust, it must be able to predict responses with small differences from to the experimental data. Thus, the validity of models was evaluated by experimentally preparing and measuring the transduction efficiency of hybrid vectors in three chosen random check points (Table 2.5). The actual results obtained, together with their predicted values generated from the equations for the D-optimal quadratic models showed a good agreement between the actual and predicted responses. The obtained biases ranged between 2.5% and 18.2% and agreements below 30% bias were considered acceptable [215]. These findings confirm the predictability of the D-optimal model and suggest the possibility of its utilization for the optimization of the transduction efficiency of PLL-g-PEG-FlAd vectors in HEK 293 and NIH 3T3 cells.

DOE allowed us to optimize the PLL-g-PEG-FLAd vector to achieve maximum TE, where we selected one hybrid vector for each cell type with the highest desirability. In CAR-positive and CAR-negative cells, $PLL_{15\text{-}30}\text{-}g_{25\%}\text{-}PEG_{0.5}$ (S_1) and $PLL_{4\text{-}15}\text{-}g_{5\%}\text{-}PEG_5$ (S_2) at 1 µg PLL-g-PEG /10^6 vp were selected as they achieved 3.5 and 10.2 folds of transduction efficiency compared to FlAd, respectively. The results suggest that hybrid vectors chosen have benefited from a combination of different factors and levels to reach the optimum TE. S_1 hybrid vector was composed of PLL (15–30 kDa) that resulted in a positive zeta potential of 11.2 mV, but yet a reasonable particle size of 193 nm. High Mwt PLL based particles are expected to form large sized particles but adding short PEG chains (0.5 kDa) at high DOP (25%) offered a steric hindrance in-between the particles ensuring their stability. At the same time, the short PEG chains allowed for a good exposure of the positively charged PLL molecules coating the virus which enabled cellular binding and internalization. S_2 hybrid vector was composed of PLL (4–15 kDa) which also resulted in a positive zeta potential of 7.5 mV, but a particle size of 270 nm. A larger particle size and a lower surface charge is expected upon using long PEG chains (5 kDa). Although the PEG chains on the PLL backbone might have shielded the virus surface but using it at a low DOP (5%) offered enough flexibility for the PEG chains to move freely to expose the positive charged PLL molecules for better binding and cellular internalization.

The differences in-between the vectors' composition that achieved high transduction efficiency was expected as we are infecting different cell types. Although hybrid vectors formed are CAR-independent, the transduction efficiency seems to depend on the cell type. Both HEK 293 and NIH 3T3 cells have different cell membrane fluidity and elasticity characteristics which affect the endocytosis of nanoparticles [216, 217]. In addition, HEK 293 is an epithelial human kidney cell while the NIH 3T3 is a mouse fibroblast cell and they use different endocytic mechanisms that would call for different characteristics of nanoparticles [218, 219]. Further studies and investigations are required to confirm these hypotheses, but we have covered some of the endocytic pathways differences as later explained in chapter 4.

2.5 CONCLUSION

This work showed that complexes of FlAd with cationic copolymer to form PLL-g-PEG-FlAd hybrid vectors enhanced the efficiency of gene expression *in vitro*. The function of the fiber of adenovirus in mediating good transduction efficiency was replaced by the physical modification of the virus with PLL-g-PEG copolymer. The physicochemical properties as well as the efficiency of gene expression of PLL-g-PEG based vectors depended on several factors, including PLL Mwt, PEG Mwt, DOP, and the amount of copolymer/virus. Hybrid vectors showed good gene expression in a CAR-independent way. Therefore, these vectors may increase gene transfer to different cell types irrespective of CAR. In this study, hybrid vectors were optimized to increase their transduction efficiency in specific cell types and results cannot be generalized to all cells. Considering the effect of cell type on the vector gene expression efficiency is essential when vectors are designed to be used *in vivo* in other cell types. With improvement in the gene delivering efficiency of the vectors, it may be possible to deliver lower concentrations of the vector and thus reduce toxicity and any associated adverse effects with the use of high viral dose. The subsequent increase in the therapeutic index would further improve the vector and potentially lead to successful gene therapy.

CHAPTER III

HYBRID ADENOVIRAL VECTORS OVERCOMING ADENOVIRUS LIMITATIONS: IMMUNOGENICITY, SERUM STABILITY, AND TROPISM

3.1 INTRODUCTION

An efficient yet safe and non-toxic gene delivery vector is a necessity in the field of gene therapy research. Adenovirus (Ad) is among the most widely used vectors for gene therapy [220]. Ad can transduce a broad range of cells including dividing and non-dividing cells and produce high levels of gene transfer relative to other currently available vectors [162, 221-223]. Despite its advantages, Ad gene delivery vectors suffer from serious limitations like immunogenicity and promiscuous tropism. Shortly after systemic administration of Ad vectors, pathogen-associated molecular patterns (PAMPs) such as capsid, fiber, or DNA of the virus activate an inflammatory response. This results in the release of cytokines/chemokines such as interleukin-6 and interleukin -12 (IL-6, IL-12) and tumor necrosis factor (TNFα), and Interferon gamma-induced protein 10 (IP-10) causing the activation of an innate immune response [101, 163, 224, 225]. The elicited innate immune response leads to the rapid clearance of the Ad vector from the body before the desired therapeutic response is achieved [72, 226].

Previous researchers have attempted to reduce the immunogenicity of adenovirus vectors through genetic or chemical/physical modification. Ablation of Coxsackievirus Adenovirus Receptor (CAR) (primary receptor), αv integrin binding (secondary receptor), and heparan sulfate

glycosaminoglycan (HSG) (third receptor) binding have been reported to reduce liver toxicity and IL-6 production [227]. Chemical /physical modification was also accomplished through coating or conjugating the vector to polyethylene glycol (PEG), poly-N-(2-hydroxy propyl) methacrylamide (pHPMA), poly(ethylenimine) (PEI), poly (L-lysine) (PLL), and chitosan [188, 194, 203, 228, 229]. PEGylation is the most popular approach to shield the surface of the vector from aggregation, opsonization, and phagocytosis, reducing liver biodistribution, as well as weakening the immune responses and prolonging the circulation time of the vector [39, 228, 230]. Not only PEGylation has addressed the immunogenicity of the virus but PEGylation was also used to manage viral tropism problem. Ad cellular attachment primarily depends on the ubiquitously found CAR, which results in widespread infection of many cell types [61]. Dependency on this receptor also limits the ability of Ad-based vectors to transform cells that lack CAR, such as advanced tumor cells, peripheral blood cells, vascular smooth muscle cells, and cancer cells where CAR is down-regulated. PEGylation reduces adenovirus transduction efficiency in CAR-positive or CAR-negative cells through non-specific steric hindrance [231, 232]. This simultaneous ability to reduce immunogenicity and lower transduction efficiency in cells is known as the “PEG dilemma” [196]. To solve this dilemma, researchers have investigated the use of cationic polymers such as PEI and PLL to complement the function of PEGylation and increase adenovirus transduction efficiency [12,27]. These polymers carry highly positive charges, allowing them to coat the anionic adenovirus particles. This strategy usually improves transduction efficiency but also increases cytotoxicity, as observed when coating adenovirus with high-molecular-weight PEI or PLL [203]. Therefore, a good balance between PEG Mwt, degree of PEGylation, PLL Mwt, and PLL-g-PEG/FlAd ratio can ameliorate the cytotoxicity of the vector. The charged particles can easily interact with serum proteins when systemically administrated [24, 25]. This interaction would reduce the distribution of the vectors *in vivo* resulting in rapid clearance from the body.

In this chapter, we combine the two approaches of removing the fiber of Ad with the PLL-g-PEG coating to address the aforementioned problems in the gene delivery. We selected the PLL-g-PEG-FlAd vectors with the highest transduction efficiency from chapter 2 to examine their immunogenicity, toxicity, serum stability, and transduction in CAR-low and CAR-negative cells.

3.2 MATERIALS AND METHODS

Cell culture

Mouse fibroblast cell line (NIH 3T3), and human embryonic kidney cell line (HEK 293), Chinese hamster ovary (CHO), and breast cancer cell line (MCF-7) were purchased from the American Type Culture Collection (ATCC) (Manassas, VA). The HEK 293, CHO, and MCF-7 were cultured in Dulbecco's Modified Eagle Medium (DMEM) (Gibco-BRL, Grand Island, NY) supplemented with 10% fetal bovine serum (FBS) (Mediatech, Inc., Manassas, VA). The NIH 3T3 cells were cultured in DMEM with 10% calf serum (CS) (Mediatech, Inc., Manassas, VA). Cells were maintained in a humidified atmosphere at 37ºC and 5% CO_2.

Adenovirus

Recombinant adenovirus type 5 (Ad) encoding *lac*Z reporter gene and lacking the E1 and E3 native genes was generated from the native adenoviral plasmid, pAdEasy-1(Addgene plasmid 16400) and pShuttle-CMV-lacZ (Agilent, CA) [197, 198]. The virus was amplified in HEK 293 cells and purified using ion-exchange chromatography in a Vivapure Adenopack purification kit following the manufacturer's protocol (Sartorius Stedim, CO). Ad was concentrated and stored in phosphate-buffered saline (PBS), pH 7.4. The number of virus particles (vp) was determined by measuring UV absorbance at 260 nm (1 U $\approx 10^{12}$ virus particles/ml) [198].

Fiberless Adenovirus generation

A FlAd plasmid (pAd5-FlAd) was generated using homologous recombination to remove the fiber gene from the native Ad plasmid (pAdEasy-1) [184]. Since the removal of the fiber

severely reduced the infectivity of the virus, amplification of FlAd is required in 633 cell line that stably expresses fiber protein. Transfection of 633 cells with pAd5-FlAd produced a virus with fiber protein but lacking the fiber gene. Passaging the virus on 633 cells enriched the virus titer. The enriched virus was then used to produce FlAd through a final passage on HEK 293 cells. The virus was collected and purified using the Vivapure Adenopack purification kit following the manufacturer's protocol (Sartorius Stedim Arvada, CO). The virus was quantified by measuring the absorbance of the viral DNA at a wavelength of 260 nm (1 U $\approx 10^{12}$ virus particles/ml).

FlAd is unable to infect cells since it lacks the fiber protein. While generally the virus is referred to as infectious particles, it is better to think about the particles as being potentially infectious. Not all NtAd or FlAd particles, however, are infectious or potentially infectious. Mittereder et al. showed that only about 5% of adenovirus particles are infectious [199]. The other 95% of the virus particles are thought to be inactive due to harsh conditions the viral particles go through during the purification steps. An assumption made in the present study was that only 5% of FlAd is potentially infectious.

PLL-g-PEG copolymer synthesis

PLL-g-PEG was synthesized via reacting the primary amines (-NH2) on the lysine chains of PLL-HBr (Sigma, Aldrich) with the succinimidyl ester group on the mPEG-NHS (Creative PEGworks, NC). For these studies, we prepared, $PLL_{15\text{-}30}\text{-}g_{25\%}\text{-}PEG_{0.5}$ and $PLL_{4\text{-}15}\text{-}g_{5\%}\text{-}PEG_{5}$ to use in preparing hybrid viral vectors to transduce the cells, respectively. $PLL_{15\text{-}30}\text{-}g_{25\%}\text{-}PEG_{0.5}$-FlAd was prepared by adding 14 mg of 0.55 kDa mPEG-NHS to 15 mg of 15-30 kDa PLL-HBr dissolved in 200 µl of phosphate-buffered saline (PBS). $PLL_{4\text{-}15}\text{-}g_{5\%}\text{-}PEG_{5}$ was prepared by adding 25 mg of 5 kDa mPEG-NHS to the dissolved 15-30 kDa PLL-HBr. The mixtures were allowed to react for 2 hours before being washed with ultrapure water in a 10 kDa centrifugal concentrator. After 3 washes, each grafted copolymer was lyophilized and stored at -20°C.

Formation of PLL-g-PEG-FlAd vectors

PLL-g-PEG-FlAd vectors were prepared through electrostatic attraction between the positively charged copolymer and the negatively charged FlAd). PLL-g-PEG was dissolved in PBS, pH 7.4, prior to the dropwise addition of the virus so that the concentration of PLL-g-PEG was 1 μg/10^6vp. Subsequently, the solution was mixed by gentle aspiration with the pipet tip and allowed to incubate for 10–30 min at room temperature before further use.

Evaluation of the innate immune response of PLL-g-PEG-FlAd vectors *in-vitro*

To evaluate the effect of modified Ad on the innate immune response, the amount of pro-inflammatory cytokines, interleukin 6 (IL-6), and tumor necrosis factor (TNFα), produced by murine macrophage RAW 264.7 cells were measured. Raw 264.7 cells were seeded 18–24 hours before transduction in 12-well plates at a seeding density of 2×10^5 cells/well. The cells were treated with NtAd, FlAd and $PLL_{15\text{-}30}$-$g_{25\%}$-$PEG_{0.5}$-FlAd and $PLL_{4\text{-}15}$-$g_{5\%}$-PEG_5-FlAd vectors for 32 hours at a MOI of 100. The cell-free supernatants were then collected and the levels of IL-6 and TNFα were then quantified using an IL-6 and a TNFα ELISA kit (BD Biosciences, Sparks, MD) following the manufacturer's protocols. Briefly, ELISA plates precoated with monoclonal antibodies against murine IL-6 or TNFα were used. Fifty microliters of IL-6 standards and samples were incubated on the pre-coated plates for 2 h at room temperature. The plates were washed and biotinylated anti-mouse IL-6 antibodies, together with streptavidin–HRP conjugates were added for another hour. The plates were again washed, and TMB One-Step reagent was added for 30 min. The reactions were stopped with 50 μl of 2 N H_2SO_4. The amount of IL-6 and TNFα was determined by measuring absorbance at 450 nm and compared to a standard curve with known IL-6 and TNFα concentration, respectively.

Effect of serum on transduction efficiency of PLL-g-PEG-FlAd

The transduction efficiency of Ad, FlAd, and PLL-g-PEG-FlAd vectors was studied on HEK 293 and NIH 3T3 cells. Cells were seeded for 24 hours before infection at 5×10^4 cells per

well in 24 well plates. The cell culture medium was replaced with serum-free DMEM at 50% of the typical well culture volume (for example, 0.5 ml in a 12-well plate). The cells were then infected with the virus or hybrid viral vector using a MOI of 100 for HEK 293 cells and 250 for NIH 3T3 cells. Four hours later, the medium was again replaced with fresh cell culture medium containing 10%, 20%, 30%, 40% or 50% of serum, and cells were incubated for 48 hours. LacZ expression was quantified using the chemiluminescence based Beta-Glo assay (Promega Inc., Madison, WI). The reporter gene expression was measured in terms of relative light units (RLU) with a Lumat LB9507 luminometer (EG&G, Berthold, Bundoora, Australia). The gene expression was then normalized to total cellular protein determined using the bicinchoninic acid assay (BCA assay) (Pierce, Rockford, IL). All gene expression results were normalized to the infectivity in serum free medium.

Cytotoxicity of PLL-g-PEG-FlAd vectors

Cytotoxicity of PLL-g-PEG-FlAd vectors was measured using a Cell Titer-Blue® Cell Viability assay (Promega, Madison, WI). HEK 293 and NIH-3T3 cells were seeded in 96-well plates for 18–24 hours at 2×10^4 cells/well. Before transduction, the growth medium on the cells was replaced with fresh growth medium. $PLL_{15\text{-}30}\text{-}g_{25\%}\text{-}PEG_{0.5}$-FlAd and $PLL_{4\text{-}15}\text{-}g_{5\%}\text{-}PEG_{5}$-FlAd were prepared and added to HEK 293 and NIH 3T3, respectively and incubated for 48 hours at 37 °C and 5% CO_2. Cell Titer-Blue® Reagent was added to each well following manufacturer's protocol. Twenty µl of CellTiter-BlueTM reagent was added to each well 24 h after the addition of drugs. The cells were incubated further for 1– 4 h at 37°C. Fluorescence at 560/590 nm was measured in a SpectraMax Gemini XPS spectrophotometer (Molecular Devices, Sunnyvale, CA).

Transduction of PLL-g-PEG-FlAd in CAR-low and CAR-negative cells

The transduction efficiency of Ad, FlAd, and PLL-g-PEG-FlAd vectors was studied on MCF-7 (CAR-low), NIH 3T3, and CHO (CAR-negative) cells. MCF-7 and CHO cells were grown in DMEM with10% FBS, while NIH 3T3 cells were grown in DMEM with 10% CS. All cells were maintained at 37ºC in a humidified 5% CO_2 incubator. Cells were seeded for 24 hours

before infection at 5×10^4 cells per well in 24 well plates. The cell culture medium was replaced with serum-free DMEM at 50% of the typical well culture volume (for example, 0.25 ml in a 24-well plate). The cells were then infected with the virus or hybrid viral vector using a MOI of 250 and 500 for the three cell lines. Four hours later, the medium was again replaced with fresh cell culture medium (containing serum), and cells were incubated for 48 hours. LacZ expression was quantified using the chemiluminescence based Beta-Glo assay (Promega Inc., Madison, WI). The reporter gene expression was measured in terms of relative light units (RLU) with a Lumat LB9507 luminometer (EG&G, Berthold, Bundoora, Australia). The gene expression was then normalized to total cellular protein determined using the bicinchoninic acid assay (BCA assay) (Pierce, Rockford, IL). All gene expression results were normalized to the infectivity of the unmodified virus.

Statistical analysis

All statistical analyses mentioned in this study were done using the ANOVA analysis followed by a post-ad-hoc test. A result was deemed not significant (ns) if $p > 0.05$. (#$p < 0.05$; ##$p < 0.01$; ###$p < 0.001$; *$p< 0.0001$).

3.3 RESULTS

Innate immune response

The systemic administration of Ad vectors initiates cytokine induction in innate effector cells such as dendritic cells, macrophages, or peripheral blood mononuclear cells [72]. This innate immune response limits the effectiveness of Ad vectors for gene therapy [18]. We assessed the levels of pro-inflammatory cytokines, IL-6, and TNFα, produced by macrophage RAW 264.7 cells to evaluate the innate immune response of PLL-g-PEG-FlAd hybrid vectors compared to NtAd, FlAd reduced the elicited IL-6 and TNFα production by 60% and 15%, respectively, due to removing the fiber protein. Modification of FlAd with PLL-g-PEG showed a 20–30% further reduction in IL-6 production and a 40–45% further reduction in TNFα compared to FlAd. Upon

comparing our hybrid vectors to NtAd, RAW 264.7 cells produced 80 pg/ml of IL-6 after exposure to NtAd and only 26 and 23 pg/ml after exposure to $PLL_{15\text{-}30}$-$g_{25\%}$-$PEG_{0.5}$-FlAd (S_1) and $PLL_{4\text{-}15}$-$g_{5\%}$-PEG_5-FlAd (S_2) vectors, respectively (Fig. 3.1A). Similarly, RAW 264.7 cells produced 542 pg/ml of TNFα after exposure to NtAd and this value was reduced to 246 and 277 pg/ml after exposure to $PLL_{15\text{-}30}$-$g_{25\%}$-$PEG_{0.5}$-FlAd (S_1) and $PLL_{4\text{-}15}$-$g_{5\%}$-PEG_5-FlAd (S_2) vectors, respectively (Figure 3.1B).

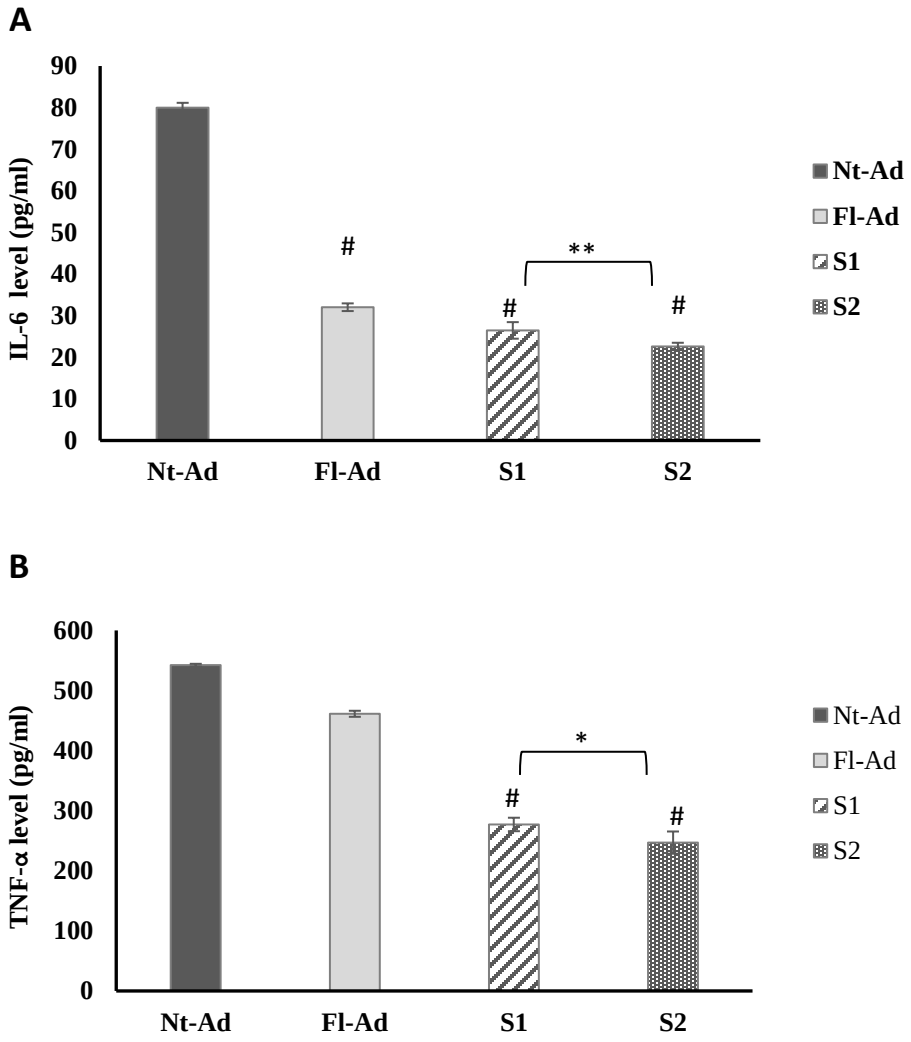

Figure 3.31: Expression of inflammatory cytokine (A) IL-6 and (B) TNFα produced by RAW 264.7 macrophage cells upon exposure to NtAd, FlAd, $PLL_{15\text{-}30}$-$g_{25\%}$-$PEG_{0.5}$-FlAd (S_1) and $PLL_{4\text{-}15}$-$g_{5\%}$-PEG_5-FlAd (S_2), vectors. #$p<0.0001$, ***$p<0.001$, **$p<0.01$, *$p<0.05$.

Effect of serum on the transduction efficiency of PLL-g-PEG-FlAd vectors

Serum proteins can easily interact with gene delivery vectors and inhibit their transduction in cells [211, 233]. For efficacious systemic gene delivery, the delivery system has to resist these non-specific interactions with serum. To examine the effect of serum on the transduction efficiency of PLL-g-PEG-FlAd, vectors were incubated in the presence and absence of up to 50% serum, since serum constitutes 50% (v:v) of blood [234]. Figure 3.2 shows that NtAd and FlAd lost ~45% and 55% of their efficiency when subjected to 50% serum in both cell lines. In contrast, the transduction efficiency of PLL-g-PEG-FlAd hybrid vectors decreased only by a range of 15-20% in the presence of 50% serum. These results indicate that there is a decreased possibility of the vector binding to serum protein allowing improved blood circulation and entering the cells at a higher concentration to provide successful gene delivery.

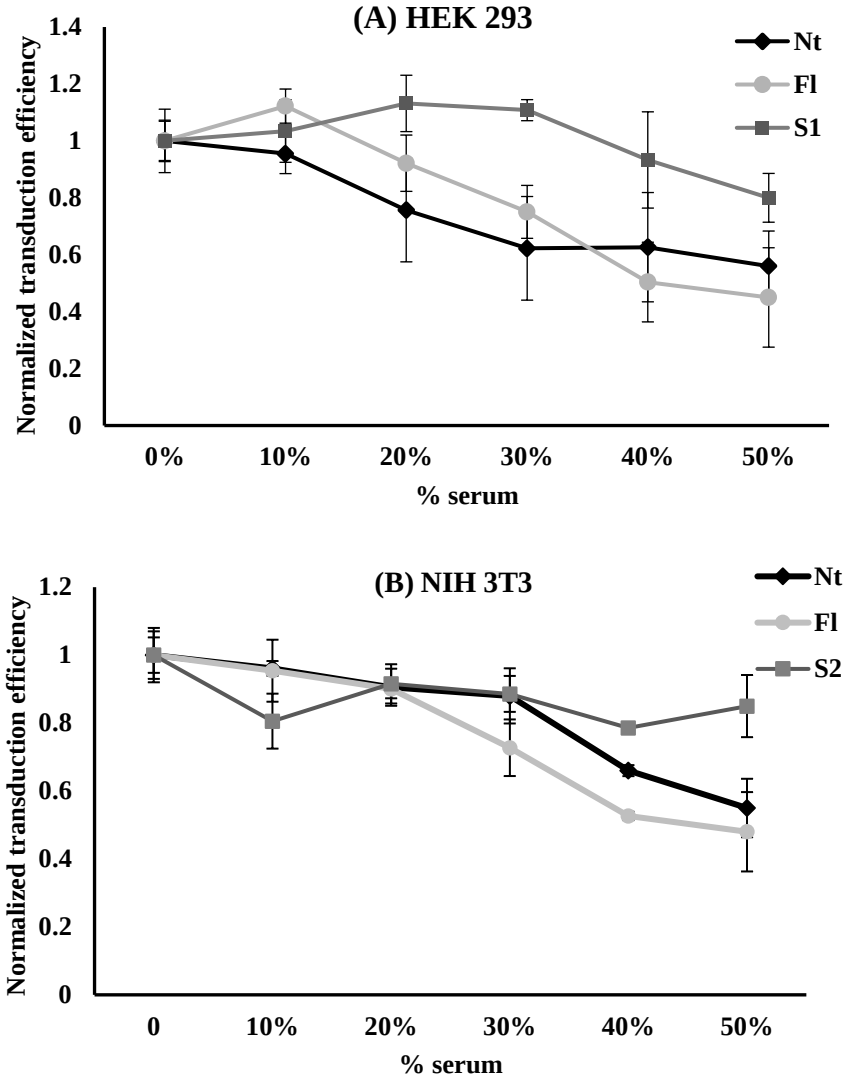

Figure 3.3: Transduction Efficiency NtAd, FlAd, $PLL_{15\text{-}30}$-$g_{25\%}$-$PEG_{0.5}$-FlAd (S_1), and $PLL_{4\text{-}15}$-g5%-PEG_5-FlAd (S_2), at 1 µg /10^6vp in the presence of 0-50% serum in (A) HEK 293, (B) NIH 3T3. Y-axis – Normalized transduction efficiency to the same expression at 0% serum for every tested vector. X-axis – Serum (%) in transduction media.

Cytotoxicity of PLL-g-PEG-FlAd vectors

PLL-g-PEG is biodegradable and hence is more desirable to use as a cationic component in gene delivery vectors compared to other polymers like PEI or PLL [235]. We investigated the cytotoxicity of hybrid vectors prepared with PLL-g-PEG compared to those prepared with PEI or PLL using an assay of cellular metabolic activity (Cell-Titer Blue ™) on HEK 293 and NIH 3T3 cells. Vectors prepared with PEI showed the most toxic effect, where the viability of both cell

lines decreased to 16% and 36% in HEK 293 and NIH 3T3 cells, respectively (Figure 3.3A). In contrast, vectors prepared with PLL-g-PEG had lower cytotoxicity as the cell viability was maintained >85% in both cell lines (Figure 3.3B). These results suggest that PLL-g-PEG-FlAd hybrid vectors have a good safety profile that enables them to be used at higher concentrations if needed *in vivo*.

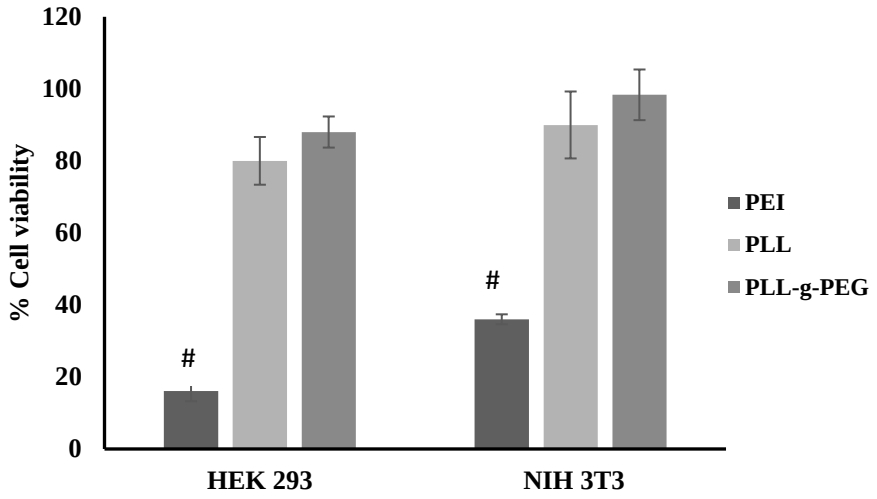

Figure 3.3A: Cytotoxicity of $PLL_{15\text{-}30}$-FlAd, and PEI_{25}-FlAd and $PLL_{15\text{-}30}$-$g_{25\%}$-$PEG_{0.5}$-FlAd (S_1) on HEK 293 and of $PLL_{4\text{-}15}$-FlAd, and PEI_{10}-FlAd, and $PLL_{4\text{-}15}$-$g_{5\%}$-PEG_{5}-FlAd (S_2) on NIH 3T3 #p<0.0001.

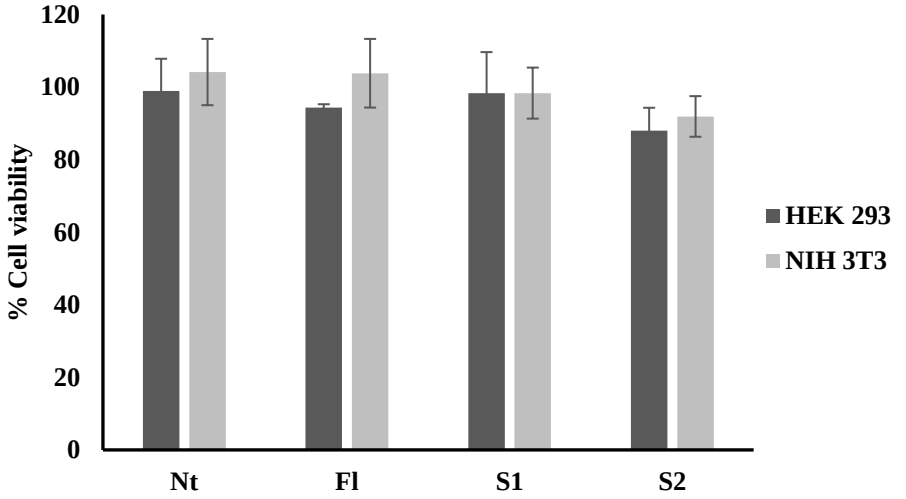

Figure 3.3B: Cell viability of HEK 293 and NIH 3T3 cells when incubated with $PLL_{4\text{-}15}$-$g_{5\%}$-PEG_{5}-FlAd (S_2), $PLL_{15\text{-}30}$-$g_{25\%}$-$PEG_{0.5}$-FlAd (S_1) at 1 µg /10^6vp.

Transduction efficiency of PLL-g-PEG-FlAd across a panel of CAR-low and CAR-negative cell lines

Ad infection depends primarily on the binding of the virus fiber to CAR [61]. Ad was reported to have a variable ability to infect different CAR-negative cell lines like cancer cells where CAR are downregulated [201, 236-238]. Therefore, we chose CAR-low cells like human breast cancer cells (MCF-7) and CAR-negative cells like NIH 3T3 and Chinese hamster ovary (CHO), to study the requirement for a CAR-mediated binding event in adenovirus infection.

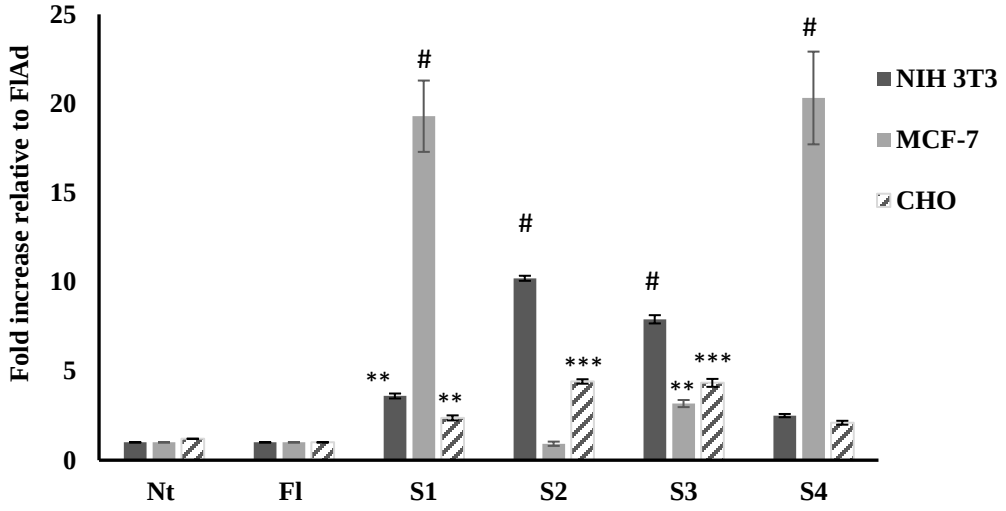

Figure 3.3: Transduction efficiency of the PLL-g-PEG-FlAd in CAR-deficient cells. NIH 3T3, CHO, or MCF7 cells were transduced with NtAd, FlAd, PLL-g-PEG-FlAd at a MOI of 250. PLL_{15-30}-$g_{25\%}$-$PEG_{0.5}$-FlAd (S_1), PLL_{4-15}-g5%-PEG_5-FlAd (S_2), PLL_{1-5} $g_{25\%}$-PEG_2-FlAd (S_3), and PLL_{1-5}-$g_{10\%}$-PEG_5-FlAd (S_4) at 1 µg /10^6vp was used. Results were normalized to RLU/µg total protein of FlAd (Relative Light Units per µg total protein in cellular lysate). Relative transduction efficiency of PLL-g-PEG-FlAd to FlAd was expressed as a fold increase relative to FlAd. Data represent the means and standard deviations of triplicate experiments. #-$p < 0.0001$, ***-$p<0.001$, **-$p<0.01$, *-$p<0.05$ versus FlAd.

To compare the gene transfer effect of PLL-g-PEG-FlAd in different cell lines, we measured the transduction efficiency in MCF-7, NIH 3T3, and CHO cells. Cells were transduced at a MOI of 250 of NtAd, FlAd or PLL-g-PEG-FlAd, and the transduction efficiency was estimated by B-glo assay.

As shown in Figure 3.4, the transduction efficiency of PLL-g-PEG-FlAd was significantly greater than that for FlAd in all cell lines. Interestingly, hybrid vectors' transduction in NIH 3T3, CHO, and MCF-7 reached 10.2, 4.4 and 20-folds compared to FlAd. The variable transduction of PLL-g-PEG-FlAd in CAR-deficient cells demonstrates their ability to transduce a broader range of cells.

3.4 DISCUSSION

A major obstacle in gene therapy is the shortage of efficient, non-toxic, non-immunogenic gene delivery agents. Having demonstrated that our adenoviral vectors improved *in vitro* transduction efficiency through ablating CAR binding with the removal of Ad fiber and replacing its function with cationic PLL-g-PEG copolymer. Since fiber removal and PEG reduces immune response and transduction, while PLL and PEG worsen serum stability and cytotoxicity, it was necessary to assess hybrid vectors' immunogenicity, serum stability, and cytotoxicity as well as its ability to transduce CAR-deficient cells.

The innate immune response is a barrier to the effective application of Ad vectors in humans [154]. Systemic administration of Ad rapidly recruits macrophages, inducing secretion of pro-inflammatory cytokines such as interleukin-6 (IL-6) and tumor necrosis factor (TNFα) [72, 225]. To understand how the removal of Ad fiber proteins and modification with the PLL-g-PEG copolymer affects the innate immune response, RAW 264.7 macrophage cells were incubated with NtAd, FlAd and our selected hybrid vectors (S_1 and S_2), then IL-6 and TNF α cytokine production was quantified using an ELISA assay. Macrophages produced 15% and 60% lower levels of IL-6 and TNF α when incubated with FlAd compared to NtAd (Figures 3.1). This may be due to the absence of fiber protein-receptor interaction, which triggers a cascading effect on the innate immune system [129]. The knob of the fiber was reported to be necessary for adenoviral uptake in macrophages via the scavenger receptor A [239]. Modification of FlAd with electrostatically bound PLL-g-PEG reduced the secretion of IL-6 and TNFα by almost 70% and

50% compared to NtAd, respectively. This reduction may be due to PEG shielding the epitopes on the virus capsid from macrophage uptake and activation [126, 129]. Previous studies have also shown a significantly lower secretion of the proinflammatory cytokines IL-6 and TNFα after delivery of PEGylated vectors [124, 126, 194, 203]. Higher Mwt PEG (5 kDa), used in preparing $PLL_{4\text{-}15}$-$g_{5\%}$-PEG_{5}-FlAd (S_2) hybrid vector, showed a more significant effect in reducing the immune response compared to lower Mwt PEG (0.5 kDa) used in preparing $PLL_{15\text{-}30}$-$g_{25\%}$-$PEG_{0.5}$-FlAd (S_1) vectors. PEG (5 kDa) resulted in a 15% and 11% reduction in IL-6 and TNFα secretion compared to PEG (0.5 kDa), respectively. This might be due to the lower efficiency of higher Mwt PEG in transducing macrophages [240].

An efficient gene delivery vector *in vivo* must also be stable under physiological conditions. The presence of serum is known to inhibit transductions of most gene delivery vectors, particularly charged species that can easily interact with the serum proteins [241, 242]. This serum interaction decreases the circulation of the vectors in the blood resulting in rapid clearance of the vectors from the body. Consequently, these undesired interactions should be minimal to deliver the required genes before the vectors are cleared out of the body. We tested the transduction efficiency of our hybrid vectors in comparison to NtAd in the presence of up to 50% serum in transduction media. NtAd and FlAd transduction efficiency was maintained at 10% serum then decreased to 56% and 45% at 50% serum compared to serum-free conditions, respectively. In contrast, PLL-g-PEG-FlAd showed better serum stability, where the transduction efficiency only decreased to a range of 80–85 % in the presence of 50% serum. PEG shields the surface of vectors due to its hydrophilic nature where PEG forms a hydrated cloud that sterically precludes vectors from interacting with neighboring vectors and/or blood components [243, 244]. The interaction of vectors with serum and their circulation time *in vivo* is controlled by different factors, like PEG molecular weight (Mwt), PEG surface density, and the charge of the vectors [243]. Recently, Yang and coworkers reported that when the grafting density is "high" PEG with a Mwt as low as 559 Da can effectively shield surfaces of 100 nm polystyrene (PS) NPs [54].

Thus, grafting lower Mwt PEG (550 Da) at a higher PEGylation ratio (25%) as in hybrid vector (S_1) may be similarly effective in stabilizing the vectors as grafting higher Mwt PEG (5kDa) at lower PEGylation ratio (5%) in hybrid vector (S_2). Both S_1 and S_2 vectors showed a 20% and 15% decrease in transduction efficiency upon incubation in 50% serum, respectively. Last, we cannot neglect the effect of the particle charge on the stability of the vectors in serum. The positive surface charge of hybrid vectors formed a steric hindrance against interaction with anionic serum proteins, leading to more stabilization of the vectors.

PEG contributed to the lower immunogenicity and the better serum stability of hybrid vectors; however, PEG might have affected the transduction efficiency of cells. Cationic polymers were combined to Ad to enhance the gene transfer into cells. PEI is a cationic polymer of good transfection efficiency, however, PEI is well known for its toxicity [245]. Upon binding to FlAd, a 64% and 84% reduction in cell viability of HEK 293 and NIH 3T3 cells was observed, respectively. PLL is a cationic polymer of lower cytotoxicity compared to PEI. This explains why the cell viability of HEK 293 and NIH 3T3 cells decreased by only 10% and 20% n respectively, when subjected to PLL-FlAd. To ameliorate the cytotoxicity of PLL, PEG was conjugated to PLL to form a more biocompatible and biodegradable copolymer. The results of the cytotoxicity of PLL-g-PEG-FlAd showed a low level of cytotoxicity that was similar to NtAd alone where the cell viability exceeded 85% with all hybrid vectors.

The variable level of CAR expression on cells is another major limitation that inhibits effective Ad delivery *in vitro* and *in vivo* due to the dependence of Ad infection on CAR binding [33]. Cationic polymers can enhance Ad-mediated gene transfer and infection through CAR-independent pathways. In this chapter, combined with chapter 2 findings, we demonstrated that hybrid vectors enhanced transduction efficiency in cells regardless of the CAR expression level. The transduction efficiency of the FlAd coated with PLL-g-PEG was significantly increased where it reached 20, 4.4, and 10 folds in both CAR-low (MCF-7) and CAR-negative (CHO and NIH 3T3) expressing cells compared to FlAd, respectively. Enhanced transduction efficiency of

PLL-g-PEG-FlAd was more evident in CAR-low than CAR-negative cells. Previous studies also showed that gene expression levels in MCF-7 (CAR-low) was more profound compared to that in HT1080 or C2C12 (CAR-negative) cells after transduction with polymer-modified Ad complex [246]. Another study has shown that the fold increase in gene transfer efficiency of polymer based adenoviral vector was inversely correlated to the level of CAR expression in cancer cells [136]. These data lead to the conclusion that cationic copolymers can improve the gene transfer efficiency of Ad to cells with variable CAR expression taking advantage of the surface charge of the vector.

3.5 CONCLUSION

In this chapter, we demonstrated that the PLL-g-PEG-FlAd hybrid vectors previously selected for their high transduction efficiency showed lower cytotoxicity and better serum stability than NtAd *in vitro*. The vectors have also evoked a weaker innate immune response as we have seen lower cytokine production amid macrophage incubation with the vectors. These effects are likely because the PEG chains masked the epitopes on the Ad surface from the surrounding environment. The vectors were able to transduce efficiently CAR-deficient cell lines like NIH 3T3, MCF-7, and CHO, proving their potential to deliver genes to different cell lines with poor CAR expression. Given these results, the removal of the fiber protein combined with viral surface modification with PLL-g-PEG can be anticipated as an effective way to further expand the applicability of adenovirus-derived vectors.

CHAPTER IV

INTRACELLULAR TRAFFICKING OF HYBRID ADENOVIRAL VECTORS

4.1 INTRODUCTION

In earlier chapters, we discussed the design of PLL-g-PEG-FlAd hybrid vectors. Ad has been engineered by removing the virus fiber and replacing its function with a synthetic PLL-g-PEG copolymer. This modification affected the physicochemical properties of hybrid vectors as well as their transduction efficiencies. The intracellular trafficking of hybrid vectors is also expected to be modulated by this modification. In this chapter, we describe the different cellular mechanisms leading to different transduction efficiencies of hybrid vectors in HEK 293 cells and NIH 3T3 cells.

The intracellular trafficking pathway of Ad serotype C, type 5 (Ad5) is demonstrated in Figure 4.1. Ad5 binds *via* its fiber knob to Coxsackie and Adenovirus Receptor (CAR), a 46 kDa cell receptor abundant in human tissues [61, 247, 248]. CAR binding is followed by secondary interactions of the RGD motifs in the virus penton base proteins with αvß3 or αvß5 integrins in the cells to initiate endocytosis and viral entry [62]. In addition to the classical CAR binding and the RGD-interaction, Ad might use alternative entry pathways like heparan sulfate proteoglycans (HSPGs) as receptors [62] and lactoferrin as a bridge between viral particles and the cell surface [249].

Once bound to the cell surface, the virus enters the cell by clathrin-mediated endocytosis [250]. Endocytosis appears to be rapid, as up to 30% of bound Ad is internalized within 15 minutes [62]. After the clathrin-coated pit separates from the plasma membrane as an endocytic vesicle, vacuolar H+-ATPase acidifies the endosomes. This acidification triggers conformational changes in the adenovirus capsid exposing the lytic factor identified as protein VI [251]. The protein VI facilitates the escape of the partially uncoated Ad particles from the early endosomes to be released into the cytosol before being degraded by lysosomal proteases [251-253]. After escaping to the cytosol, Ad particles are rapidly (30-60 min) translocated along microtubules to the nucleus via dynein motor protein to accumulate at the nuclear periphery and then docks at the nuclear pore complex [254-256]. Biochemical analysis has indicated that the majority of the viral capsid remains in the cytoplasm and is gradually dismantled by a combination of step-wise dissociation and proteolytic degradation [257]. Finally the liberated viral genome enters the nucleus via nuclear pores to be stored as an episome [258, 259]. Once in the nucleus, viral genes are expressed and ultimately result in the generation of transgene products.

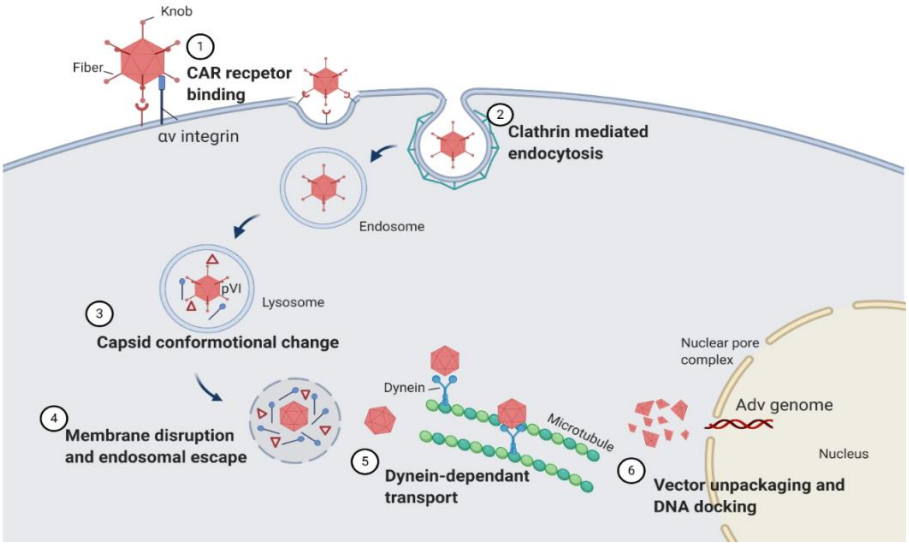

Figure 4.1: Infection pathway of adenovirus. The fiber protein of the virus binds to CAR, the Penton base binds to integrin which promotes clathrin mediated endocytosis. After cellular internalization, the virus capsid undergoes conformational changes and escapes the endosome to bind to microtubule/dynein for transport across the nucleus. The virus disassembles and releases the viral gene close to the nuclear pore to be taken up by the nucleus.

Gene delivery vectors tend to deliver their cargo into the cells via two key pathways: endocytic pathways or non-endocytic pathways [260]. Fusion and penetration are amongst the non-endocytic mechanisms, but this capability is possessed by only a few vectors; typically vectors with an associated fusogenic peptide or penetrating peptide which our current design of hybrid vectors lacks. Endocytic pathways have been known as the primary transport mechanisms for both viral and non-viral vectors into cells [261]. Endocytosis includes three major types: clathrin-mediated endocytosis (CME), caveolae-mediated endocytosis (CavME), and macropinocytosis (MP). The clathrin-mediated endocytosis depends on the formation of coated pits through the assembly of the protein clathrin and other adapter proteins enveloping the endocytic vesicles [262]. These small coated pits (approximately 100 nm in diameter) can uptake particles up to 200 nm [263], and form a vesicle after endocytosis, later maturing into late endosomes and fusing with lysosomes. In contrast, caveolae are small flask-shape invaginations of the plasma membrane that resemble the shape of a cave (hence the name caveolae) [261]. Caveolae consist of the cholesterol-binding protein caveolin with a bilayer enriched in cholesterol and glycolipids. The size of a particle that is internalized by caveolae-mediated endocytosis ranges from 200 nm to 500 nm [263]. Macropinocytosis refers to the fusion of ruffling plasma membranes which enfold surrounding fluids within 0.5–5 μm vesicles. The filling of the vesicles occurs in a non-specific manner and results in pinosomes that travel into the cytosol and fuses with other vesicles such as endosomes and lysosomes [264].

Endocytosis differs according to the cell type and characteristics of the endocytosed particles such as size and type of material [263, 265-267]. Studies have reported that cationic polymer-based gene delivery vectors enter cells via clathrin-dependent, as well as clathrin-independent endocytosis, caveolae-mediated endocytosis, and macropinocytosis [136, 267-270]. The major obstacle to efficient gene delivery is generally believed to be failure of endosomal escape, leading to vector degradation in lysosomes. Depending on the synthetic part of the hybrid

vector, different escape mechanisms from the endosomal compartment have been proposed. These include endosomal membrane destabilization [268, 271], free polymer-mediated membrane permeability and nanoscale hole formation [272], and endosomolysis caused by osmotic swelling [273, 274]. PLL does not have the ability to mediate a proton sponge effect like PEI leading to lower transduction of polyplexes compared to PEI-based polyplexes [275].

The purpose of our study was to examine the effect of replacing the virus fiber with PLL-g-PEG copolymer on the intracellular trafficking pathways. We wanted to investigate whether there is any difference in internalization and intracellular trafficking of our hybrid vector compared to the native adenovirus and whether these differences affect intracellular fate and transduction efficiency. Our experiments were based on a fibreless adenovirus that avoids CAR receptor binding as the first step in cell trafficking. We hypothesized that our hybrid vectors bind to the negatively charged components on the cell membrane. Next, we investigated the trafficking mechanisms of our hybrid vectors $PLL_{15\text{-}30}$-$g_{25\%}$-$PEG_{0.5}$-FlAd (S_1) in CAR-positive (HEK 293) cells and $PLL_{4\text{-}15}$-$g_{5\%}$-PEG_5-FlAd (S_2) in CAR-negative (NIH 3T3) cells via cellular uptake and transductions studies in the presence of various drug inhibitors that would affect specific pathways within the cell. We hypothesized that replacing the virus fiber with a synthetic copolymer would affect the hybrid vector internalization and trafficking pathways relative to the virus.

4.2 MATERIALS AND METHODS

Cell culture

Mouse fibroblast cell line (NIH 3T3), and human embryonic kidney cell line (HEK 293) were purchased from the American Type Culture Collection (ATCC) (Manassas, VA). The HEK 293 was cultured in Dulbecco's Modified Eagle Medium (DMEM) (Gibco-BRL, Grand Island, NY) supplemented with 10% fetal bovine serum (FBS) (Mediatech, Inc., Manassas, VA). The

NIH 3T3 cells were cultured in DMEM with 10% calf serum (CS) (Mediatech, Inc., Manassas, VA). Cells were maintained in a humidified atmosphere at 37ºC and 5% CO_2.

Adenovirus

Recombinant adenovirus type 5 (Ad) encoding *lac*Z reporter gene and lacking the E1 and E3 native genes were generated from the native adenoviral plasmid, pAdEasy-1 (Addgene plasmid 16400) and pShuttle-CMV-lacZ (Agilent, CA) [197, 198]. The virus was amplified in HEK 293 cells and purified using ion-exchange chromatography in a Vivapure Adenopack purification kit following the manufacturer's protocol (Sartorius Stedim, CO). Ad was concentrated and stored in phosphate-buffered saline (PBS), pH 7.4. The number of virus particles (vp) was determined by measuring UV absorbance at 260 nm (1 U ≈ 10^{12} virus particles/ml) [198].

Fiberless Adenovirus generation

A FlAd plasmid (pAd5-FlAd) was generated using homologous recombination to remove the fiber gene from the native Ad plasmid (pAdEasy-1) [184]. Since the removal of the fiber severely reduced the infectivity of the virus, amplification of FlAd is required in 633 cell line that stably expresses fiber protein. Transfection of 633 cells with pAd5-FlAd produced a virus with fiber protein but lacking the fiber gene. Passaging the virus on 633 cells enriched the virus titer. The enriched virus was then used to produce FlAd through a final passage on HEK 293 cells. The virus was collected and purified using the Vivapure Adenopack purification kit following the manufacturer's protocol (Sartorius Stedim Arvada, CO). The virus was quantified by measuring the absorbance of the viral DNA at a wavelength of 260 nm (1 U ≈ 10^{12} virus particles/ml).

FlAd is unable to infect cells since it lacks the fiber protein. While generally the virus is referred to as infectious particles, it might be better to think about the particles as being potentially infectious. Not all NtAd or FlAd virus particles, however, are infectious or potentially infectious. Mittereder et al. showed that only about 5% of adenovirus particles are infectious [199]. The other 95% of the virus particles are thought to be inactive due to harsh conditions the

viral particles go through during the purification steps. An assumption made in the present study was that only 5% of fiberless Ad is potentially infectious.

PLL-g-PEG copolymer synthesis

PLL-g-PEG was synthesized via reacting the primary amines (-NH2) on the lysine chains of PLL-HBr (Sigma, Aldrich) with the succinimidyl ester group on the mPEG-NHS (Creative PEGworks, NC). For these studies, we prepared, $PLL_{15\text{-}30}\text{-}g_{25\%}\text{-}PEG_{0.5}$ and $PLL_{4\text{-}15}\text{-}g_{5\%}\text{-}PEG_{5}$ to use in preparing hybrid vectors to transduce HEK 293 and NIH 3T3 cells, respectively. $PLL_{15\text{-}30}\text{-}g_{25\%}\text{-}PEG_{0.5}$ was prepared by adding 14 mg of 0.5 kDa mPEG-NHS to 15 mg of 15–30 kDa PLL-HBr dissolved in 200 µl of phosphate-buffered saline (PBS). $PLL_{4\text{-}15}\text{-}g_{5\%}\text{-}PEG_{5}$ was prepared by adding 25 mg of 5 kDa mPEG-NHS to the dissolved 15-30 kDa PLL-HBr. The mixtures were allowed to react for 2 hours before being washed with ultrapure water in a 10 kDa centrifugal concentrator. After 3 washes, each grafted copolymer was lyophilized and stored at -20°C.

Formation of PLL-g-PEG-FlAd hybrid vector

PLL-g-PEG-FlAd hybrid vectors were prepared through electrostatic attraction between the positively charged copolymer and the negatively charged FlAd. PLL-g-PEG was dissolved in PBS, pH 7.4, prior to the dropwise addition of the virus so that the concentration of PLL-g-PEG was 1 µg/ 10^6vp. Subsequently, the solution was mixed by gentle aspiration with the pipet tip and allowed to incubate for 10–30 min at room temperature before further use.

Transduction efficiency studies

The transduction efficiency of NtAd, FlAd, and PLL-g-PEG-FlAd hybrid vectors was studied on HEK 293 and NIH 3T3 cells. Cells were seeded for 24 hours before infection at 5×10^4 cells per well in 24 well plates. The cell culture medium was replaced with serum-free DMEM at 50% of the typical well culture volume (for example, 0.5 ml in a 12-well plate). The cells were then infected with the virus or hybrid viral vector using a MOI of 100 for HEK 293 cells and 250 for NIH 3T3 cells. Four hours later, the medium was again replaced with fresh cell culture medium (containing serum), and cells were incubated for 48 hours. LacZ expression was

quantified using the chemiluminescence based Beta-Glo assay (Promega Inc., Madison, WI). The reporter gene expression was measured in terms of relative light units (RLU) with a Lumat LB9507 luminometer (EG&G, Berthold, Bundoora, Australia). The gene expression was then normalized to total cellular protein determined using the bicinchoninic acid assay (BCA assay) (Pierce, Rockford, IL). All gene expression results were normalized to the infectivity of the unmodified virus.

qPCR assay for quantitation of Ad cellular uptake

DNA isolation. Total cellular DNA was purified using DNeasy Blood and Tissue Kit (Qiagen, Valencia, CA, USA), following the manufacturer's protocol. Total DNA was eluted in a final volume of 50 µl, aliquoted, and stored in -20°C until quantitation by qPCR assay.

Primer design and HRM melting predictions. Nucleic acid sequences used to design primers for Ad (AC-000008.1), HEK 293, and NIH 3T3 were retrieved from NCBI. For Ad, primers were designed using the consensus gene region of *E2* gene in Primer 3 (v.4.0.0)[276, 277]. The HRM melting temperature (HRM Tm) of the expected PCR product was predicted with uMELT ^{SM} [278]. To serve as an internal control, Beta-actin (*ACTB*) primer pair for either HEK 293 or NIH 3T3 was designed. Primers generated for the virus were then uploaded to the NCBI Primer BLAST database to predict *in silico* primer specificity.

Gradient PCR assays. To determine the optimal annealing temperature for each primer pair, 20 µl PCR reactions were performed as follows: 10 µl GoTaq (Promega, Madison, WI), 6 µl nuclease-free water, 2 µl of each forward and reverse primer (10 µM), and 2 µl of DNA. The thermocycler conditions for each reaction were as follows: four minutes at 95°C, 40 cycles of 20 seconds at 95°C, 20 seconds at a 50–62°C gradient, 20 seconds at 72°C, followed by a final extension for four minutes at 72°C. PCR was performed in a gradient capable Biometra Thermocycler (Biosciences, Dublin, Ireland). PCR products were then visualized using gel electrophoresis with SYBR™ Safe stain (Invitrogen, Carlsbad, CA) and visualized in a Gel Doc™ XR+ (Biorad, Hercules, CA).

qPCR reaction mix and reaction conditions. The optimized master mix (20 µl) was comprised of 10.5 µl of Hot Start master mix (Thermofisher, Waltham, MA), 5 µl nuclease-free water, 1 µl of each 10 µM forward and reverse primer, 1 µl LC Green (BioFire, Salt Lake City, UT), and 1 µl of DNA. PCR was performed in a Corbett Research Rotorgene (QIAGEN, Hilden, Germany) and the thermocycler profile used was 95°C for 4 minutes, 40 cycles of 95°C for 20 seconds, 55°C for 20 seconds, 72°C for 20 seconds, followed by a final extension of 72°C for 5 minutes, and an HRM ramping from 50°C to 90°C, increasing by 0.25°C every second. The concentration of purified Ad was measured using PicoGreen® dsDNA quantitation assay, following the manufacturer's protocol [279, 280]. Six-fold dilution from 1 ng to 1 fg/µl was prepared to generate a standard calibration curve by plotting C_t against each concentration. For comparison of results of drug-treated versus untreated samples, the livak method ($\Delta\Delta C_t$) was used (Appendix II).

Binding and internalization studies

HEK 293 and NIH 3T3 cells were seeded 24 h before transduction at 10^5 cells/well in 12-well plates. Cells and plates were transferred to 4 °C for 30 min before growth media containing serum was replaced with serum-free DMEM. Viral samples, NtAd, FlAd, or PLL-g-PEG-FlAd, were immediately added to the samples and cells were incubated for 1 hr on ice to halt endocytosis. Before measuring the amount of bound virus, unbound viruses were removed by washing the cells with cold trypsin followed by cold PBS. The cells were then scraped and pelleted by centrifugation. Viral and cellular DNA were isolated, and qPCR was used to measure viral titer, which was normalized to the housekeeping gene *ACTB*.

To measure the amount of internalized virus, unbound viruses were first removed by rinsing with cold trypsin followed by cold PBS. Warm growth medium was then added to the cells, which were transferred to an incubator at 37°C. After incubation at 37°C for 4 h, the cells were scraped and pelleted by centrifugation. Cellular DNA was isolated, and qPCR was used to quantify viral titer (as explained before), which was normalized to the housekeeping *ACTB* gene.

Drug cytotoxicity and compatibility studies

The toxicity of drugs was determined using the Cell Titer- BlueTM Cell Viability Assay. HEK 293 and NIH 3T3 cells were seeded in a 96-well plate at 2–2.5 x 10^4 cells/well 24 h before the addition of drugs. Different concentrations of drugs were added to the cells in a serum-free medium and left for 4 h before the medium was replaced with complete media. Twenty µl of CellTiter-BlueTM reagent was added to each well 24 h after the addition of drugs. The cells were incubated further for 1–4 h at 37°C. Fluorescence at 560/590 nm was measured in a SpectraMax Gemini XPS spectrophotometer (Molecular Devices, Sunnyvale, CA).

Competitive heparin assay

HEK 293 and NIH 3T3 cells were plated in a 12-well plate for 24 hours, then media was replaced with DMEM and treated with heparin (100 µg/mL) for 1 h at 37ºC. Either NtAd or PLL-g-PEG-FlAd was then added to the cells and incubated for 24–36 h. The transduction efficiency was measured as mentioned before and data were compared to untreated controls.

Drug inhibitor-based trafficking studies (Transduction)

HEK 293 and NIH 3T3 cells were seeded 24 h before transduction at 10^5 cells/well in 12-well plates. Growth media containing serum was replaced with serum-free DMEM along with the addition of predetermined concentrations of drugs. After 1 h of incubation with drugs, NtAd, FlAd, or hybrid vectors were added dropwise. The transduction media was replaced again with complete media 4 h post-transduction. Transduction efficiency was measured 48 h post-transduction as mentioned above.

Drug inhibitor-based trafficking studies (Cellular uptake)

HEK 293 and NIH 3T3 cells were seeded 24 h before transduction at 10^5 cells/well in 12-well plates. Growth media containing serum was replaced with serum-free DMEM along with the addition of predetermined concentrations of drugs. After 1 h of incubation with drugs, NtAd, FlAd, or hybrid vectors were added dropwise. The cells were washed with PBS containing 0.001% SDS 4 h post-transduction to remove surface-bound, uninternalized vectors. Cells were

then washed twice with room temperature PBS and harvested by scraping into PBS, centrifuging at 100 × *g* for 4 minutes at 4°C, and resuspending in PBS.

Statistical analysis

All statistical analyses mentioned in this study were done using the ANOVA analysis followed by a post-ad-hoc test. A result was deemed not significant (ns) if $p > 0.05$. (# $p < 0.05$; ## $p < 0.01$; ### $p < 0.001$; * $p < 0.0001$).

4.3 RESULTS

The role of heparan sulfate proteoglycans in vector transduction

Ad5 primarily binds to CAR via its fiber protein, followed by secondary interactions of the virus penton base protein with αv integrins on the cell [62]. Heparan sulphate proteoglycans (HSPGs) are also involved in the binding of Ad5 as receptors [281, 282]. Since we are studying a fiberless adenovirus, CAR interactions do not appear to be the key mechanism for cell binding. An alternative cell surface interaction, however, is the electrostatic attraction between vector cations and highly anionic cell surface proteoglycans. We wanted to verify that our hybrid vector interacts with HSPGs and uses them as receptors to bind to the cells. We treated HEK 293 (CAR-positive) and NIH 3T3 cells (CAR-negative) cells with heparin to competitively bind to HSPGs. In HEK 293 cells, heparin decreased the transduction efficiency of PLL-g-PEG-FlAd by 50%, while no inhibitory effect on the transduction of NtAd was observed. In contrast, the addition of heparin reduced transduction of NIH 3T3 by NtAd and PLL-g-PEG-FlAd by 30% and 58%, respectively (Figure 4.2).

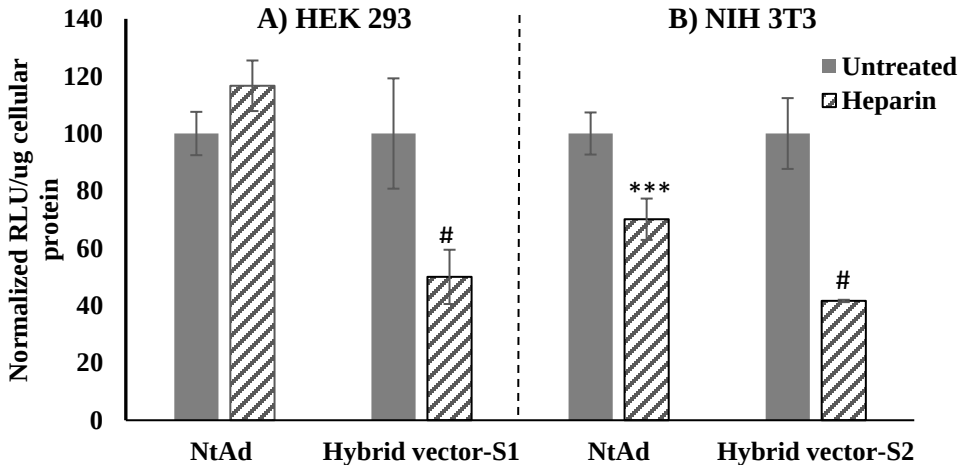

Figure 4.2: Transduction efficiency of A) NtAd and hybrid vector S_1 ($PLL_{15\text{-}30}$-$g_{25\%}$-$PEG_{0.5}$-FlAd) in HEK 293 cells and B) NtAd and hybrid vector S_2 ($PLL_{4\text{-}15}$-$g_{5\%}$-PEG_5-FlAd) in NIH 3T3 cells after treating both cell lines with heparin. Y-axis – Normalized RLU/µg total protein = Relative Light Units per µg total protein in cellular lysate normalized to the same expression for untreated cells. #$p<0.0001$, ***$p<0.001$.

Binding and internalization studies

We measured the binding and internalization of PLL-g-PEG-FlAd to investigate whether the lower level of transduction efficiency observed for PLL-g-PEG-FlAd in HEK 293 and NIH 3T3 cells (compared to NtAd) was caused by low levels of binding and/or inefficient internalization of the vector.

The binding amount of the virus/ hybrid vector was determined by halting the endocytosis of the virus/hybrid vector at low temperature, followed by removal of unbound virus then quantitation of the remaining bound virus/hybrid vector to the cell membrane. The internalized amount was then compared to the respective amount of the virus/hybrid vector bound to the cell membrane. The binding and internalization of FlAd and PLL-g-PEG-FlAd on HEK 293 cells (CAR-positive) were lower compared to that of NtAd (Figure 4.A). In CAR-positive (HEK 293) cells, removal of the fiber and knob protein decreased the binding of the virus to only 17% compared to the native virus. Although, not able to completely restore cell binding, addition of the copolymer significantly improved the cell binding to 76%. FlAd showed good internalization results where all of the virus bound to the cells was internalized inside. While 63% of the bound hybrid vectors were internalized inside the cells. The same study was carried in CAR-negative (NIH 3T3) to investigate the relatively high level of transduction efficiency observed for PLL-g-PEG-FlAd compared to NtAd or FlAd. Hybrid vectors showed a 55-fold increase in binding levels compared to NtAd and FlAd that barely bound to the cells (Figure 4.B). In contrast, at least 80% of the NtAd, FlAd, and the hybrid vector cell bound particles were internalized into the cells.

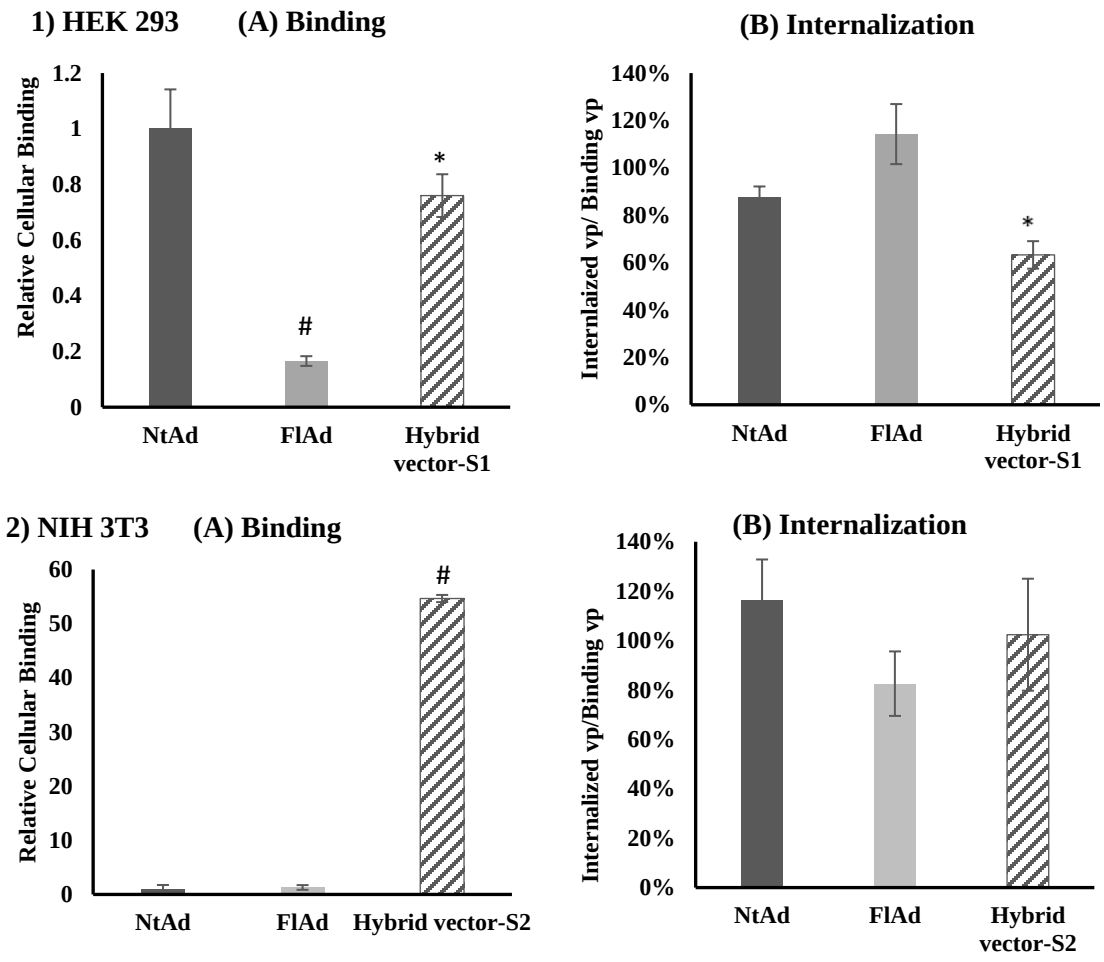

Figure 4.3: (1) Binding (A) and internalization (B) of NtAd, FlAd, and $PLL_{15\text{-}30}$-$g_{25\%}$-$PEG_{0.5}$-FlAd in HEK 293 cells, (2) Binding (A) and internalization (B) of NtAd, FlAd, $PLL_{4\text{-}15}$-$g_{5\%}$-PEG_{5}-FlAd in NIH 3T3 cells. In (A) Binding results are normalized to NtAd values. In (B) Internalization results are normalized to the respective binding values of each vector. *p<0.05, **p<0.01, ***p<0.001, #p<0.0001.

Effect of pharmacological inhibitors on cellular uptake and transduction efficiency of NtAd, FlAd, and PLL-g-PEG-FlAd hybrid vectors

Determining the optimal concentration of drug inhibitors. The use of pharmacological inhibitors is a well-known method to study the intracellular trafficking mechanisms of drug and gene delivery vectors [260]. These drugs inhibit specific intracellular pathways leading to modified trafficking mechanisms and/or shut down of the pathway which would be observed in the decrease in the transduction efficiency. By studying the results of the various inhibitions, a map for the trafficking of hybrid vectors through the cells would be designed.

These drug inhibitors, however, are cytotoxic beyond certain concentrations and can affect the transgene expression via non-specific mechanisms [283]. Therefore, the drug inhibitors cytotoxicity was studied to optimize the concentration to be used in HEK 293 and NIH 3T3 cells. The optimal concentration was decided based on the highest drug concentration that resulted in > 90% cell viability.

Table 4.1 summarizes the mechanism of the action of the drugs on intracellular trafficking as well as the concentration for their optimal use to study their inhibitory effect.

Table 4.1: Mechanism of action and optimal concentration of drug inhibitors

Drug	Effect and Mechanism of action	Optimal Concentration	Reference
Chlorpromazine (CPZ)	Disrupts assembly and disassembly of clathrin from coated pits (CME)	10 μg/ml	[284]
Amiloride (AMD)	Inhibition of Na^+/H^+ exchange protein (MP)	10 μg/ml	[285]
Genistein (GST)	Inhibition of tyrosine kinase preventing caveolae formation (CavME)	0.1 μg/ml	[286]
Bafilomycin A1 (BAF)	Blocks the v-ATPase proton pumps which prevents acidification of endosomal vesicles inhibiting release of endosomal cargo	100 nM	[287, 288]
Cytochalasin D (CCN)	Inhibits actin microfilaments depolymerization that can inhibit caveolae formation and macropinocytosis (CavMe,MP)	0.1 μg/ml	[289]
Colchicine (CLC)	Inhibits microtubule polymerization	0.1 μg/ml	[290, 291]

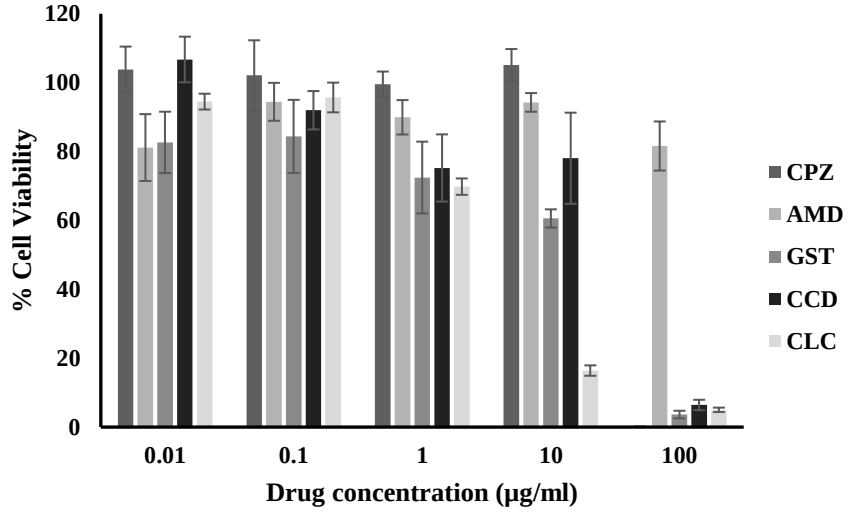

Figure 4.4: Cytotoxicity on HEK 293 cells after exposure to different concentrations of drug inhibitors (CPZ, AMD, GST, CCD, and CLC). Y-axis – % Cell viability, X-axis – Concentration (µg/ml).

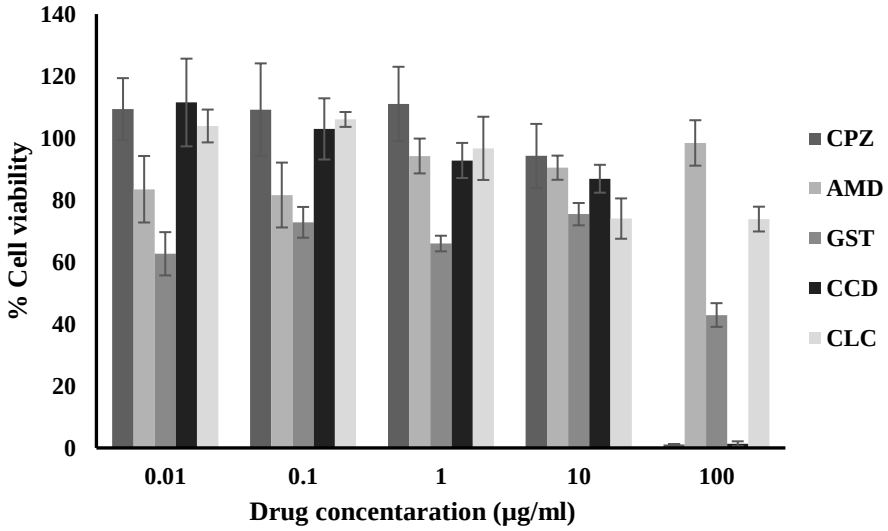

Figure 4.5: Cytotoxicity on NIH 3T3 cells after exposure to different concentrations of drug inhibitors (CPZ, AMD, GST, CCD, and CLC). Y-axis – % Cell viability, X-axis – Concentration (µg/ml).

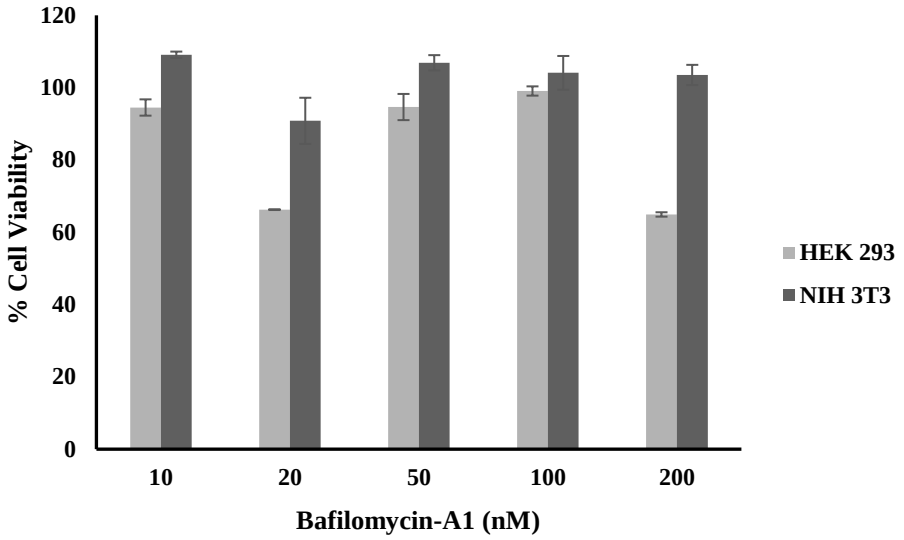

Figure 4.6: Cytotoxicity on HEK 293 and NIH 3T3 cells after exposure to different concentrations of Bafilomycin A1 (BAF). Y-axis – % Cell viability, X-axis – Concentration (nM).

Development of qPCR assay method for the quantitation of viral DNA

Primer design and HRM melting predictions. Three primer pairs were designed, one for Ad *E2* gene and two *ACTB* primers as housekeeping / internal control genes for HEK 293 and NIH 3T3 cells. All three primers are capable of being used in end-point PCR, qPCR, and HRM. Table 4.2 compiles thermodynamic features of designed primer sequences such as annealing temperature (Tm), predicted amplicon melting point (HRM Tm), oligo self-complementary score (Any), and oligo 3′ self-complementarity at the 3′ termini (3′). Primers for Ad *E2* gene amplify a segment of 194 bp of Ad genome. Primers for *ACTB*-HEK 293 and *ACTB*-NIH 3T3 amplify a 171 and 195 bp fragment of each cell line genome, respectively.

Table 4.2: Primer sequences for Ad E2 primers and the two ACTB housekeeping genes primers along with the corresponding thermodynamic values calculated by Primer 3 (v.0.4.0) for each.

	Target	Primer	Primer Sequence (5′ - 3′)	Tm (°C) *	Amplicon Size (bp)*	HRM Tm (°C) *	Any*	3′*
Ad	**NtAd or FlAd**	**Ad-*E2*-Fw**	AGGCTAAGTGGG AGGGGTAG	59.59	194	88.5	3	0
		Ad-*E2*-Rv	CGATGCGGAAG AGAGTGAG	59.67			2	0
Internal control	**HEK**	***ACTB*-Fw**	AAACTGGAACG GTGAAGGTG	60.01	171	84.5	3	0
		***ACTB*-Rv**	AGAGAAGTGGG GTGGCTTTT	60.11			3	0
	3T3	***ACTB*-Fw**	GCTGCGTTTTAC ACCCTTTC	59.75	195	74, 76.7	3	0
		***ACTB*-Rv**	CCTTCACCGTTC CAGTTTTT	59.07			3	0

*The thermodynamic metrics listed include primer annealing temperature (Tm), amplicon size (Size) predicted amplicon melting point (HRM Tm), oligo self-complementary score (Any), and oligo 3′ self-complementarity at the 3′ termini (3′).

Gradient PCR assays. Primers designed for Ad and the internal control genes successfully amplified their respective expected products, which matched predicted lengths. Gradient PCR was used to assess the optimal annealing temperature of each designed primer pair (Figure 4.7).Each of the primer pairs performed according to optimal thermodynamic values in Table 4.2. The annealing temperatures studied ranged from 50−62 °C, producing a clear, bright PCR product of the predicted length. When used to amplify NtAd or FlAd, the primer pair produced lower DNA yields when used at annealing temperatures above 60 °C as determined by visual assessment of DNA yields. 55°C was chosen as an annealing temperature as it showed bright, clear bands for all sets of primers.

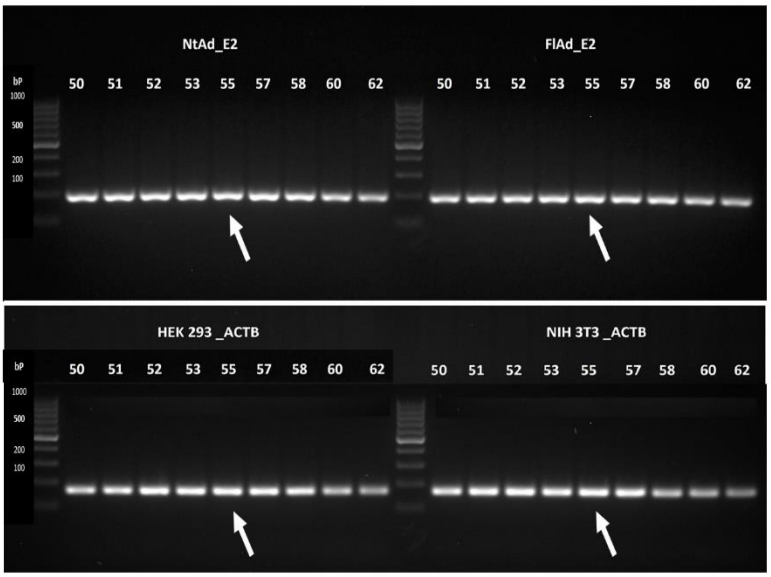

Figure 4.7*:* Gradient PCR of each primer pair and target template for Ad- E2, ACTB-HEK 293, *ACTB*-NIH 3T3 from 50 to 62 °C. Gel electrophoresis was performed on a 2% agarose gel in 0.5 x TAE at 95 V for approximately 45 min, alongside a 100 bp ladder (New England Biolabs, Ipswich, MA).

qPCR reaction mix and reaction conditions. A standard calibration curve was developed by measuring the quantity of purified FlAd in a serial dilution from 1 ng to 1 fg/µl. As shown in Figure 4.8.A each serial dilution generated separated real-time reactions with distinct threshold cycle values (Ct). The correlation coefficient (R2) for the line is 0.995 with an efficiency of 1.02 (Figure 4.8C). This plot is then used as a calibration curve for extrapolating relative expression levels of *E2* gene in unknown experimental samples. Absolute quantification of samples was used for determining binding and internalization levels of virus or hybrid vectors. Relative quantification of samples using the livak method ($\triangle\triangle C_t$) was used for comparing the cellular uptake of virus or hybrid vectors in untreated and drug inhibitor-treated cells. The relative quantification calibration curve results were normalized to that of a housekeeping gene in the same sample, and then the normalized numbers are compared between samples.

High-Resolution Melting Analysis (HRM) is a recently developed technique for fast, high-throughput post-PCR analysis of genetic mutations or variance in nucleic acid sequences.

After completion of the PCR step, the amplified target is gradually denatured by increasing the temperature in small increments, to produce a characteristic melting profile; this is termed melting analysis. The amplified target denatures gradually, releasing a specialized dye, which results in a decrease in fluorescence. HRM curve shows differentiation in the rates at which PCR products of each concentration of Ad degraded as temperature increased (Figure 4.8B).

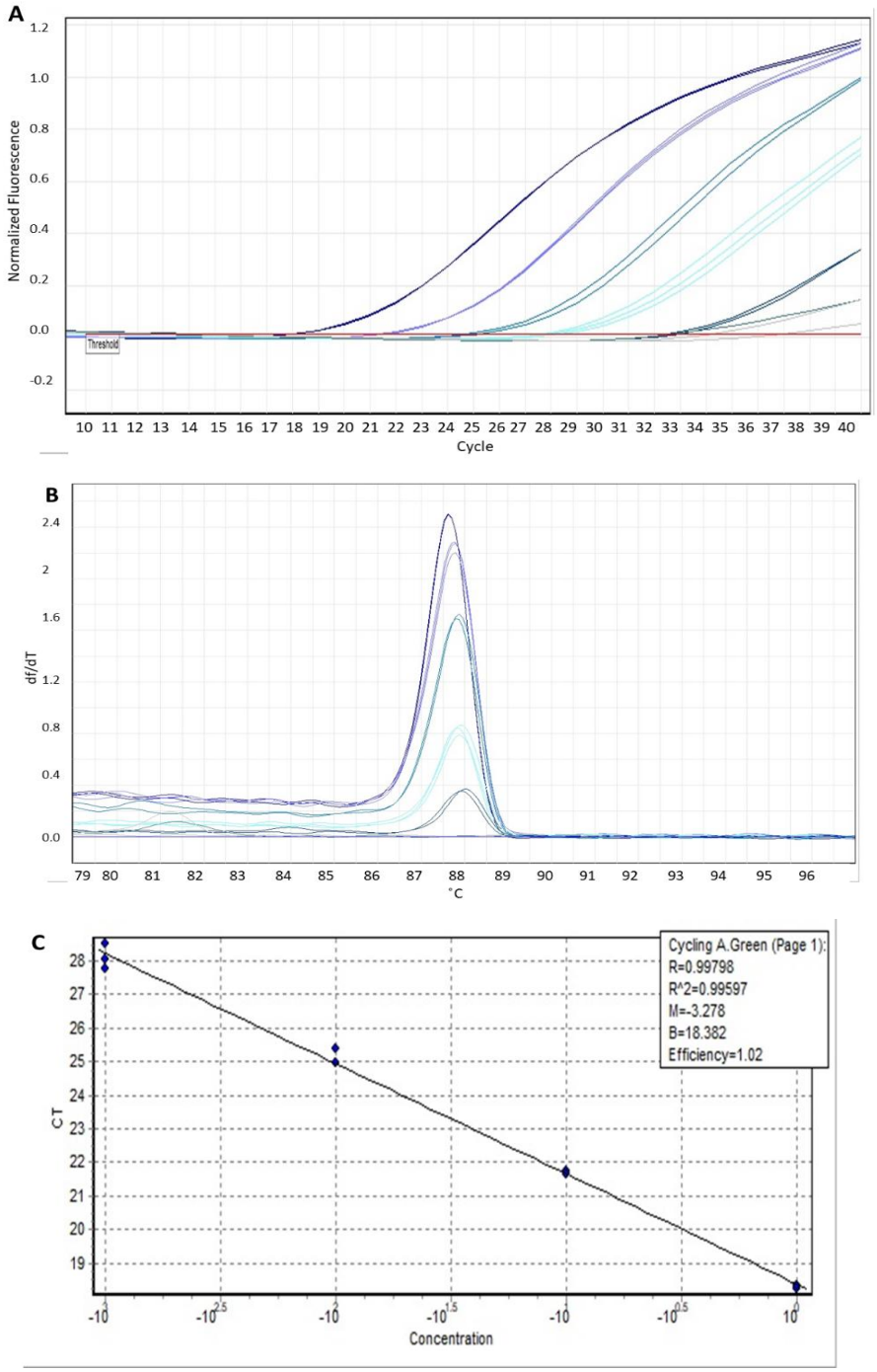

Figure 4.8: qPCR standard curve. A) A representative amplification plot, B) HRM df/dT melting curve, and C) a standard curve is shown. A six-fold serial dilution of purified Ad, ranging from 1 ng to 1 fg/µl, was used to generate both plots.

Cellular internalization mechanism of the hybrid vector (PLL-g-PEG-FlAd) in CAR-positive cells (HEK 293) and CAR-negative cells (NIH 3T3)

A hybrid viral vector is a promising tool for gene therapy approaches. Analyzing the vector internalization and trafficking pathways within the cell is crucial nowadays. This is especially essential when comparing to viral vectors that benefit from their inherent high cell transduction efficiency. Understanding uptake mechanisms and intracellular pathways of the vector will lead to improvement in the design of hybrid vectors for further applications.

We studied the cellular uptake of PLL-g-PEG-FlAd in CAR-positive (HEK 293) and CAR-negative (NIH 3T3) cells. The cellular uptake of NtAd and FlAd served as effective controls for elucidating the changes that occur in the trafficking mechanism due to the presence of the copolymer (PLL-g-PEG) as a synthetic part that functions in place of the fiber of the virus.

Clathrin-, caveolin-, and macropinocytosis- mediated pathways are proposed to be the main routes of endocytosis for viral vectors [261, 292]. To assess the role of these three endocytic pathways in the entry of PLL-g-PEG-FlAd hybrid vectors, each pathway was blocked by a specific drug inhibitor. Chlorpromazine is known to block clathrin-mediated internalization [284], while genistein inhibits tyrosine kinase preventing caveolae dependent pathway [293], and amiloride is used to inhibit the macropinocytosis [294] by preventing the induction of membrane ruffling.

The cellular uptake of the virus and hybrid vectors in HEK 293 cells in the presence of inhibitors of clathrin- or caveolae- or macropinocytosis mediated uptake is represented in figure 4.9A. The cellular uptake of NtAd decreased significantly (to 30%) when clathrin-mediated endocytosis was blocked by CPZ ($p<0.0001$). The uptake of the virus was also reduced (to 60%) when macropinocytosis was blocked by AMD ($p<0.0001$). This data is consistent with the major role of clathrin-mediated endocytosis and the minor role of macropinocytosis in the internalization of Ad [295]. The same effect was shown with the cellular uptake of FlAd, where the uptake decreased to 60% ($p<0.01$) and 40% ($p<0.0001$) after treating cells with CPZ and

AMD, respectively. For PLL-g-PEG-FlAd, the uptake was significantly reduced to 60% ($p<0.05$) when either clathrin or macropinocytosis pathways was blocked. We observed that neither the cellular uptake of the virus nor the hybrid vector was affected upon treating the cells with GST, as caveolin was not reported to be a pathway for internalization of Ad.

As the cellular uptake is not indicative of gene expression, gene expression experiments in the presence of the same drug inhibitors were performed. As shown in Figure 4.9B, CPZ significantly reduced the transduction efficiency of NtAd and FlAd, to 35% and 45% ($p<0.0001$), respectively. Similarly, CPZ caused a 50% ($p<0.0001$) reduction in the transduction efficiency of PLL-g-PEG-FlAd. Interestingly, pre-treatment with AMD inhibited the gene expression of PLL-g-PEG-FlAd to a significantly greater degree (80%) ($p<0.0001$) than that of NtAd (45%) ($p<0.01$).

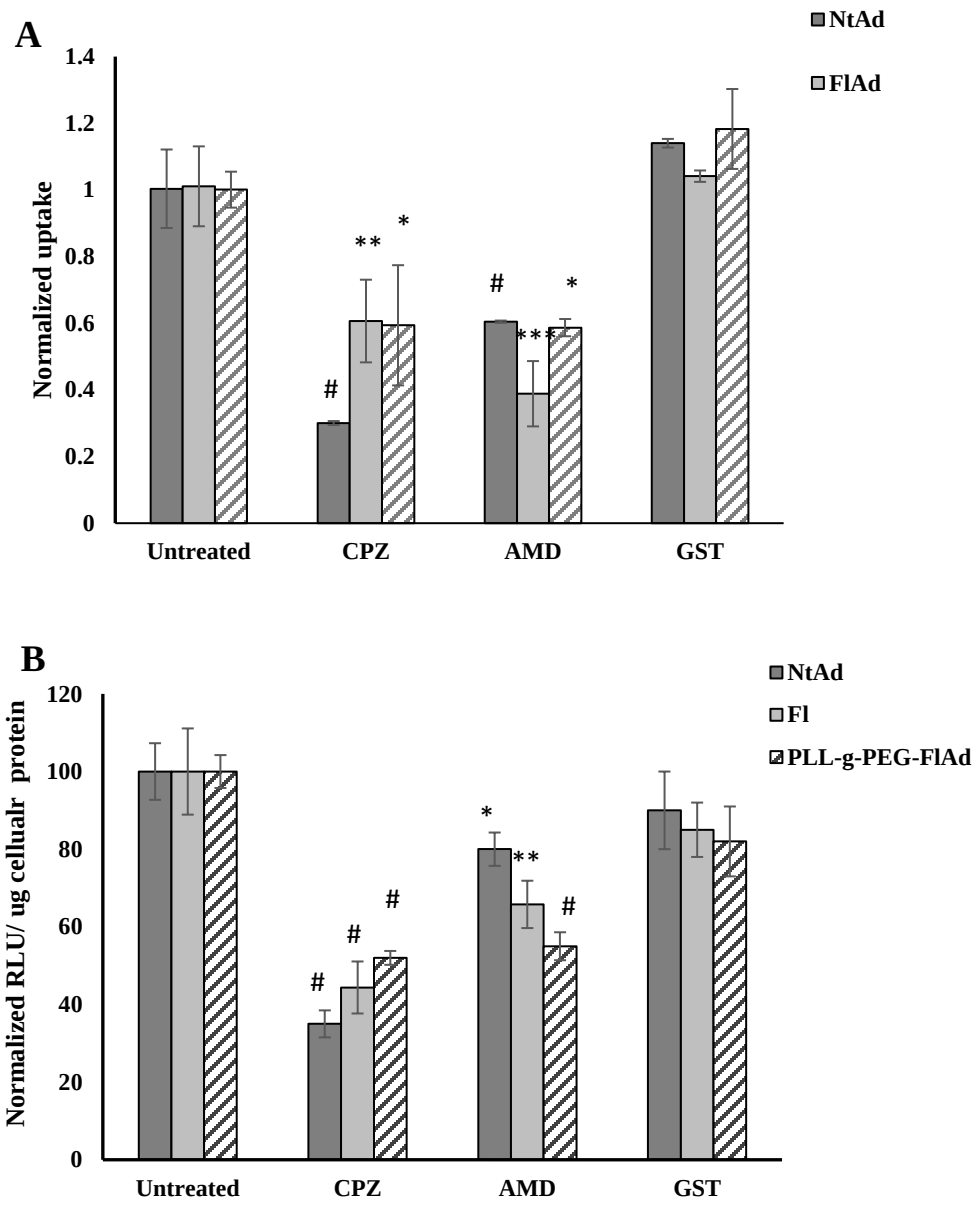

Figure 4.3: A) Cellular uptake and B) transduction efficiency of NtAd, FlAd, and $PLL_{15\text{-}30}\text{-}g_{25\%}\text{-}PEG_{0.5}$-FlAd in the presence of drug inhibitors in HEK 293 cells. Y-axis – Normalized values of the virus or hybrid vector normalized to the same uptake for untreated cells. X-axis – Drugs at optimal concentrations. * $p<0.05$, ** $p<0.01$, *** $p<0.001$, # $p<0.0001$.

Since cellular trafficking is cell dependent, we studied the internalization mechanism of PLL-g-PEG-FlAd in CAR-negative (NIH 3T3) cells. The cells were treated with the same drug inhibitors to block the three endocytic pathways, clathrin, caveolar, and macropinocytosis mediated endocytosis. The cellular uptake of PLL-g-PEG-FlAd hybrid vector was measured and compared to that of NtAd as represented in Figure 4.10A. The cellular uptake of NtAd decreased to 42% ($p<0.001$) and to 22% ($p<0.0001$) when clathrin-mediated endocytosis and macropinocytosis were blocked by CPZ and AMD, respectively. The uptake of PLL-g-PEG-FlAd, in contrast, was diminished by the clathrin- and caveolae-mediated endocytic drug inhibitors to 47%, and 65%, respectively. The transduction efficiency was also studied as demonstrated in Figure 4.10B. The transduction efficiency of NtAd decreased to 45% ($p<0.0001$) and 81% ($p<0.01$) after using clathrin- and macropinocytosis mediated endocytosis drug inhibitors, respectively. While the transduction efficiency of PLL-g-PEG-FlAd decreased to 55% ($p<0.0001$), and 75%($p<0.01$) after treating the cells with clathrin- and caveolar-mediated endocytosis drug inhibitors, respectively.

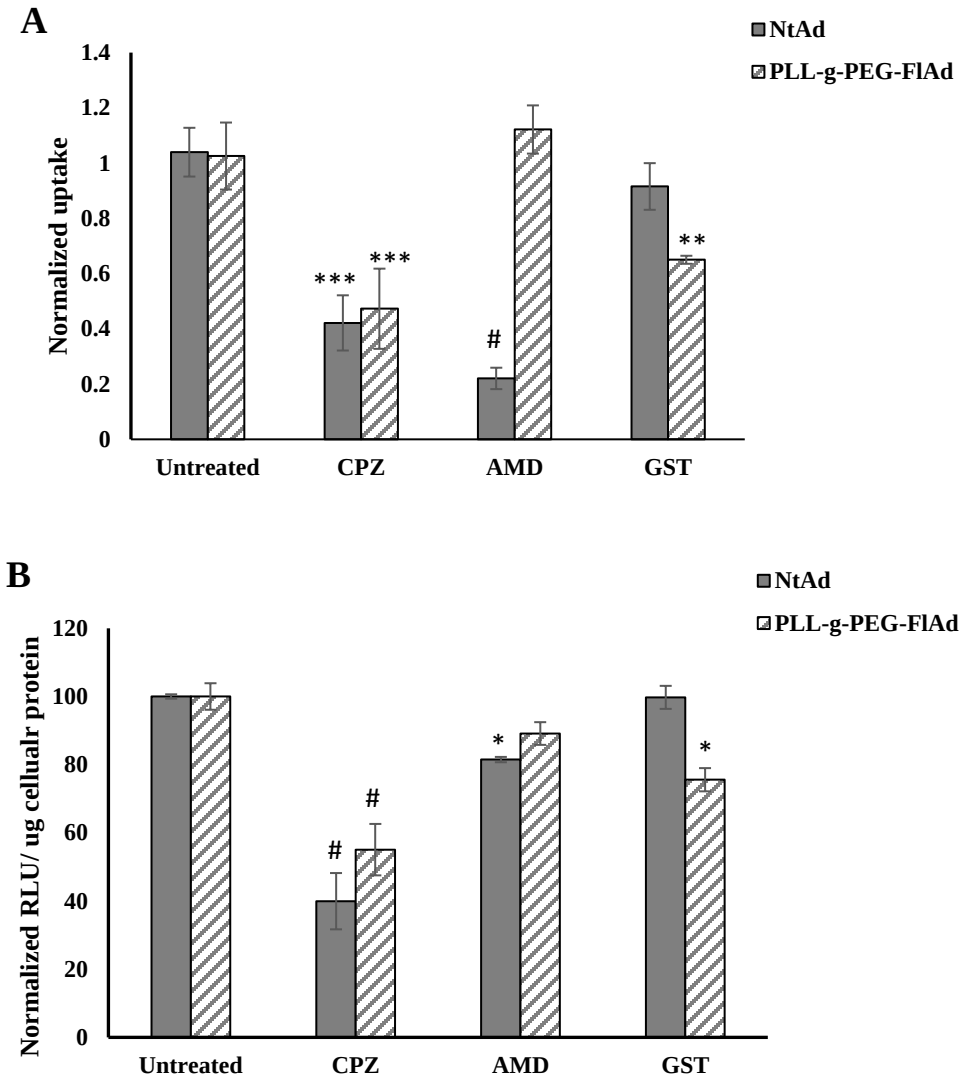

Figure 10: A) Cellular uptake and B) transduction efficiency of NtAd, and $PLL_{4\text{-}15}$-$g_{5\%}$-PEG_5-FlAd in the presence of drug inhibitors in NIH 3T3 cells. Y-axis – Normalized values of the virus or hybrid vector normalized to the same uptake for untreated cells. X-axis – Drugs at optimal concentrations. * $p<0.05$, ** $p<0.01$, *** $p<0.001$, # $p<0.0001$.

Endolysosomal escape of the hybrid vector (PLL-g-PEG-FlAd) in CAR-positive cells (HEK 293) and CAR-negative cells (NIH 3T3)

After internalization of the hybrid vector into endosomes, the hybrid vector must escape the endosomal vesicles to be released into the cytoplasm before being degraded by the lysosomal proteases. A drop in pH is concomitant with the escape of Ad from the endocytic vesicle. Yet, the precise role of pH in virus disassembly is under investigation [296]. The cellular uptake and the transduction efficiency of NtAd, FlAd, and PLL-g-PEG-FlAd in the presence of BAF were studied in HEK 293 cells as shown in Figure 4.11A and B, respectively. The cellular uptake of either the virus or the hybrid vector was unaffected when BAF was used as this drug does not affect internalization, rather it inhibits the acidification of endosomes. To investigate whether the endosomal acidification is required for transduction of PLL-g-PEG-FlAd vectors, BAF was added to the cells prior to their transduction by hybrid vectors. The transduction efficiencies of hybrid vectors were compared to that of NtAd and FlAd under the same conditions. Figure 4.11B shows that the transduction efficiency of NtAd was significantly decreased (to 65%) ($p<0.0001$), while that of FlAd was further reduced (to 38%) ($p<0.0001$. In case of PLL-g-PEG FlAd, the transduction efficiency decreased to almost the same level as NtAd (to 65%). This indicates that low-pH endosomal processes are essential for the productive transduction of the virus and hybrid vectors.

The effect of acidification inhibition on the endosomal escape of PLL-g-PEG-FlAd vectors in CAR-negative (NIH 3T3) cells was also studied. No significant change in the cellular uptake of NtAd or PLL-g-PEG-FlAd was noticed upon treating the cells with BAF as represented in Figure 4.12A. However, BAF inhibited the acidification of endosomes in NIH 3T3 cells which lead to a reduction in the transduction efficiency of NtAd and PLL-g-PEG FlAd to 79% ($p<0.01$) and 30% ($p<0.0001$), respectively (Figure 4.12B).

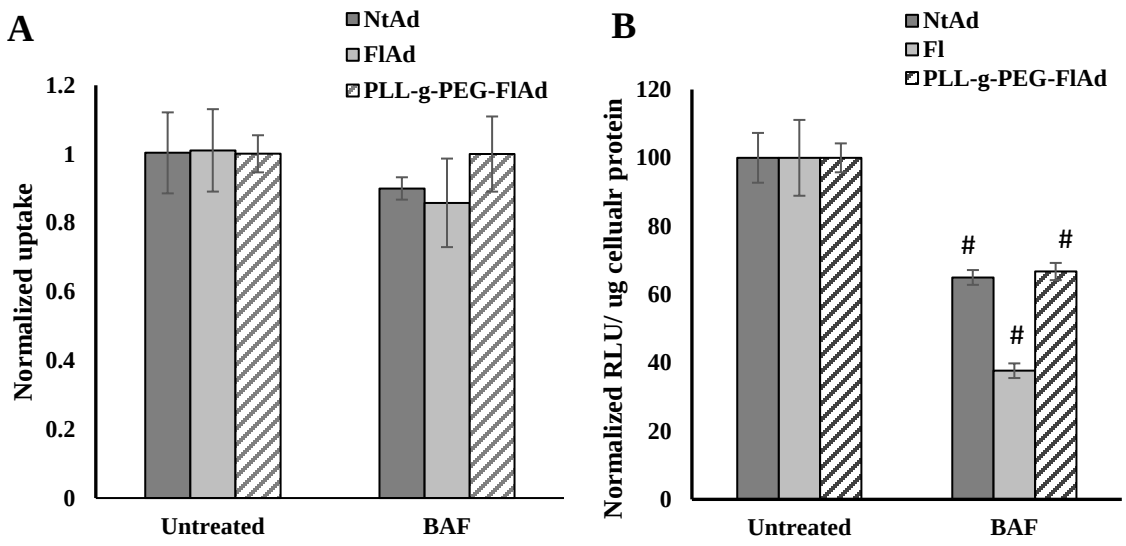

Figure 4.11: A) Cellular uptake and B) transduction efficiency of NtAd, and $PLL_{15\text{-}30}$-$g_{25\%}$-$PEG_{0.5}$-FlAd in the presence of Bafilomycin (BAF) in HEK 293 cells. Y-axis – Normalized values of the virus or hybrid vector normalized to the same uptake for untreated cells. X-axis – Drugs at optimal concentrations. * p<0.05, **p<0.01, ***p<0.001, #p<0.0001**.**

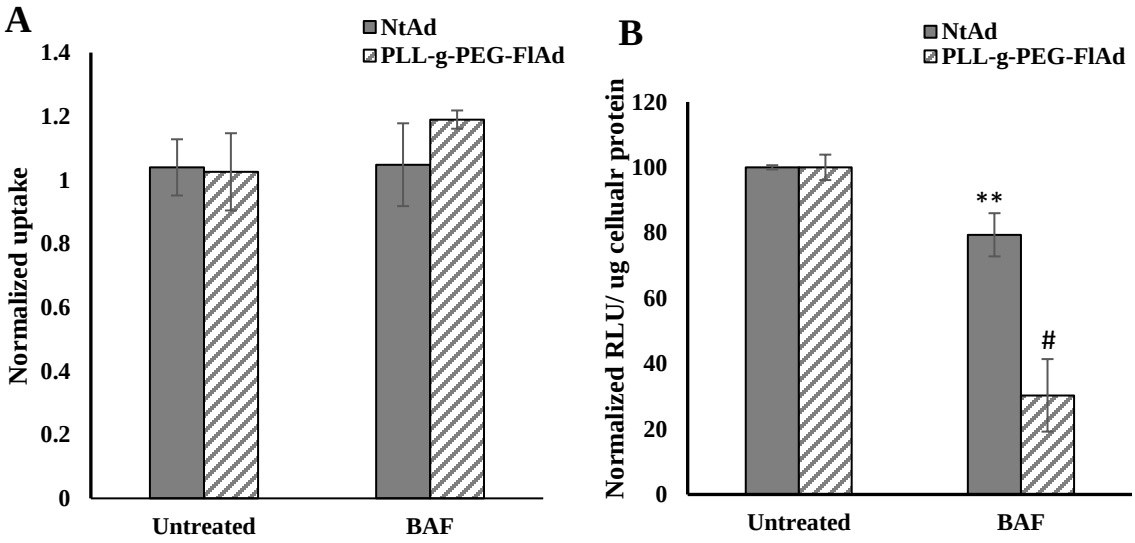

Figure 4.12: A) Cellular uptake and B) transduction efficiency of NtAd, and $PLL_{4\text{-}15}$-$g_{5\%}$-PEG_5-FlAd in the presence of Bafilomycin (BAF) in NIH 3T3 cells. Y-axis – Normalized values of the virus or hybrid vector normalized to the same uptake for untreated cells. X-axis – Drugs at optimal concentrations. * p<0.05, **p<0.01, ***p<0.001, #p<0.0001.

Intracellular trafficking of the hybrid vector (PLL-g-PEG-FlAd) in CAR-positive cells (HEK 293) and CAR-negative cells (NIH 3T3)

After endosomal escape, the virus/hybrid vector is released into the cytosol to complete its journey to deliver the transgenes to the nucleus. To be transported across the cytoplasm, particles can interact with the cytoskeletal network including the microtubules and/or actin filaments to be directed towards the nucleus. The cellular uptake and the transduction efficiency of NtAd, FlAd, and PLL-g-PEG-FlAd were studied in HEK 293 cells after disruption of the microtubules or the actin filaments with CLC or CCD, respectively (Figure 4.13A and B). Upon treating the cells with CLC, no significant change in the cellular uptake of NtAd, FlAd or PLL-g-PEG-FlAd was observed as this drug does not affect their internalization. However, the transduction efficiency of NtAd, FlAd, and PLL-g-PEG-FlAd significantly decreased to 40%, 30%, and 15% after treating the cells with CLC respectively ($p<0.0001$). Upon treating the cells with CCD, the drug prevented the polymerization of actin filaments leading to their destabilization. The cellular uptake of NtAd was unaffected, while that of FlAd and PLL-g-PEG-FlAd significantly decreased to 45% and 65% ($p<0.05$), respectively. Regarding the virus/hybrid vector ability to deliver genes into the nucleus after actin filaments destabilization by CCD. We observed a decrease in the transduction efficiency of NtAd, FlAd, and PLL-g-PEG-FlAd by 35% ($p<0.001$), 45% ($p<0.0001$) and 30% ($p<0.01$), respectively.

We studied the effect of microtubule disruption or actin filament depolarization on the cellular uptake and the transduction efficiency of the hybrid vector in NIH 3T3 cells as well. The cellular uptake of the hybrid vector was unaffected upon treatment with either CLC or CCD (Figure 4.14A). The transduction efficiency of PLL-g-PEG-FlAd significantly decreased after treating cells with CLC, to 62% ($p<0.001$) (Figure 4.14B). The same effect was seen upon disrupting the actin microfilaments with CCD, where the transduction efficiency of PLL-g-PEG-FlAd decreased to 40% ($p<0.0001$). In contrast, the transduction efficiency of NtAd was not affected by either drug inhibitors.

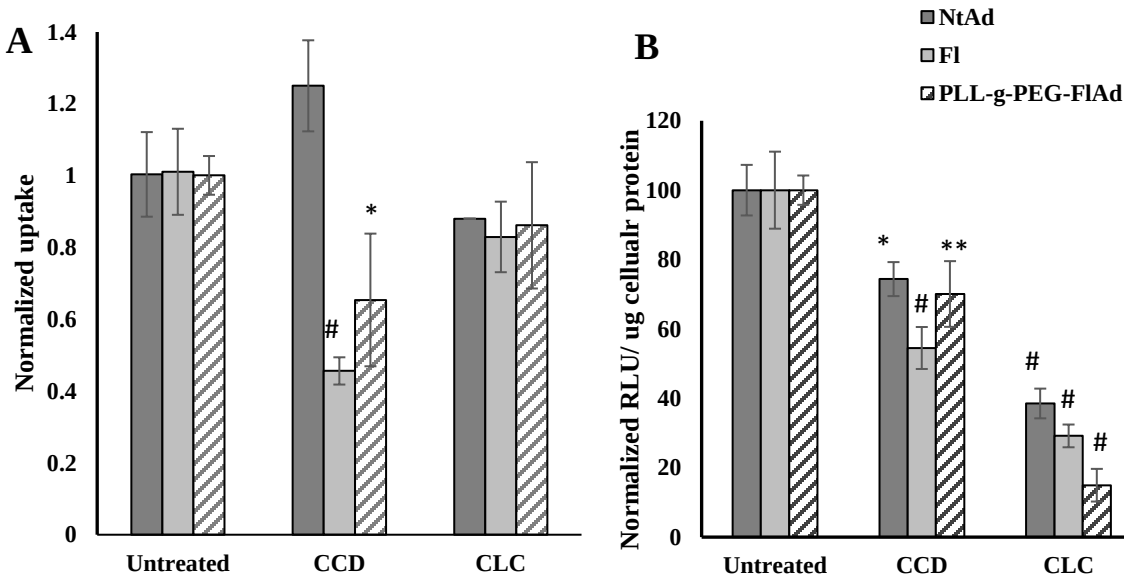

Figure 4.3: A) Cellular uptake and B) transduction efficiency of NtAd, and $PLL_{15\text{-}30}\text{-}g_{25\%}\text{-}PEG_{0.5}$-FlAd in the presence of drug inhibitors in HEK 293. Y-axis – Normalized values of the virus or hybrid vector normalized to the same uptake for untreated cells. X-axis – Drugs at optimal concentrations. * $p<0.05$, ** $p<0.01$, *** $p<0.001$, # $p<0.0001$.

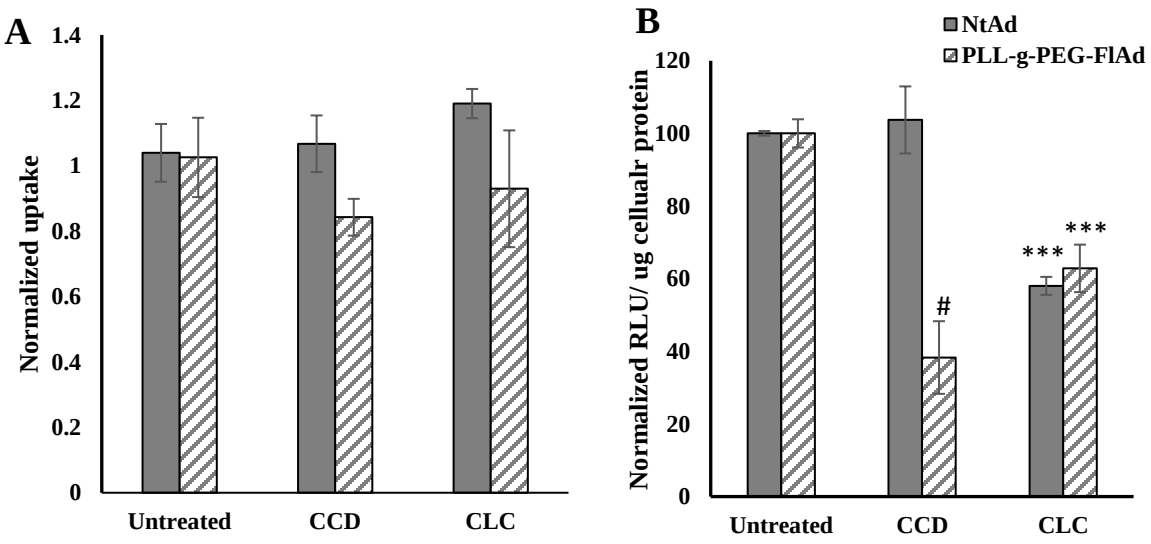

Figure 4.3: A) Cellular uptake and B) transduction efficiency of NtAd, and $PLL_{4\text{-}15}\text{-}g_{5\%}\text{-}PEG_{5}$-FlAd in the presence of drug inhibitors in NIH 3T3. Y-axis – Normalized values of the virus or hybrid vector normalized to the same uptake for untreated cells. X-axis – Drugs at optimal concentrations. * $p<0.05$, ** $p<0.01$, *** $p<0.001$, # $p<0.0001$.

4.4 DISCUSSION

Accounting for the effects of intracellular trafficking is of critical importance to ensure that engineered viral vectors can induce good gene expression in target cells. In our study, the adenovirus fiber protein was removed to eliminate the dependency of the virus on the CAR, which led to the virus losing its ability to bind to cells. We replaced the function of the fiber with PLL-g-PEG and wanted to study how the properties of this synthetic coating would affect the gene delivery trafficking pathway. By comparing the hybrid vector performance to the native virus, we can determine the important steps in the gene delivery process and design better materials accordingly. Cellular trafficking experiments were based on quantifying the virus *via* a qPCR technique, which was designed to amplify the adenoviral *E2* gene. Since the expression of Ad *E2* gene starts to increase between 12 and 13 hours after infection [297], quantifying the viruses within the first few hours guaranteed that the measured viruses were the experimentally added viruses to the cell and not any of their progeny.

The first step to Ad transduction is the binding of the virus to the cell surface followed by internalization. We studied the binding and internalization of PLL-g-PEG-FlAd and compared it to NtAd and FlAd in CAR-positive (HEK 293) and CAR-negative (NIH 3T3) cells. FlAd had a poor binding ability to HEK 293 cells because of the absence of the key binding pathway which is the interaction of the knob domain of the fiber protein and CAR. Upon modifying FlAd with PLL-g-PEG copolymer, the ability of the hybrid vector to bind to the cell was partially restored. The affinity of NtAd to CAR is much higher compared to the lower electrostatic attraction between the cationic hybrid vectors and the anionic cell membrane[298]. All NtAd bound to cells were internalized while only approximately two thirds of hybrid vectors that bound to cells were internalized. This might explain the observed lower transduction efficiency of the hybrid vector compared to NtAd. The results infer that internalization of the hybrid vector is a bottleneck towards achieving better gene delivery in CAR-positive cell. In contrast, the hybrid vector

showed high binding levels in CAR-negative cells that were 55-fold higher compared to NtAd and FlAd. Both NtAd and FlAd virus lacked an efficient way to bind to the cell membrane while the hybrid vector used electrostatic attraction to mediate good binding to CAR-negative cells. All the NtAd, FlAd, and hybrid vectors achieved high levels of internalization (> 80% of the respective virus/hybrid vector bound to the cells). These results suggest that if we were able to design vectors with higher binding capacity to CAR-negative cells, we would have a greater number of internalized viruses and thus better gene delivery efficiency.

HSPGs are glycoproteins with a heparan sulfate moiety and are ubiquitously expressed by most mammalian cell types [299]. HSPGs can serve as a co-receptor for Ad thereby increasing the concentration of virus at the cell surface and leading to more efficient interaction with CAR [281, 282]. HSPGs possess an overall negative charge and can interact electrostatically with cationic viral capsid proteins [300]. We hypothesized that our cationic hybrid vectors would attach to the cells *via* electrostatic interactions with HSPGs. Since heparin has a structure that is similar to heparan sulfate [301], heparin acts as a competitive inhibitor and decreases the hybrid vector electrostatic interactions with heparan sulfate. We demonstrated here that the addition of heparin immediately before transduction with hybrid vectors reduced the levels of gene delivery. This suggests that binding to heparan sulfate may play a role in the transduction of our hybrid vectors in the absence of higher affinity interactions like CAR binding.

Next, we studied the endocytic pathways in CAR-positive (HEK 293) cells that the hybrid vector uses compared to the native virus. Cellular entry of NtAd was primarily based on clathrin-mediated endocytosis as indicated by the reduction in cellular uptake and transduction efficiency in the presence of CPZ (Figure 9A and B). Although not as impactful as CPZ, AMD also reduced the uptake and transduction of NtAd proving that macropinocytosis is an additional route that the virus uses to enter cells. Our findings are consistent with other studies that state that Ad uses macropinocytosis in addition to clathrin-mediated endocytosis for cell entry [302, 303]. While NtAd used clathrin-mediated endocytosis more than macropinocytosis; FlAd used both

pathways almost equally to enter the cells. This observed effect might be attributed to the fact that FlAd lacks the fiber-CAR interaction that prompts clathrin mediated endocytosis and instead binds to αv integrin which triggers macropinocytosis [304]. Our study shows that the virus fiber is not required for viral entry and is supported by previous findings reporting that the shedding the fiber and viral entry *via* endocytosis appear to be independent events during adenovirus cell entry [305].The hybrid vector entered the cell *via* clathrin-mediated endocytosis and macropinocytosis equally as shown in Figure 4.9A and B. Several studies have reported that cellular internalization of cationic polyplexes (ex: PLL-DNA) was through clathrin-dependent and independent endocytosis and macropinocytosis pathways [267, 270, 306].

After endocytosis, we studied endolysosomal escape and the cytoplasmic transport using BAF and CLC, respectively. At first, we evaluated the effect of each drug on the cellular uptake of hybrid vectors to confirm that the decrease in transduction efficiency was due to impaired endolysosomal escape or cytoplasmic transport and not by the inhibition of cellular uptake. Neither drug showed a significant effect on the cellular uptake of the virus or the hybrid vector (Figure 4.11A and Figure 4.13A).

Endosomal escape is known as a possible rate-limiting step and may explain the differences in gene expression. There has been some debate on whether or not acidification of endosomes (pH 4.6 – 6.0) is necessary for infection by NtAd [305], with some arguments stating that acidification triggers conformational changes that lead to release of the membrane lytic protein VI [307] and others arguing that different mechanical stresses between the virus and integrins in the cell plasma membrane during cellular entry may initiate disassembly of the virus particle even before it reaches the early endosome to help release protein VI [308]. Regardless of what leads to release of protein VI, once the protein is released a membrane lytic region is inserted into the endosomal membrane imparting partial membrane rupture and release of the virus into the host cell cytoplasm [251].

Our results suggest that both mechanisms for release of protein VI may be relevant. Blocking acidification of endosomes appears to have some effect on the performance of NtAd with a 35% decrease in its transduction efficiency as shown in Figure 4.11B. Although blocking acidification negatively impacted the performance of the virus, it did not completely eliminate its ability to infect. This may be because the virus has undergone conformational changes through mechanical stresses created by the virus binding to integrins that leads to some exposure of protein VI and endosomal escape of the virus [309]. FlAd is expected to also be sensitive to blocking acidification of endosomes since the fiber is not present to undergo a pH-induced conformation transformation that leads to release of protein VI. Further, the absence of the fiber protein will greatly reduce the mechanical stresses that would normally occur as a result of fiber protein binding to CAR and integrin receptors[305]. Consistent with this was our observation that blocking acidification of endosomes reduced transduction efficiency of FlAd by 70%. Our results show that the Ad fiber protein plays an important role in Ad disassembly and escape from the endolysosomal pathway and that its role requires acidification of the endosome, consistent with the mechanistic studies mentioned above.

Interestingly, the addition of PLL-g-PEG to FlAd appears to offset the impact of BAF on a fiberless virus particle. Blocking acidification still reduces the transduction efficiency of the hybrid vector but only by ~35% not the ~70% experienced by the fiberless virus. Different hypotheses have been postulated to explain how cationic polymers such as PLL-g-PEG are able to escape from endosomes [41]. We attribute the endosomal escape of hybrid vectors to either of the two following theories. First, the cationic hybrid vector might have interacted with the endosomal membrane leading to membrane damage/permeability and nanoscale hole formation [268, 271, 272]. Banaszak Holl and his group investigated a broad range of cationic polymers including PLL and identified membrane damages like membrane thinning and transient membrane hole formation which lead to leakage of nanosized cargo [310]. Second, the free cationic PLL-g-PEG chains might have intercalated into the endosomal membrane to cause

defects in the lipid layer and leakage of the nanosized vectors. Previous studies have reported the effect of the free polymer-mediated membrane permeability in endosomal escape [311].

After endosomal escape, the virus is released into the cytosol to be transported to the nucleus. There are two main types of cytoskeletal polymers, actin filaments and microtubules, that are responsible for transport of intracellular cargo [312]. CLC disrupted microtubules without significantly affecting the cellular uptake of NtAd or hybrid vectors (Figure 4.13A). However, the transduction efficiency of NtAd decreased by 60%, while that of the hybrid vector transduction further decreased by 85% compared to untreated cells (Figure 4.13 B). Previous studies showed that drug inhibitors like CLC that disrupt microtubules had no effect on cell entry but prevented viral translocation to the nucleus [313]. Based on our data, we can deduce that the hybrid vector is more highly dependent on microtubules as a cytosolic transport mechanism than NtAd.

Actin microfilaments are the other cytoskeletal protein polymer that were studied. Actin microfilaments are present throughout the entire cytosol, but the highest concentration forms a network of actin microfilaments directly beneath the plasma membrane (i.e., actin cortex). The actin cortex plays a role in endocytosis of particles into cells as well as provide mechanical strength to cells grown in cell culture [314]. Actin filaments mediate various intracellular transport processes as well as assist in genome replication inside the nucleus [315].

CCD is a drug that prevents the polymerization of actin filaments affecting adenovirus entry and infection [250]. The role of CCD in cellular uptake is debatable. Several studies have reported that early endocytic events are at least partially inhibited by CCD [316, 317]; others reported no effect on receptor-mediated endocytosis [318, 319] with no obligatory role in endocytic vesicle formation in cultured mammalian cells [320]. Because of the potential dual roles of actin in both cellular uptake and cellular transport its necessary to understand how CCD affects both of these aspects of the transduction process.

Treating cells with CCD increased the uptake of NtAd (Figure 4.13A), however, it decreased uptake of both FlAd and PLL-g-PEG-FlAd. This effect can be explained based on the

following : a) electrostatic attraction between FlAd or hybrid vectors and the cell membrane is weaker than NtAd-CAR binding, b) HEK 293 cells can round up and lose cell-cell contacts as a response to CCD action [321]. Therefore, cell rounding might have caused more NtAd to be uptaken. In contrast, the electrostatic attraction between FlAd/hybrid vector and the cell membrane might has been compromised upon cell rounding leading to the lower uptake observed upon CCD addition. We did not observe an increase in cellular uptake of NtAd in NIH 3T3 cells as observed in HEK 293 cells (Figure 4.14A) .Because no cell rounding was observed upon CCD treatment owing to the rigidity of the cell membrane of NIH 3T3 compared to HEK 293 cells [216].

Although cellular uptake of NtAd was not affected by CCD, the transduction efficiency of NtAd decreased by 25% (Figure 4.13B). Ad is known to primarily use microtubules for cytoplasmic transport, which might cause one to question why disruption of actin microfilaments would hinder intracellular transport of the virus. Whether or not actin microfilaments play a role in virus transport, however, remains uncertain. In fact, some researchers have found that Ad can interact with different cytoskeletal systems and utilize both microtubule-dependent and microtubule-independent mechanisms [322, 323]. Previous studies have also reported that Ad infection not only depends on actin dynamics for transport, but nuclear actin polymerization is also needed for efficient viral gene transcription [315]. Consequently, disruption of actin microfilaments by CCD may have decreased intracellular transport of the virus or compromised reporter gene expression or some combination of these two mechanisms.

Treatment with CCD reduced the transduction efficiency of PLL-g-PEG FlAd to levels similar to the NtAd. This reduction in gene delivery efficiency is likely to be related to cellular uptake of the hybrid vector. As seen in Figure 4.13A, CCD decreased uptake of the hybrid vector by about 65%. Reporter gene expression from the hybrid vector also decreased by about 55% when cells were treated with CCD. Since reporter gene expression is ultimately reliant on both uptake and intracellular transport, we would expect gene expression to be reduced by more than

55% if CCD were further affecting cellular transport in addition to cellular uptake. Consequently, the hybrid vector does not appear to use actin microfilaments for intracellular transport and instead relies entirely on microtubules for transport through the cell cytosol.

Based on the intracellular trafficking of the hybrid vector in CAR-positive cells, the hybrid vector was internalized *via* clathrin-mediated endocytosis and macropinocytosis; the levels of internalization of hybrid vectors into the cells, however, were lower compared to the native virus. Subsequently, despite of the removal of the fibers that played a role in virus release from the endosomes, the copolymer coating helped the hybrid vectors to achieve similar transduction efficiencies as the native virus upon inhibiting acidification of endosomes. Lastly, the hybrid vector relied primarily on microtubules to reach the nucleus and did not show good transduction upon microtubule disruption. We can conclude that internalization and cytosolic transport of hybrid vectors appear to be important steps in transducing CAR-positive cells that subsequently lead to low levels of transduction efficiency relative to NtAd.

In addition to studying how the hybrid vector transduces CAR-positive cells, we were also interested to know how the vector transduces cells that the native virus would not normally be capable of infecting. For this purpose, we studied the hybrid vector transduction of CAR-negative (NIH 3T3) cells. As different cells vary in their morphology and functions, it would be surprising if all cells interacted with viral vectors in identical manners. The internalization pathways were studied using the same drug inhibitors. CPZ and AMD significantly reduced the cellular uptake(Figure 4.10A)) and the transduction efficiency (Figure 4.10B) of NtAd in NIH 3T3 cells. This indicated that NtAd entered NIH 3T3 cells *via* clathrin-mediated endocytosis and macropinocytosis. The hybrid vector entered the cells via clathrin- and caveolae- mediated endocytosis as the cellular uptake was reduced by 50% and 35% upon using CPZ and GST, respectively. The transduction efficiency results of the hybrid vector supported the same findings where we observed a 45% and a 25% decrease in the transduction efficiency of the hybrid vector after inhibition with CPZ and GST, respectively. Endocytosis depends on different properties,

such as the polymer molecular weight, type of polymer used to create the nanoparticle, and cell type. Caveolae are preferentially involved in the internalization of larger particles, i.e. with diameters exceeding 200 nm [263]. Our hybrid vectors transducing NIH 3T3 cells have a particle size of 270 nm and thus have the potential to be endocytosed *via* a caveolae-mediated pathway. Moreover, caveolae are not common to all eukaryotic cells but are abundantly present in many cell types including fibroblasts and adipocytes [324]. Previous studies have also shown that modification of the adenoviral tropism can induce deficient clathrin-mediated endocytosis of the viral particles, which can infect refractory CAR-negative cells through a non-clathrin-mediated endocytosis pathway [325].

Next, we studied the endosomal escape of hybrid vectors. Cellular uptake of NtAd and PLL-g-PEG-FlAd after inhibition with BAF was unaffected (Figure 4.12A). This is not surprising as we expect the drug to play no role in the uptake of the virus or the hybrid vector. The transduction efficiency of the NtAd and the hybrid vector was significantly reduced after treating cells with BAF (Figure 4.12 B). Inhibition of endosomal acidification affected the gene expression of NtAd in NIH 3T3 similar to how it did in HEK 293 cells. The fact that BAF reduces transduction efficiency of the hybrid vector by ~70% seems to suggest that the vector primarily relied on pH-induced conformational changes that led to exposure of protein VI. The native virus, however, was not impacted as severely as the hybrid vector. This might be due to the native virus have a better chance for protein VI exposure compared to the polymer-coated hybrid vector. There are several possible explanations for how the hybrid vector was able to escape the endosomal pathway and transduce at all in the presence of BAF. One potential explanation may be that mechanical stresses were created that led to exposure of protein VI in a pH-independent manner. These mechanical stresses may have been induced by the polymer or maybe by integrin binding. Another possible explanation is that transduction resulted from the portion of the vector that entered through the caveolae-mediated pathway. This pathway is known to avoid acidification and release endosomal contents through a process that involves merging with the

golgi and endoplasmic reticulum [326]. A third possible explanation is that the PLL polymer facilitated release of the virus in a pH-independent manner. The endosomal escape of hybrid vectors was difeerent in between HEK 293 and NIH 3T3 cells. Hybrid vectors transducing NIH 3T3 were prepared with a PLL of lower Mwt (4-15 kDa) and were less cationic (7.5 mV) compared to vectors used in HEK 293 cells and prepared with PLL of higher Mwt (15-30 kDa). This resulted in a better transduction efficiency from hybrid vectors in HEK 293 cells compared to NIH 3T3 cells upon inhibiting acidification by BAF. Previous researchers have shown that different degrees of membrane damages were influenced by the polymer molecular weight, charge density, and concentration [204, 272, 327].

After release into the cytoplasm, we studied the cellular uptake of NtAd and PLL-g-PEG-FlAd after inhibition with CLC and CCD, which was not significantly affected (Figure 4.14A). This indicates that both drugs played no role in cellular entry in NIH 3T3 cells. The transduction efficiency of NtAd was not impacted significantly by disruption of actin microfilaments by CCD but decreased upon microtubule disruption by CLC (Figure 4.14B). The hybrid vector used both microtubules and actin microfilaments for cytosolic transport to the nucleus as their transduction efficiency was reduced by 36% and 62% after treating the cells with CLC and CCD, respectively (Figure 4.14B). The ability of the hybrid vector to use both actin microfilaments and microtubulin in cytoplasmic transport in CAR-negative cells might help explain the overall improved transduction efficiency of the hybrid vector relative to NtAd.

Based on the intracellular trafficking studies of hybrid vectors in CAR-negative cells. Hybrid vectors showed higher binding levels compared to NtAd in CAR-negative (NIH 3T3). Nearly all of the bound NtAd and hybrid vector were internalized, and both vectors used more than one pathway to enter the cell. The hybrid vector was internalized *via* clathrin-mediated endocytosis and caveola-mediated endocytosis. Although acidification of the endosomal network is more important for the hybrid vector, it is not clear how well the virus escapes the endosomal network under normal conditions. Next, hybrid vectors used more than one pathway for

cytoplasmic transport to reach the nucleus including microtubules and actin microfilaments. However, there is only a 10-fold improvement in transduction efficiency, while we achieved 55-fold increase in cellular attachment. These results indicate that the hybrid vector must perform better compared to the native virus when it comes to attachment but poorly when it comes to either endosomal escape, intracellular trafficking, or nuclear entry.

Table 4.3: Summary of uptake mechanisms and trafficking pathways of NtAd and PLL-g-PEG-FlAd hybrid vector in CAR-positive and CAR-negative cells.

		CAR-positive cells		CAR-negative cells	
		NtAd	**Hybrid vector**	**NtAd**	**Hybrid vector**
Binding to cell		+++	++	-	++
Internalization		+++	+	++	++
Endocytic pathway	**Clathrin**	+++	++	+++	++
	Caveolae				+
	Macropinocytosis	+	++	+	-
Role of pH on Endosomal Escape		++	++	+	+++
Cytosolic transport	**Microtubule**	+++	++	+++	++
	Actin Filaments	+	+		++

4.5 CONCLUSION

Hybrid vectors are promising vehicles for delivering therapeutic genes because of their relatively safe profile compared to their viral counterparts. However, the transduction efficiency of hybrid vectors is less than satisfactory for clinical purposes. Vector-mediated transduction efficiency reflects the sum of the vector binding, internalizing, and undergoing intracellular trafficking. An ideal gene delivery vector should facilitate cellular uptake, promote endosomal escape, and release transgenes within the nucleus

In our study, the adenovirus fiber protein was removed, and its function replaced *via* PLL-g-PEG copolymer. The surface modification with a cationic copolymer allowed for electrostatic

association with anionic heparan sulfate proteoglycan receptors on the cell membrane, which eliminated the dependence on CAR and facilitated the use of an alternative pathway for cell binding. In CAR-positive cells, including design features that improve internalization and cytosolic transport would result in hybrid vectors that have potential to better transduce these cells. In CAR-negative cells, designing a hybrid vector with better binding is a key mechanism to enhance transduction of these cells. The stepwise approach in replacing viral vector proteins with synthetic components would enable the development of a completely non-viral vector that transfects as efficiently as viral vectors yet avoids the disadvantages of a viral vector.

CHAPTER V

CONCLUSIONS AND FUTURE DIRECTIONS

Adenovirus is the most commonly used viral vector in gene therapy clinical trials. While this viral vector is highly efficient and can transduce a wide profile of cells including dividing and non-dividing cells as well as accommodating large transgenes up to 8.5 kbp, it suffers from many issues such as broad tropism making it difficult for specific targeting for different cell lines and high immunogenicity. These disadvantages are particularly associated with the presence of the fiber protein on the capsid of the adenovirus. The fiber protein, however, is solely responsible for binding to target cells having coxsackie adenovirus receptor (CAR) without which the adenoviral particle is ineffective. In this dissertation, we explored the possibility of removing the fiber protein and replacing it with poly-l-lysing grafted poly-ethylene glycol (PLL-g-PEG) copolymer to mediate effective transduction by effectively performing the functions of the native fiber protein.

This replacement of the fiber protein would also provide certain advantages of synthetic agents with respect to clinical implementation of human gene therapy while still maintaining the good transduction capabilities of adenovirus thereby leading to the design of a novel hybrid gene delivery vector.

As per our results reported in this document, the function of the fiber of adenovirus in mediating good transduction efficiency was replaced by the physical modification of the virus with PLL-g-PEG copolymer. To achieve small particle size, high cationic charge and good transduction efficiency, there should be a balance between PLL Mwt, PEG Mwt, DOP, and the amount of copolymer/virus. Hybrid vectors prepared with high PLL Mwt (up to 30 kDa) is better to be combined with either low PEG Mwt (0.5 or 2 kDa) at high degree of PEGylation (25%) or with high PEG Mwt (5 kDa) at low degree of PEGylation (5%) to achieve a good balance between the particle size and the exposed cationic charge on the PLL chain for better transduction efficiency. Low Mwt PEG (5kDa) have the advantage of reacting with high Mwt PEG (5kDa) at high degree of PEGylation and still resulting in small particle sized hybrid vectors with high transduction efficiency. Multifactor testing via statistical model design (Design of experiment generated a D-optimal design) allowed us to optimize hybrid vectors to achieve the highest transduction efficiency in CAR-positive (HEK 293) and CAR- negative (NIH 3T3) cells. PLL-g-PEG-FLAd hybrid vectors were more efficient at transducing CAR-positive (HEK293) cells in vitro with 3.5-fold increase compared to FlAd. Those hybrid vectors restored 85% of the lost infectivity due to fiber removal. PLL-g-PEG-FLAd hybrid vectors were also more efficient at transducing CAR-negative (NIH 3T3) cells in vitro with 10-fold increase compared to FlAd that was refractory to transduce the cells. Hybrid vectors showed good gene expression in a CAR-independent way. Since results cannot be generalized to every cell type, a design of experiment is recommended as a future direction to achieve the required responses in terms of particle size, zeta potential and transduction efficiency in the cells of interest. This design can be used as a guide towards that with some recommendations like excluding high PLL Mwt as 30-70 kDa and extending PEG Mwt to higher molecular weights. Different PEG Mwt can be aslo tested *in vivo* to correlate the results with *in vitro* results for better optimization.

Optimized hybrid vectors were tested for their cytotoxicity, serum stability, innate immunogenicity, and transduction of various CAR- negative cells. PLL-g-PEG proved to be highly biocompatible as compared to PEI and PLL exhibiting much lower toxicity in HEK293 and NIH 3T3 cells. Hybrid vectors have also induced a weaker innate immune response as we have seen lower production of proinflammatory cytokine. Hybrid vectors exhibited better serum resistance compared to NtAd and FlAd, as they showed better transduction efficiencies in both HEK 293 and NIH 3T3 cells in different serum concentrations up to 50%. We have shown that excellent *in vitro* transduction efficiency can be potentially achieved using hybrid vectors designed to transduce CAR- negative cells. These hybrid vectors showed high transduction efficiency of 20- fold and 4-fold increase compared to FlAd in CAR low cells as MCF-7 cancer cells and in CAR-negative cells as CHO, respectively. The future directions for the design of adenoviral based hybrid vectors should be directed towards optimization of the morphology of vectors through optimal combination of PLL, PEG at an optimal DOP and concentration to achieve highest transduction efficiency in MCF-7 cells. Breast cancer cells are recommended as a target for our hybrid vectors. This can be achieved through either of the following two approaches or combining both: (1) Further optimization of our hybrid vectors to better transduce breast cancer cells to be used as an intratumoral injection into breast cancer cells, or (2) Conjugating a target ligand to hybrid vectors to either target epidermal growth factor receptor (EGFR) or HER2 receptor to be systemically administrated to target breast cancer cells. The resulting hybrid vectors can be potentially used for breast cancer gene therapy following appropriate characterization of the biodistribution and efficacy of these hybrid vectors *in vivo*.

The cellular uptake and intracellular trafficking of hybrid vectors explained their attachment, internalization, endosomal escape and cytosolic transport to the cell nucleus. The surface modification with a cationic copolymer as PLL-g-PEG eliminated the dependence on CAR and facilitated electrostatic association with anionic heparan sulfate proteoglycan receptors on the cell membrane for cellular

attachment. In CAR-positive cells, the lower internalization levels achieved by hybrid vectors compared to NtAd is a major cause of the lower performance of hybrid vectors and restoring only 85% of the infectivity lost due to fiber removal. In CAR-negative cells, the superiority of the binding levels compared to NtAd explains the better performance of hybrid vectors in transducing those cells. The intracellular trafficking significantly differed based on the type of cells as well as the composition of PLL-g-PEG used for FlAd. NtAd used clathrin-mediated endocytosis and macropinocytosis to enter CAR-positive and CAR-negative cells, as known in literature. In contrast, hybrid vectors used the same pathways as NtAD to enter CAR-positive, whereas they used clathrin- and caveola-mediated endocytosis to enter CAR-negative cells. After being endocytosed, surface modification of FlAd with PLL-g-PEG restored the endosomal escape efficiency to the same level of NtAd in CAR-positive cells. In contrast, this modification failed to help vectors to escape from endosomes in CAR-negative cells. The endosomal escape of hybrid vectors showed high dependence on pH change (acidification) in CAR-positive compared to CAR-negative cells. After release into cytosol, hybrid vectors relied on microtubules in CAR-positive cells, whereas hybrid vectors were flexible to use microtubules or microfilaments for transport across the cytosol. Future directions of designing a hybrid vector with better binding is a key mechanism to enhance transduction of CAR-negative cells. This enhancement can be achieved via including ligands to interact with either nonspecific cell receptors as saccharide receptors or with specific receptors according to targeted cells. In addition, including design features that improve endosomal escape of hybrid vectors in CAR-negative cells is recommended like lactosylated PLL, histidine modified PLL or bioreducible PLL derivatives or incorporation of proteins as GALA or KALA into the design. If CAR-positive cells are a target of future studies, it is recommended to including design features that improve internalization like cell penetrating peptides or lipid enhancers as phosphatidylcholine, phosphatidylserine, or sphingomyelins. Moreover, better binding of hybrid vectors to dynein motor proteins would enhance transport along microtubules in CAR-positive cells.

We wholly expect that the design of hybrid vectors (CAR-negative design) can be extended towards treating cancer cells. Hybrid vectors can benefit from the fact that endosomes of cancer cells have lower pH to help better escape and release of vectors into the cytosol. Also, the ability of using different cytosolic transport mechanisms can be an advantage in cancer cells when microtubule function and activity changes. Future studies should be targeted towards design of therapeutic hybrid vectors that have a clinically useful target gene or an RNAi construct for cancer gene therapy.

Finally, future studies may include the effect of fiber removal and surface modification on transduction of hepatic cells and inducing liver toxicity as we expect both effects to decrease. Therefore, improvement of hybrid vector efficiency would result in lower dose administration which decreases accompanying adverse effects. A balance between efficacy and toxicity of hybrid vectors is very essential in clinical gene therapy. Furthermore, studying the suitable route of administration for these hybrid vectors wither by local administration or systemic administration is important to reduce immunotoxicity, inflammatory response and systemic effects. Finally, the ultimate goal should be replacing viral vector parts with synthetic components to develop a non-viral vector that transfect as efficiently as a virus yet avoids the disadvantages of viral vectors.

REFERENCES

1. Omenn, G.S., et al., *Metrics for the Human Proteome Project 2016: progress on identifying and characterizing the human proteome, including post-translational modifications.* Journal of proteome research, 2016. 15(11): p. 3951-3960.

2. Hood, L. and L. Rowen, *The Human Genome Project: big science transforms biology and medicine.* Genome medicine, 2013. 5(9): p. 79-79.

3. *Finishing the euchromatic sequence of the human genome.* Nature, 2004. 431(7011): p. 931-45.

4. Hanna, E., et al., *Gene therapies development: slow progress and promising prospect.* Journal of market access & health policy, 2017. 5(1): p. 1265293.

5. Mountain, A., *Gene therapy: the first decade.* Trends in biotechnology, 2000. 18(3): p. 119-128.

6. Lechardeur, D., et al., *Metabolic instability of plasmid DNA in the cytosol: a potential barrier to gene transfer.* Gene therapy, 1999. 6(4): p. 482-497.

7. Friedmann, T., *Stanfield Rogers: insights into virus vectors and failure of an early gene therapy model.* Molecular Therapy, 2001. 4(4): p. 285-288.

8. Ferrari, G., et al., *An in vivo model of somatic cell gene therapy for human severe combined immunodeficiency.* Science, 1991. 251(4999): p. 1363-1366.

9. Sheridan, C., *Gene therapy finds its niche.* Nature biotechnology, 2011. 29(2): p. 121-128.

10. Wirth, T., N. Parker, and S. Ylä-Herttuala, *History of gene therapy.* Gene, 2013. 525(2): p. 162-169.

11. Couzin, J. and J. Kaiser, *As Gelsinger case ends, gene therapy suffers another blow*. 2005, American Association for the Advancement of Science.

12. Stolberg, S.G., *The biotech death of Jesse Gelsinger.* NY Times Mag, 1999. 28: p. 136-140.

13. Raper, S.E., et al., *Fatal systemic inflammatory response syndrome in a ornithine transcarbamylase deficient patient following adenoviral gene transfer.* Molecular genetics and metabolism, 2003. 80(1-2): p. 148-158.

14. Inui, K., S. Okada, and G. Dickson, *Gene therapy in Duchenne muscular dystrophy.* Brain and Development, 1996. 18(5): p. 357-361.

15. Griesenbach, U., D.M. Geddes, and E. Alton, *Gene therapy progress and prospects: cystic fibrosis.* Gene therapy, 2006. 13(14): p. 1061.

16. McNeish, I., S. Bell, and N. Lemoine, *Gene therapy progress and prospects: cancer gene therapy using tumour suppressor genes.* Gene therapy, 2004. 11(6): p. 497-503.

17. Katz, M.G., et al., *Cardiac gene therapy: optimization of gene delivery techniques in vivo.* Human gene therapy, 2010. 21(4): p. 371-380.

18. Verma, I.M., et al., *Gene therapy: promises, problems and prospects*, in *Genes and Resistance to Disease*. 2000, Springer. p. 147-157.

19. Hidai, C. and H. Kitano, *Nonviral gene therapy for cancer: a review.* Diseases, 2018. 6(3): p. 57.

20. Prakash, V., M. Moore, and R.J. Yáñez-Muñoz, *Current progress in therapeutic gene editing for monogenic diseases.* Molecular Therapy, 2016. 24(3): p. 465-474.

21. Prondzynski, M., G. Mearini, and L. Carrier, *Gene therapy strategies in the treatment of hypertrophic cardiomyopathy.* Pflügers Archiv-European Journal of Physiology, 2019. 471(5): p. 807-815.

22. Ibraheem, D., A. Elaissari, and H. Fessi, *Gene therapy and DNA delivery systems.* International journal of pharmaceutics, 2014. 459(1-2): p. 70-83.

23. Ginn, S.L., et al., *Gene therapy clinical trials worldwide to 2017: An update.* The journal of gene medicine, 2018. 20(5): p. e3015.

24. Wilson, J.M., *Gendicine: The first commercial gene therapy product; Chinese translation of editorial.* Human gene therapy, 2005. 16(9): p. 1014-1015.

25. Guo, J. and H. Xin, *Splicing out the West?* 2006, American Association for the Advancement of Science.

26. Ylä-Herttuala, S., *Endgame: glybera finally recommended for approval as the first gene therapy drug in the European union.* Molecular Therapy, 2012. 20(10): p. 1831-1832.

27. Prasad, V., *Tisagenlecleucel—the first approved CAR-T-cell therapy: implications for payers and policy makers.* Nature Reviews Clinical Oncology, 2018. 15(1): p. 11-12.

28. Yip, A. and R.M. Webster, *The market for chimeric antigen receptor T cell therapies*. 2018, Nature Publishing Group.

29. Smalley, E., *First AAV gene therapy poised for landmark approval*. 2017, Nature Publishing Group.

30. Urquhart, L., *FDA new drug approvals in Q2 2019.* Nature reviews. Drug discovery, 2019. 18(8): p. 575.

31. Goswami, R., et al., *Gene therapy leaves a vicious cycle.* Frontiers in oncology, 2019. 9: p. 297.

32. Houk, B.E., G. Hochhaus, and J.A. Hughes, *Kinetic modeling of plasmid DNA degradation in rat plasma.* AAPS PharmSci, 1999. 1(3): p. 15-20.

33. Sternberg, B., et al., *Ultrastructural characterization of cationic liposome-DNA complexes showing enhanced stability in serum and high transfection activity in vivo.* Biochimica et Biophysica Acta (BBA)-Biomembranes, 1998. 1375(1-2): p. 23-35.

34. Sakurai, F., et al., *Interaction between DNA–cationic liposome complexes and erythrocytes is an important factor in systemic gene transfer via the intravenous route in mice: the role of the neutral helper lipid.* Gene therapy, 2001. 8(9): p. 677-686.

35. McCray Jr, P.B., et al., *Alveolar macrophages inhibit retrovirus-mediated gene transfer to airway epithelia.* Human gene therapy, 1997. 8(9): p. 1087-1093.

36. Chen, D., et al., *Adaptive and innate immune responses to gene transfer vectors: role of cytokines and chemokines in vector function.* Gene therapy, 2003. 10(11): p. 991-998.

37. Fausther-Bovendo, H. and G.P. Kobinger, *Pre-existing immunity against Ad vectors: humoral, cellular, and innate response, what's important?* Human vaccines & immunotherapeutics, 2014. 10(10): p. 2875-2884.

38. Fan, G., et al., *Bio-inspired polymer envelopes around adenoviral vectors to reduce immunogenicity and improve in vivo kinetics.* Acta biomaterialia, 2016. 30: p. 94-105.

39. O'Riordan, C.R., et al., *PEGylation of adenovirus with retention of infectivity and protection from neutralizing antibody in vitro and in vivo.* Human gene therapy, 1999. 10(8): p. 1349-1358.

40. Koltover, I., et al., *An inverted hexagonal phase of cationic liposome-DNA complexes related to DNA release and delivery.* Science, 1998. 281(5373): p. 78-81.

41. Bus, T., A. Traeger, and U.S. Schubert, *The great escape: how cationic polyplexes overcome the endosomal barrier.* Journal of Materials Chemistry B, 2018. 6(43): p. 6904-6918.

42. Dauty, E. and A. Verkman, *Actin cytoskeleton as the principal determinant of size-dependent DNA mobility in cytoplasm a new barrier for non-viral gene delivery.* Journal of Biological Chemistry, 2005. 280(9): p. 7823-7828.

43. Alberts, B., et al., *The transport of molecules between the nucleus and the cytosol*, in *Molecular Biology of the Cell. 4th edition*. 2002, Garland Science.

44. Brunner, S., et al., *Cell cycle dependence of gene transfer by lipoplex, polyplex and recombinant adenovirus.* Gene therapy, 2000. 7(5): p. 401-407.

45. Schaffer, D.V., et al., *Vector unpacking as a potential barrier for receptor‐mediated polyplex gene delivery.* Biotechnology and bioengineering, 2000. 67(5): p. 598-606.

46. Grigsby, C.L. and K.W. Leong, *Balancing protection and release of DNA: tools to address a bottleneck of non-viral gene delivery.* Journal of the Royal Society Interface, 2010. 7(suppl_1): p. S67-S82.

47. Tatum, E.L., *Molecular biology, nucleic acids, and the future of medicine.* Perspect Biol Med, 1966. 10(1): p. 19-32.

48. Nayerossadat, N., T. Maedeh, and P.A. Ali, *Viral and nonviral delivery systems for gene delivery.* Advanced biomedical research, 2012. 1: p. 27-27.

49. Richardson, T.P., W.L. Murphy, and D.J. Mooney, *Polymeric delivery of proteins and plasmid DNA for tissue engineering and gene therapy.* Critical Reviews™ in Eukaryotic Gene Expression, 2001. 11(1-3).

50. Gigante, A., et al., *Non-viral transfection vectors: are hybrid materials the way forward?* Medchemcomm, 2019. 10(10): p. 1692-1718.

51. Rowe, W.P., et al., *Isolation of a cytopathogenic agent from human adenoids undergoing spontaneous degeneration in tissue culture.* Proceedings of the Society for Experimental Biology and Medicine, 1953. 84(3): p. 570-573.

52. Buckwalter, S.P., et al., *Real-time qualitative PCR for 57 human adenovirus types from multiple specimen sources.* Journal of clinical microbiology, 2012. 50(3): p. 766-771.

53. Wild, D., *The immunoassay handbook: theory and applications of ligand binding, ELISA and related techniques*. 2013: Newnes.

54. Van Oostrum, J. and R.M. Burnett, *Molecular composition of the adenovirus type 2 virion.* Journal of virology, 1985. 56(2): p. 439-448.

55. Brenner, S. and R. Horne, *A negative staining method for high resolution electron microscopy of viruses.* Biochimica et biophysica acta, 1959. 34: p. 103-110.

56. Valentine, R. and H. Pereira, *Antigens and structure of the adenovirus.* Journal of molecular biology, 1965. 13(1): p. 13-IN13.

57. Rux, J.J. and R.M. Burnett, *Adenovirus structure.* Human gene therapy, 2004. 15(12): p. 1167-1176.

58. Russell, W., *Adenoviruses: update on structure and function.* Journal of General Virology, 2009. 90(1): p. 1-20.

59. Devaux, C., et al., *Structure of adenovirus fibre: I. Analysis of crystals of fibre from adenovirus serotypes 2 and 5 by electron microscopy and X-ray crystallography.* Journal of molecular biology, 1990. 215(4): p. 567-588.

60. Henry, L.J., et al., *Characterization of the knob domain of the adenovirus type 5 fiber protein expressed in Escherichia coli.* Journal of virology, 1994. 68(8): p. 5239-5246.

61. Bergelson, J.M., et al., *Isolation of a common receptor for Coxsackie B viruses and adenoviruses 2 and 5.* Science, 1997. 275(5304): p. 1320-1323.

62. Wickham, T.J., et al., *Integrins αvβ3 and αvβ5 promote adenovirus internalization but not virus attachment.* Cell, 1993. 73(2): p. 309-319.

63. Roth, M.D., et al., *Helper-dependent adenoviral vectors efficiently express transgenes in human dendritic cells but still stimulate antiviral immune responses.* The Journal of Immunology, 2002. 169(8): p. 4651-4656.

64. Kafri, T., et al., *Cellular immune response to adenoviral vector infected cells does not require de novo viral gene expression: implications for gene therapy.* Proceedings of the National Academy of Sciences, 1998. 95(19): p. 11377-11382.

65. Meier, O., et al., *Early steps of clathrin-mediated endocytosis involved in phagosomal escape of Fcγ receptor-targeted adenovirus.* Journal of virology, 2005. 79(4): p. 2604-2613.

66. Takeuchi, O. and S. Akira, *Innate immunity to virus infection.* Immunological reviews, 2009. 227(1): p. 75-86.

67. Benihoud, K., et al., *Efficient, repeated adenovirus-mediated gene transfer in mice lacking both tumor necrosis factor alpha and lymphotoxin α.* Journal of virology, 1998. 72(12): p. 9514-9525.

68. Muruve, D.A., et al., *Adenoviral gene therapy leads to rapid induction of multiple chemokines and acute neutrophil-dependent hepatic injury in vivo.* Human gene therapy, 1999. 10(6): p. 965-976.

69. Schagen, F.H., et al., *Immune responses against adenoviral vectors and their transgene products: a review of strategies for evasion.* Critical reviews in oncology/hematology, 2004. 50(1): p. 51-70.

70. Smith, L. and J.F. Byers, *Gene therapy in the post-Gelsinger era.* JONA'S healthcare law, ethics and regulation, 2002. 4(4): p. 104-110.

71. Marshall, E., *Gene therapy death prompts review of adenovirus vector.* Science, 1999. 286(5448): p. 2244-2245.

72. Muruve, D.A., *The innate immune response to adenovirus vectors.* Human gene therapy, 2004. 15(12): p. 1157-1166.

73. Shayakhmetov, D.M., et al., *Adenovirus binding to blood factors results in liver cell infection and hepatotoxicity.* Journal of virology, 2005. 79(12): p. 7478-7491.

74. Thomas, C.E., et al., *Acute direct adenoviral vector cytotoxicity and chronic, but not acute, inflammatory responses correlate with decreased vector-mediated transgene expression in the brain.* Molecular Therapy, 2001. 3(1): p. 36-46.

75. Smith, T., et al., *Transient immunosuppression permits successful repetitive intravenous administration of an adenovirus vector.* Gene therapy, 1996. 3(6): p. 496-502.

76. Rahman, A., et al., *Specific depletion of human anti-adenovirus antibodies facilitates transduction in an in vivo model for systemic gene therapy.* Molecular Therapy, 2001. 3(5): p. 768-778.

77. Noutsias, M., et al., *Human coxsackie-adenovirus receptor is colocalized with integrins αvβ3 and αvβ5 on the cardiomyocyte sarcolemma and upregulated in dilated cardiomyopathy: implications for cardiotropic viral infections.* Circulation, 2001. 104(3): p. 275-280.

78. Raschperger, E., et al., *The coxsackie-and adenovirus receptor (CAR) is an in vivo marker for epithelial tight junctions, with a potential role in regulating permeability and tissue homeostasis.* Experimental cell research, 2006. 312(9): p. 1566-1580.

79. Cohen, C.J., et al., *The coxsackievirus and adenovirus receptor is a transmembrane component of the tight junction.* Proceedings of the National Academy of Sciences, 2001. 98(26): p. 15191-15196.

80. Kim, M., et al., *The therapeutic efficacy of adenoviral vectors for cancer gene therapy is limited by a low level of primary adenovirus receptors on tumour cells.* European Journal of Cancer, 2002. 38(14): p. 1917-1926.

81. Vigne, E., et al., *Genetic manipulations of adenovirus type 5 fiber resulting in liver tropism attenuation.* Gene Therapy, 2003. 10(2): p. 153-162.

82. Smith, T., et al., *In vivo hepatic adenoviral gene delivery occurs independently of the coxsackievirus–adenovirus receptor.* Molecular Therapy, 2002. 5(6): p. 770-779.

83. Kalyuzhniy, O., et al., *Adenovirus serotype 5 hexon is critical for virus infection of hepatocytes in vivo.* Proceedings of the National Academy of Sciences, 2008. 105(14): p. 5483-5488.

84. Seiradake, E., et al., *The cell adhesion molecule "CAR" and sialic acid on human erythrocytes influence adenovirus in vivo biodistribution.* PLoS pathogens, 2009. 5(1).

85. Lundstrom, K., *Viral vectors in gene therapy.* Diseases, 2018. 6(2): p. 42.

86. Jaffe, H., et al., *Adenovirus–mediated in vivo gene transfer and expression in normal rat liver.* Nature genetics, 1992. 1(5): p. 372-378.

87. Buckley, R.H., *Gene therapy for SCID--a complication after remarkable progress.* The Lancet, 2002. 360(9341): p. 1185-1186.

88. Giacca, M. and S. Zacchigna, *Virus-mediated gene delivery for human gene therapy.* Journal of controlled release, 2012. 161(2): p. 377-388.

89. Kotterman, M.A., T.W. Chalberg, and D.V. Schaffer, *Viral vectors for gene therapy: translational and clinical outlook.* Annual review of biomedical engineering, 2015. 17: p. 63-89.

90. Leggiero, E., et al., *Helper-dependent adenovirus-mediated gene transfer of a secreted LDL receptor/transferrin chimeric protein reduces aortic atherosclerosis in LDL receptor-deficient mice.* Gene therapy, 2019. 26(3): p. 121-130.

91. Maggio, I., et al., *Selection-free gene repair after adenoviral vector transduction of designer nucleases: rescue of dystrophin synthesis in DMD muscle cell populations.* Nucleic acids research, 2016. 44(3): p. 1449-1470.

92. Zhang, C. and D. Zhou, *Adenoviral vector-based strategies against infectious disease and cancer.* Human vaccines & immunotherapeutics, 2016. 12(8): p. 2064-2074.

93. Smaill, F., et al., *A human type 5 adenovirus–based tuberculosis vaccine induces robust T cell responses in humans despite preexisting anti-adenovirus immunity.* Science translational medicine, 2013. 5(205): p. 205ra134-205ra134.

94. Buchbinder, S.P., et al., *Efficacy assessment of a cell-mediated immunity HIV-1 vaccine (the Step Study): a double-blind, randomised, placebo-controlled, test-of-concept trial.* The Lancet, 2008. 372(9653): p. 1881-1893.

95. Hill, A.V., et al., *Prime-boost vectored malaria vaccines: progress and prospects.* Human vaccines, 2010. 6(1): p. 78-83.

96. Scallan, C.D., et al., *An adenovirus-based vaccine with a double-stranded RNA adjuvant protects mice and ferrets against H5N1 avian influenza in oral delivery models.* Clin. Vaccine Immunol., 2013. 20(1): p. 85-94.

97. Mennechet, F.J., et al., *Ebola virus vaccine: benefit and risks of adenovirus-based vectors.* Expert review of vaccines, 2015. 14(11): p. 1471-1478.

98. Maggio, I., et al., *Adenoviral vectors encoding CRISPR/Cas9 multiplexes rescue dystrophin synthesis in unselected populations of DMD muscle cells.* Scientific reports, 2016. 6(1): p. 1-12.

99. Bett, A.J., L. Prevec, and F.L. Graham, *Packaging capacity and stability of human adenovirus type 5 vectors.* Journal of virology, 1993. 67(10): p. 5911-5921.

100. Graham, F.L., et al., *Characteristics of a human cell line transformed by DNA from human adenovirus type 5.* Journal of general virology, 1977. 36(1): p. 59-72.

101. Liu, Q. and D. Muruve, *Molecular basis of the inflammatory response to adenovirus vectors.* Gene therapy, 2003. 10(11): p. 935-940.

102. Wen, S., et al., *Second-generation adenoviral vectors do not prevent rapid loss of transgene expression and vector DNA from the arterial wall.* Arteriosclerosis, thrombosis, and vascular biology, 2000. 20(6): p. 1452-1458.

103. Sakhuja, K., et al., *Optimization of the generation and propagation of gutless adenoviral vectors.* Human gene therapy, 2003. 14(3): p. 243-254.

104. Stevenson, S.C., et al., *Human adenovirus serotypes 3 and 5 bind to two different cellular receptors via the fiber head domain.* Journal of virology, 1995. 69(5): p. 2850-2857.

105. Krasnykh, V.N., et al., *Generation of recombinant adenovirus vectors with modified fibers for altering viral tropism.* Journal of virology, 1996. 70(10): p. 6839-6846.

106. Koizumi, N., et al., *Reduction of Natural Adenovirus Tropism to Mouse Liver by Fiber-Shaft Exchange in Combination with both CAR-andαv Integrin-Binding Ablation.* Journal of virology, 2003. 77(24): p. 13062-13072.

107. Hesse, A., et al., *Tropism modification of adenovirus vectors by peptide ligand insertion into various positions of the adenovirus serotype 41 short-fiber knob domain.* Journal of virology, 2007. 81(6): p. 2688-2699.

108. Shayakhmetov, D.M. and A. Lieber, *Dependence of adenovirus infectivity on length of the fiber shaft domain.* Journal of virology, 2000. 74(22): p. 10274-10286.

109. Van Beusechem, V., et al., *Recombinant adenovirus vectors with knobless fibers for targeted gene transfer.* Gene therapy, 2000. 7(22): p. 1940-1946.

110. Glasgow, J.N., et al., *An adenovirus vector with a chimeric fiber derived from canine adenovirus type 2 displays novel tropism.* Virology, 2004. 324(1): p. 103-116.

111. Nakayama, M., et al., *An adenovirus serotype 5 vector with fibers derived from ovine atadenovirus demonstrates CAR-independent tropism and unique biodistribution in mice.* Virology, 2006. 350(1): p. 103-115.

112. Shayakhmetov, D.M., et al., *The interaction between the fiber knob domain and the cellular attachment receptor determines the intracellular trafficking route of adenoviruses.* Journal of virology, 2003. 77(6): p. 3712-3723.

113. Sakurai, F., et al., *Adenovirus serotype 35 vector-induced innate immune responses in dendritic cells derived from wild-type and human CD46-transgenic mice: Comparison with a fiber-substituted Ad vector containing fiber proteins of Ad serotype 35.* Journal of controlled release, 2010. 148(2): p. 212-218.

114. Bradley, R.R., et al., *Adenovirus serotype 5 neutralizing antibodies target both hexon and fiber following vaccination and natural infection.* Journal of virology, 2012. 86(1): p. 625-629.

115. Molinier-Frenkel, V., et al., *Adenovirus hexon protein is a potent adjuvant for activation of a cellular immune response.* Journal of virology, 2002. 76(1): p. 127-135.

116. Bruder, J.T., et al., *Modification of Ad5 hexon hypervariable regions circumvents pre-existing Ad5 neutralizing antibodies and induces protective immune responses.* PLOS one, 2012. 7(4).

117. Särkioja, M., et al., *Changing the adenovirus fiber for retaining gene delivery efficacy in the presence of neutralizing antibodies.* Gene therapy, 2008. 15(12): p. 921-929.

118. Ma, J., et al., *Manipulating adenovirus hexon hypervariable loops dictates immune neutralisation and coagulation factor X-dependent cell interaction in vitro and in vivo.* PLoS pathogens, 2015. 11(2).

119. Irons, E.E., et al., *Coagulation factor binding orientation and dimerization may influence infectivity of adenovirus-coagulation factor complexes.* Journal of virology, 2013. 87(17): p. 9610-9619.

120. Kreppel, F. and S. Kochanek, *Modification of adenovirus gene transfer vectors with synthetic polymers: a scientific review and technical guide.* Molecular Therapy, 2008. 16(1): p. 16-29.

121. Pearce, O.M., et al., *Glycoviruses: chemical glycosylation retargets adenoviral gene transfer.* Angewandte Chemie International Edition, 2005. 44(7): p. 1057-1061.

122. Montaguti, P., E. Melloni, and E. Cavalletti, *Acute intravenous toxicity of dimethyl sulfoxide, polyethylene glycol 400, dimethylformamide, absolute ethanol, and benzyl alcohol in inbred mouse strains.* Arzneimittel-Forschung, 1994. 44(4): p. 566-570.

123. Eto, Y., et al., *Development of PEGylated adenovirus vector with targeting ligand.* International journal of pharmaceutics, 2008. 354(1-2): p. 3-8.

124. Croyle, M.A., et al., *"Stealth" adenoviruses blunt cell-mediated and humoral immune responses against the virus and allow for significant gene expression upon readministration in the lung.* Journal of virology, 2001. 75(10): p. 4792-4801.

125. Croyle, M.A., Q.-C. Yu, and J.M. Wilson, *Development of a rapid method for the PEGylation of adenoviruses with enhanced transduction and improved stability under harsh storage conditions.* Human gene therapy, 2000. 11(12): p. 1713-1722.

126. Mok, H., et al., *Evaluation of polyethylene glycol modification of first-generation and helper-dependent adenoviral vectors to reduce innate immune responses.* Molecular Therapy, 2005. 11(1): p. 66-79.

127. Benihoud, K., et al., *Respective roles of TNF-α and IL-6 in the immune response-elicited by adenovirus-mediated gene transfer in mice.* Gene therapy, 2007. 14(6): p. 533-544.

128. Croyle, M.A., et al., *PEGylated helper-dependent adenoviral vectors: highly efficient vectors with an enhanced safety profile.* Gene therapy, 2005. 12(7): p. 579-587.

129. Coughlan, L., et al., *Tropism-modification strategies for targeted gene delivery using adenoviral vectors.* Viruses, 2010. 2(10): p. 2290-2355.

130. Fisher, K.D. and L.W. Seymour, *HPMA copolymers for masking and retargeting of therapeutic viruses.* Advanced drug delivery reviews, 2010. 62(2): p. 240-245.

131. Kang, E.-A. and C.-O. Yun, *Current advances in adenovirus nanocomplexes: more specificity and less immunogenicity.* BMB reports, 2010. 43(12): p. 781-788.

132. Fisher, K., et al., *Polymer-coated adenovirus permits efficient retargeting and evades neutralising antibodies.* Gene therapy, 2001. 8(5): p. 341-348.

133. Kasala, D., et al., *Utilizing adenovirus vectors for gene delivery in cancer.* Expert opinion on drug delivery, 2014. 11(3): p. 379-392.

134. Park, J.W., H. Mok, and T.G. Park, *Physical adsorption of PEG grafted and blocked poly-L-lysine copolymers on adenovirus surface for enhanced gene transduction.* Journal of Controlled Release, 2010. 142(2): p. 238-244.

135. Singarapu, K., I. Pal, and J.D. Ramsey, *Polyethylene glycol–grafted polyethylenimine used to enhance adenovirus gene delivery.* Journal of Biomedical Materials Research Part A, 2013. 101(7): p. 1857-1864.

136. Lee, C.-H., et al., *Enhanced therapeutic efficacy of an adenovirus-PEI-bile-acid complex in tumors with low coxsackie and adenovirus receptor expression.* Biomaterials, 2014. 35(21): p. 5505-5516.

137. Kasman, L.M., et al., *Polymer-enhanced adenoviral transduction of CAR-negative bladder cancer cells.* Molecular pharmaceutics, 2009. 6(5): p. 1612-1619.

138. Choi, J.-W., et al., *Tuning surface charge and PEGylation of biocompatible polymers for efficient delivery of nucleic acid or adenoviral vector.* Bioconjugate chemistry, 2015. 26(8): p. 1818-1829.

139. Kim, J., et al., *Therapeutic efficacy of a systemically delivered oncolytic adenovirus–biodegradable polymer complex.* Biomaterials, 2013. 34(19): p. 4622-4631.

140. Dodds, E., et al., *Cationic lipids and polymers are able to enhance adenoviral infection of cultured mouse myotubes.* Journal of neurochemistry, 1999. 72(5): p. 2105-2112.

141. Zeng, Q., et al., *Protection of adenovirus from neutralizing antibody by cationic PEG derivative ionically linked to adenovirus.* International journal of nanomedicine, 2012. 7: p. 985.

142. Yao, X., et al., *Polyethyleneimine-coating enhances adenoviral transduction of mesenchymal stem cells.* Biochemical and biophysical research communications, 2014. 447(3): p. 383-387.

143. Toyoda, K., H. Nakane, and D.D. Heistad, *Cationic polymer and lipids augment adenovirus-mediated gene transfer to cerebral arteries in vivo.* Journal of Cerebral Blood Flow & Metabolism, 2001. 21(9): p. 1125-1131.

144. Lee, S.G., et al., *Enhancement of adenoviral transduction with polycationic liposomes in vivo.* Cancer gene therapy, 2000. 7(10): p. 1329-1335.

145. Chillón, M., et al., *Adenovirus complexed with polyethylene glycol and cationic lipid is shielded from neutralizing antibodies in vitro.* Gene Ther, 1998. 5(7): p. 995-1002.

146. Natsume, A., et al., *Cationic liposome conjugation to recombinant adenoviral vector reduces viral antigenicity.* Japanese journal of cancer research, 2000. 91(4): p. 363-367.

147. Zorko, M. and Ü. Langel, *Cell-penetrating peptides: mechanism and kinetics of cargo delivery.* Advanced drug delivery reviews, 2005. 57(4): p. 529-545.

148. Ramsey, J.D. and N.H. Flynn, *Cell-penetrating peptides transport therapeutics into cells.* Pharmacology & therapeutics, 2015. 154: p. 78-86.

149. Nigatu, A.S., et al., *Evaluation of cell-penetrating peptide/adenovirus particles for transduction of CAR-negative cells.* Journal of pharmaceutical sciences, 2013. 102(6): p. 1981-1993.

150. Lehmusvaara, S., et al., *Utility of cell-permeable peptides for enhancement of virus-mediated gene transfer to human tumor cells.* Biotechniques, 2006. 40(5): p. 573-576.

151. Nigatu, A.S., et al., *Effects of cell-penetrating peptides on transduction efficiency of PEGylated adenovirus.* Biomedicine & Pharmacotherapy, 2015. 71: p. 153-160.

152. Gratton, J.-P., et al., *Cell-permeable peptides improve cellular uptake and therapeutic gene delivery of replication-deficient viruses in cells and in vivo.* Nature medicine, 2003. 9(3): p. 357-362.

153. Váňová, J., et al., *The Utilization of Cell-Penetrating Peptides in the Intracellular Delivery of Viral Nanoparticles.* Materials (Basel, Switzerland), 2019. 12(17): p. 2671.

154. Hitt, M.M. and F.L. Graham, *Adenovirus vectors for human gene therapy.* 2000.

155. Lee, C.S., et al., *Adenovirus-mediated gene delivery: potential applications for gene and cell-based therapies in the new era of personalized medicine.* Genes & diseases, 2017. 4(2): p. 43-63.

156. Lee, M., et al., *Targeting tumor neoangiogenesis via targeted adenoviral vector to achieve effective cancer gene therapy for disseminated neoplastic disease.* Molecular Cancer Therapeutics, 2020. 19(3): p. 966-971.

157. Sharma, A., et al., *Adenovirus receptors and their implications in gene delivery.* Virus research, 2009. 143(2): p. 184-194.

158. Ma, Y.Y., et al., *Loss of coxsackie and adenovirus receptor expression in human colorectal cancer: a potential impact on the efficacy of adenovirus-mediated gene therapy in Chinese Han population.* Molecular medicine reports, 2016. 14(3): p. 2541-2547.

159. Krasnykh, V., et al., *Advanced generation adenoviral vectors possess augmented gene transfer efficiency based upon coxsackie adenovirus receptor-independent cellular entry capacity.* Cancer Research, 2000. 60(24): p. 6784-6787.

160. Walters, R.W., et al., *Basolateral localization of fiber receptors limits adenovirus infection from the apical surface of airway epithelia.* Journal of Biological Chemistry, 1999. 274(15): p. 10219-10226.

161. Wickham, T.J., et al., *Targeted adenovirus gene transfer to endothelial and smooth muscle cells by using bispecific antibodies.* Journal of virology, 1996. 70(10): p. 6831-6838.

162. Mizuguchi, H. and T. Hayakawa, *Targeted adenovirus vectors.* Human gene therapy, 2004. 15(11): p. 1034-1044.

163. Hendrickx, R., et al., *Innate immunity to adenovirus.* Human gene therapy, 2014. 25(4): p. 265-284.

164. Hedley, S., et al., *An adenovirus vector with a chimeric fiber incorporating stabilized single chain antibody achieves targeted gene delivery.* Gene therapy, 2006. 13(1): p. 88-94.

165. Sohn, J., et al., *Retargeting of adenoviral gene delivery via herceptin-peg-adenovirus conjugates; a novel strategy for breast cancer gene therapy*. 2008, AACR.

166. O'Bryan, S.M. and J.M. Mathis, *Engineering an oncolytic adenovirus targeted to the CXCR4 chemokine receptor for breast cancer therapy*. 2018, AACR.

167. Sato-Dahlman, M., et al., *CD133-targeted oncolytic adenovirus demonstrates anti-tumor effect in colorectal cancer.* Oncotarget, 2017. 8(44): p. 76044.

168. Li, Y., et al., *Potent antitumor effect of tumor microenvironment-targeted oncolytic adenovirus against desmoplastic pancreatic cancer.* International journal of cancer, 2018. 142(2): p. 392-413.

169. Niemann, J. and F. Kühnel, *Tumor Targeting of Oncolytic Adenoviruses Using Bispecific Adapter Proteins*, in *Oncolytic Viruses*. 2020, Springer. p. 31-49.

170. Kaufmann, J.K. and D.M. Nettelbeck, *Virus chimeras for gene therapy, vaccination, and oncolysis: adenoviruses and beyond.* Trends in molecular medicine, 2012. 18(7): p. 365-376.

171. Volk, A.L., et al., *Enhanced adenovirus infection of melanoma cells by fiber-modification: incorporation of RGD peptide or Ad5/3 chimerism.* Cancer biology & therapy, 2003. 2(5): p. 511-515.

172. Kuhlmann, K., et al., *Fiber-chimeric adenoviruses expressing fibers from serotype 16 and 50 improve gene transfer to human pancreatic adenocarcinoma.* Cancer gene therapy, 2009. 16(7): p. 585-597.

173. Waddington, S.N., et al., *Adenovirus serotype 5 hexon mediates liver gene transfer.* Cell, 2008. 132(3): p. 397-409.

174. Garnett, M.C., *Gene-delivery systems using cationic polymers.* Critical Reviews™ in Therapeutic Drug Carrier Systems, 1999. 16(2).

175. Sun, X. and N. Zhang, *Cationic polymer optimization for efficient gene delivery.* Mini reviews in medicinal chemistry, 2010. 10(2): p. 108-125.

176. Bhattacharya, S. and A. Bajaj, *Advances in gene delivery through molecular design of cationic lipids.* Chemical Communications, 2009(31): p. 4632-4656.

177. Martin, B., et al., *The design of cationic lipids for gene delivery.* Current pharmaceutical design, 2005. 11(3): p. 375-394.

178. Xiang, J.J., et al., *IONP-PLL: a novel non-viral vector for efficient gene delivery.* The Journal of Gene Medicine: A cross-disciplinary journal for research on the science of gene transfer and its clinical applications, 2003. 5(9): p. 803-817.

179. Wu, G.Y. and C.H. Wu, *Receptor-mediated in vitro gene transformation by a soluble DNA carrier system.* Journal of Biological Chemistry, 1987. 262(10): p. 4429-4432.

180. Godbey, W., et al., *Poly (ethylenimine)-mediated transfection: A new paradigm for gene delivery.* Journal of Biomedical Materials Research: An Official Journal of The Society for Biomaterials, The Japanese Society for Biomaterials, and The Australian Society for Biomaterials and the Korean Society for Biomaterials, 2000. 51(3): p. 321-328.

181. Erbacher, P., et al., *Chitosan-based vector/DNA complexes for gene delivery: biophysical characteristics and transfection ability.* Pharmaceutical research, 1998. 15(9): p. 1332-1339.

182. Saranya, N., et al., *Chitosan and its derivatives for gene delivery.* International journal of biological macromolecules, 2011. 48(2): p. 234-238.

183. Funhoff, A.M., et al., *Cationic polymethacrylates with covalently linked membrane destabilizing peptides as gene delivery vectors.* Journal of controlled release, 2005. 101(1-3): p. 233-246.

184. Kupgan, G., et al., *The effect of fiber truncations on the stability of adenovirus type 5.* Molecular biotechnology, 2014. 56(11): p. 979-991.

185. Kirby, I., et al., *Identification of contact residues and definition of the CAR-binding site of adenovirus type 5 fiber protein.* Journal of virology, 2000. 74(6): p. 2804-2813.

186. Molinier-Frenkel, V., et al., *The maturation of murine dendritic cells induced by human adenovirus is mediated by the fiber knob domain.* Journal of Biological Chemistry, 2003. 278(39): p. 37175-37182.

187. Breidenbach, M., et al., *Genetic replacement of the adenovirus shaft fiber reduces liver tropism in ovarian cancer gene therapy.* Human gene therapy, 2004. 15(5): p. 509-518.

188. Fasbender, A., et al., *Complexes of adenovirus with polycationic polymers and cationic lipids increase the efficiency of gene transfer in vitro and in vivo.* Journal of Biological Chemistry, 1997. 272(10): p. 6479-6489.

189. Ward, C.M., M.L. Read, and L.W. Seymour, *Systemic circulation of poly (L-lysine)/DNA vectors is influenced by polycation molecular weight and type of DNA: differential circulation in mice and rats and the implications for human gene therapy.* Blood, The Journal of the American Society of Hematology, 2001. 97(8): p. 2221-2229.

190. Lv, H., et al., *Toxicity of cationic lipids and cationic polymers in gene delivery.* Journal of Controlled Release, 2006. 114(1): p. 100-109.

191. Lee, H., J.H. Jeong, and T.G. Park, *PEG grafted polylysine with fusogenic peptide for gene delivery: high transfection efficiency with low cytotoxicity.* Journal of Controlled Release, 2002. 79(1-3): p. 283-291.

192. Ward, C.M., M.L. Read, and L.W. Seymour, *Systemic circulation of poly (L-lysine)/DNA vectors is influenced by polycation molecular weight and type of DNA: differential circulation in mice and rats and the implications for human gene therapy.* Blood, 2001. 97(8): p. 2221-2229.

193. O'Riordan, C., *Lachapelle A. Delgado C. Parkes V. Wadsworth SC Smith AE Francis GE PEGylation of adenovirus with retention of infectivity and protection from neutralizing antibody in vitro and in vivo.* Hum. Gene Ther, 1999. 10: p. 1349-1358.

194. Geest, B.D., et al., *Elimination of innate immune responses and liver inflammation by PEGylation of adenoviral vectors and methylprednisolone.* Human gene therapy, 2005. 16(12): p. 1439-1451.

195. Alemany, R., K. Suzuki, and D.T. Curiel, *Blood clearance rates of adenovirus type 5 in mice.* Journal of General Virology, 2000. 81(11): p. 2605-2609.

196. Hatakeyama, H., H. Akita, and H. Harashima, *A multifunctional envelope type nano device (MEND) for gene delivery to tumours based on the EPR effect: a strategy for overcoming the PEG dilemma.* Advanced drug delivery reviews, 2011. 63(3): p. 152-160.

197. He, T.-C., et al., *A simplified system for generating recombinant adenoviruses.* Proceedings of the National Academy of Sciences, 1998. 95(5): p. 2509-2514.

198. Sweeney, J.A. and J.P. Hennessey Jr, *Evaluation of accuracy and precision of adenovirus absorptivity at 260 nm under conditions of complete DNA disruption.* Virology, 2002. 295(2): p. 284-288.

199. Mittereder, N., K.L. March, and B.C. Trapnell, *Evaluation of the concentration and bioactivity of adenovirus vectors for gene therapy.* Journal of virology, 1996. 70(11): p. 7498-7509.

200. Jose, S., et al., *Thermo-sensitive gels containing lorazepam microspheres for intranasal brain targeting.* International journal of pharmaceutics, 2013. 441(1-2): p. 516-526.

201. Li, Y., et al., *Loss of adenoviral receptor expression in human bladder cancer cells: a potential impact on the efficacy of gene therapy.* Cancer research, 1999. 59(2): p. 325-330.

202. Küster, K., et al., *Downregulation of the coxsackie and adenovirus receptor in cancer cells by hypoxia depends on HIF-1α.* Cancer gene therapy, 2010. 17(2): p. 141-146.

203. Kim, J., et al., *Enhancing the therapeutic efficacy of adenovirus in combination with biomaterials.* Biomaterials, 2012. 33(6): p. 1838-1850.

204. Lu¨hmann, T., et al., *Cellular uptake and intracellular pathways of PLL-g-PEG-DNA nanoparticles.* Bioconjugate chemistry, 2008. 19(9): p. 1907-1916.

205. Rimann, M., et al., *Characterization of PLL-g-PEG-DNA Nanoparticles for the Delivery of Therapeutic DNA.* Bioconjugate Chemistry, 2008. 19(2): p. 548-557.

206. Karlin, S. and V. Brendel, *Charge configurations in viral proteins.* Proceedings of the National Academy of Sciences, 1988. 85(24): p. 9396-9400.

207. Zhang, X., et al., *Poly (ethylene glycol)-block-polyethylenimine copolymers as carriers for gene delivery: Effects of PEG molecular weight and PEGylation degree.* Journal of Biomedical Materials Research Part A: An Official Journal of The Society for Biomaterials, The Japanese Society for Biomaterials, and The Australian Society for Biomaterials and the Korean Society for Biomaterials, 2008. 84(3): p. 795-804.

208. Allen, C., et al., *Controlling the physical behavior and biological performance of liposome formulations through use of surface grafted poly (ethylene glycol).* Bioscience reports, 2002. 22(2): p. 225-250.

209. Hunter, R.J., *Zeta potential in colloid science: principles and applications*. Vol. 2. 2013: Academic press.

210. Lee, J.H., J. Zabner, and M.J. Welsh, *Delivery of an adenovirus vector in a calcium phosphate coprecipitate enhances the therapeutic index of gene transfer to airway epithelia.* Human gene therapy, 1999. 10(4): p. 603-613.

211. Denning, W., et al., *Optimization of the transductional efficiency of lentiviral vectors: effect of sera and polycations.* Molecular biotechnology, 2013. 53(3): p. 308-314.

212. Kwoh, D.Y., et al., *Stabilization of poly-l-lysine/DNA polyplexes for in vivo gene delivery to the liver.* Biochimica et Biophysica Acta (BBA) - Gene Structure and Expression, 1999. 1444(2): p. 171-190.

213. Czitrom, V., *One-factor-at-a-time versus designed experiments.* The American Statistician, 1999. 53(2): p. 126-131.

214. Mancinelli, S., et al., *Applying design of experiments methodology to PEI toxicity assay on neural progenitor cells*, in *Mathematical Models in Biology*. 2015, Springer. p. 45-63.

215. Palazzo, F., et al., *Development of a spray-drying method for the formulation of respirable microparticles containing ofloxacin–palladium complex.* International journal of pharmaceutics, 2013. 440(2): p. 273-282.

216. Noutsi, P., E. Gratton, and S. Chaieb, *Assessment of membrane fluidity fluctuations during cellular development reveals time and cell type specificity.* PLoS One, 2016. 11(6): p. e0158313.

217. Zhang, S., H. Gao, and G. Bao, *Physical principles of nanoparticle cellular endocytosis.* ACS nano, 2015. 9(9): p. 8655-8671.

218. Kou, L., et al., *The endocytosis and intracellular fate of nanomedicines: Implication for rational design.* Asian Journal of Pharmaceutical Sciences, 2013. 8(1): p. 1-10.

219. Behzadi, S., et al., *Cellular uptake of nanoparticles: journey inside the cell.* Chemical Society Reviews, 2017. 46(14): p. 4218-4244.

220. Vorburger, S.A. and K.K. Hunt, *Adenoviral gene therapy.* The oncologist, 2002. 7(1): p. 46-59.

221. Ghosh, S.S., P. Gopinath, and A. Ramesh, *Adenoviral vectors.* Applied biochemistry and biotechnology, 2006. 133(1): p. 9-29.

222. Gregory, R.J., et al., *Adenovirus vector for gene therapy*. 1997, Google Patents.

223. Campos, S.K. and M.A. Barry, *Current advances and future challenges in Adenoviral vector biology and targeting.* Current gene therapy, 2007. 7(3): p. 189-204.

224. Singh, S., R. Kumar, and B. Agrawal, *Adenoviral Vector-Based Vaccines and Gene Therapies: Current Status and Future Prospects*, in *Adenoviruses*. 2018, IntechOpen.

225. Zhang, Y., et al., *Acute cytokine response to systemic adenoviral vectors in mice is mediated by dendritic cells and macrophages.* Molecular Therapy, 2001. 3(5): p. 697-707.

226. Worgall, S., et al., *Innate immune mechanisms dominate elimination of adenoviral vectors following in vivo administration.* Human gene therapy, 1997. 8(1): p. 37-44.

227. Koizumi, N., et al., *Modified Adenoviral Vectors Ablated for Coxsackievirus–Adenovirus Receptor, αv Integrin, and Heparan Sulfate Binding Reduce In Vivo Tissue Transduction and Toxicity.* Human gene therapy, 2006. 17(3): p. 264-279.

228. Croyle, M.A., et al., *PEGylation of E1-deleted adenovirus vectors allows significant gene expression on readministration to liver.* Human gene therapy, 2002. 13(15): p. 1887-1900.

229. Kawamata, Y., et al., *Receptor-independent augmentation of adenovirus-mediated gene transfer with chitosan in vitro.* Biomaterials, 2002. 23(23): p. 4573-4579.

230. Wonganan, P. and M.A. Croyle, *PEGylated adenoviruses: from mice to monkeys.* Viruses, 2010. 2(2): p. 468-502.

231. Kanerva, A. and A. Hemminki, *Modified adenoviruses for cancer gene therapy.* International journal of cancer, 2004. 110(4): p. 475-480.

232. Dmitriev, I., et al., *An adenovirus vector with genetically modified fibers demonstrates expanded tropism via utilization of a coxsackievirus and adenovirus receptor-independent cell entry mechanism.* Journal of virology, 1998. 72(12): p. 9706-9713.

233. Zuhorn, I.S., et al., *Interference of serum with lipoplex–cell interaction: modulation of intracellular processing.* Biochimica et Biophysica Acta (BBA)-Biomembranes, 2002. 1560(1-2): p. 25-36.

234. Xu, L. and T. Anchordoquy, *Drug delivery trends in clinical trials and translational medicine: Challenges and opportunities in the delivery of nucleic acid-based therapeutics.* Journal of pharmaceutical sciences, 2011. 100(1): p. 38-52.

235. Kawai, F., *Biodegradation of polyethers (polyethylene glycol, polypropylene glycol, polytetramethylene glycol, and others).* Biopolymers Online: Biology• Chemistry• Biotechnology• Applications, 2005. 9.

236. Okegawa, T., et al., *The dual impact of coxsackie and adenovirus receptor expression on human prostate cancer gene therapy.* Cancer research, 2000. 60(18): p. 5031-5036.

237. Anders, M., et al., *Disruption of 3D tissue integrity facilitates adenovirus infection by deregulating the coxsackievirus and adenovirus receptor.* Proceedings of the National Academy of Sciences, 2003. 100(4): p. 1943-1948.

238. Anders, M., et al., *Inhibition of the Raf/MEK/ERK pathway up-regulates expression of the coxsackievirus and adenovirus receptor in cancer cells.* Cancer research, 2003. 63(9): p. 2088-2095.

239. Haisma, H.J., et al., *Scavenger receptor A: a new route for adenovirus 5.* Molecular pharmaceutics, 2009. 6(2): p. 366-374.

240. Wortmann, A., et al., *Fully detargeted polyethylene glycol-coated adenovirus vectors are potent genetic vaccines and escape from pre-existing anti-adenovirus antibodies.* Molecular Therapy, 2008. 16(1): p. 154-162.

241. Zhang, Y. and T.J. Anchordoquy, *The role of lipid charge density in the serum stability of cationic lipid/DNA complexes.* Biochimica et Biophysica Acta (BBA)-Biomembranes, 2004. 1663(1-2): p. 143-157.

242. Duarte, S., H. Faneca, and M.C.P. de Lima, *Non-covalent association of folate to lipoplexes: a promising strategy to improve gene delivery in the presence of serum.* Journal of controlled release, 2011. 149(3): p. 264-272.

243. Suk, J.S., et al., *PEGylation as a strategy for improving nanoparticle-based drug and gene delivery.* Advanced drug delivery reviews, 2016. 99: p. 28-51.

244. Yang, Q. and S.K. Lai, *Anti-PEG immunity: emergence, characteristics, and unaddressed questions.* Wiley Interdisciplinary Reviews: Nanomedicine and Nanobiotechnology, 2015. 7(5): p. 655-677.

245. Parhamifar, L., et al., *Polycation cytotoxicity: a delicate matter for nucleic acid therapy—focus on polyethylenimine.* Soft Matter, 2010. 6(17): p. 4001-4009.

246. Kim, P.-H., et al., *The effect of surface modification of adenovirus with an arginine-grafted bioreducible polymer on transduction efficiency and immunogenicity in cancer gene therapy.* Biomaterials, 2010. 31(7): p. 1865-1874.

247. Philipson, L., K. Lonberg-Holm, and U. Pettersson, *Virus-receptor interaction in an adenovirus system.* Journal of Virology, 1968. 2(10): p. 1064-1075.

248. Tomko, R.P., R. Xu, and L. Philipson, *HCAR and MCAR: the human and mouse cellular receptors for subgroup C adenoviruses and group B coxsackieviruses.* Proceedings of the National Academy of Sciences, 1997. 94(7): p. 3352-3356.

249. Johansson, C., et al., *Adenoviruses use lactoferrin as a bridge for CAR-independent binding to and infection of epithelial cells.* Journal of virology, 2007. 81(2): p. 954-963.

250. Patterson, S. and W. Russell, *Ultrastructural and immunofluorescence studies of early events in adenovirus-HeLa cell interactions.* Journal of General Virology, 1983. 64(5): p. 1091-1099.

251. Wiethoff, C.M., et al., *Adenovirus protein VI mediates membrane disruption following capsid disassembly.* Journal of virology, 2005. 79(4): p. 1992-2000.

252. Blumenthal, R., et al., *pH-dependent lysis of liposomes by adenovirus.* Biochemistry, 1986. 25(8): p. 2231-2237.

253. Wodrich, H., et al., *A capsid-encoded PPxY-motif facilitates adenovirus entry.* PLoS pathogens, 2010. 6(3).

254. Kelkar, S.A., et al., *Cytoplasmic dynein mediates adenovirus binding to microtubules.* Journal of virology, 2004. 78(18): p. 10122-10132.

255. Leopold, P.L., et al., *Dynein-and microtubule-mediated translocation of adenovirus serotype 5 occurs after endosomal lysis.* Human gene therapy, 2000. 11(1): p. 151-165.

256. Chardonnet, Y. and S. Dales, *Early events in the interaction of adenoviruses with Hela cells: I. Penetration of type 5 and intracellular release of the DNA genome.* Virology, 1970. 40(3): p. 462-477.

257. Greber, U.F., I. Singh, and A. Helenius, *Mechanisms of virus uncoating.* Trends Microbiol, 1994. 2(2): p. 52-6.

258. Greber, U.F., et al., *The role of the nuclear pore complex in adenovirus DNA entry.* The EMBO journal, 1997. 16(19): p. 5998-6007.

259. Trotman, L.C., et al., *Import of adenovirus DNA involves the nuclear pore complex receptor CAN/Nup214 and histone H1.* Nature cell biology, 2001. 3(12): p. 1092-1100.

260. Khalil, I.A., et al., *Uptake pathways and subsequent intracellular trafficking in nonviral gene delivery.* Pharmacological reviews, 2006. 58(1): p. 32-45.

261. Ziello, J.E., Y. Huang, and I.S. Jovin, *Cellular endocytosis and gene delivery.* Molecular Medicine, 2010. 16(5-6): p. 222-229.

262. Hernández-Alcoceba, R., *Recent advances in oncolytic virus design.* Clinical and Translational Oncology, 2011. 13(4): p. 229-239.

263. Rejman, J., et al., *Size-dependent internalization of particles via the pathways of clathrin- and caveolae-mediated endocytosis.* Biochemical journal, 2004. 377(1): p. 159-169.

264. Falcone, S., et al., *Macropinocytosis: regulated coordination of endocytic and exocytic membrane traffic events.* J Cell Sci, 2006. 119(22): p. 4758-4769.

265. Von Gersdorff, K., et al., *The internalization route resulting in successful gene expression depends on both cell line and polyethylenimine polyplex type.* Molecular therapy, 2006. 14(5): p. 745-753.

266. Midoux, P., et al., *Polymer-based gene delivery: a current review on the uptake and intracellular trafficking of polyplexes.* Current gene therapy, 2008. 8(5): p. 335-352.

267. Rejman, J., A. Bragonzi, and M. Conese, *Role of clathrin-and caveolae-mediated endocytosis in gene transfer mediated by lipo-and polyplexes.* Molecular Therapy, 2005. 12(3): p. 468-474.

268. Rehman, Z.U., D. Hoekstra, and I.S. Zuhorn, *Mechanism of polyplex-and lipoplex-mediated delivery of nucleic acids: real-time visualization of transient membrane destabilization without endosomal lysis.* ACS nano, 2013. 7(5): p. 3767-3777.

269. Gabrielson, N.P. and D.W. Pack, *Efficient polyethylenimine-mediated gene delivery proceeds via a caveolar pathway in HeLa cells.* Journal of Controlled Release, 2009. 136(1): p. 54-61.

270. Bus, T., et al., *3rd generation poly (ethylene imine) s for gene delivery.* Journal of Materials Chemistry B, 2017. 5(6): p. 1258-1274.

271. Jones, C.H., et al., *Overcoming nonviral gene delivery barriers: perspective and future.* Molecular pharmaceutics, 2013. 10(11): p. 4082-4098.

272. Mecke, A., et al., *Lipid bilayer disruption by polycationic polymers: the roles of size and chemical functional group.* Langmuir, 2005. 21(23): p. 10348-10354.

273. Boussif, O., et al., *A versatile vector for gene and oligonucleotide transfer into cells in culture and in vivo: polyethylenimine.* Proceedings of the National Academy of Sciences, 1995. 92(16): p. 7297-7301.

274. Behr, J.-P., *The proton sponge: a trick to enter cells the viruses did not exploit.* CHIMIA International Journal for Chemistry, 1997. 51(1-2): p. 34-36.

275. Itaka, K., et al., *In situ single cell observation by fluorescence resonance energy transfer reveals fast intra-cytoplasmic delivery and easy release of plasmid DNA complexed with linear polyethylenimine.* The Journal of Gene Medicine: A cross-disciplinary journal for research on the science of gene transfer and its clinical applications, 2004. 6(1): p. 76-84.

276. Koressaar, T. and M. Remm, *Enhancements and modifications of primer design program Primer3.* Bioinformatics, 2007. 23(10): p. 1289-1291.

277. Untergasser, A., et al., *Primer3—new capabilities and interfaces.* Nucleic acids research, 2012. 40(15): p. e115-e115.

278. Dwight, Z., R. Palais, and C.T. Wittwer, *uMELT: prediction of high-resolution melting curves and dynamic melting profiles of PCR products in a rich web application.* Bioinformatics, 2011. 27(7): p. 1019-1020.

279. Ahn, S.J., J. Costa, and J. Rettig Emanuel, *PicoGreen quantitation of DNA: effective evaluation of samples pre-or psost-PCR.* Nucleic acids research, 1996. 24(13): p. 2623-2625.

280. Murakami, P. and M.T. McCaman, *Quantitation of adenovirus DNA and virus particles with the PicoGreen fluorescent dye.* Analytical biochemistry, 1999. 274(2): p. 283-288.

281. Dechecchi, M., et al., *Heparan sulfate glycosaminoglycans are receptors sufficient to mediate the initial binding of adenovirus types 2 and 5.* Journal of virology, 2001. 75(18): p. 8772-8780.

282. Dechecchi, M.C., et al., *Heparan sulfate glycosaminoglycans are involved in adenovirus type 5 and 2-host cell interactions.* Virology, 2000. 268(2): p. 382-390.

283. Ivanov, A.I., *Pharmacological inhibition of endocytic pathways: is it specific enough to be useful?*, in *Exocytosis and endocytosis*. 2008, Springer. p. 15-33.

284. Wang, L.-H., K.G. Rothberg, and R. Anderson, *Mis-assembly of clathrin lattices on endosomes reveals a regulatory switch for coated pit formation.* The Journal of cell biology, 1993. 123(5): p. 1107-1117.

285. Hewlett, L.J., A.R. Prescott, and C. Watts, *The coated pit and macropinocytic pathways serve distinct endosome populations.* The Journal of cell biology, 1994. 124(5): p. 689-703.

286. Orlandi, P.A. and P.H. Fishman, *Filipin-dependent inhibition of cholera toxin: evidence for toxin internalization and activation through caveolae-like domains.* The Journal of cell biology, 1998. 141(4): p. 905-915.

287. Pérez, L. and L. Carrasco, *Involvement of the vacuolar H+-ATPase in animal virus entry.* Journal of general virology, 1994. 75(10): p. 2595-2606.

288. Bayer, N., et al., *Effect of bafilomycin A1 and nocodazole on endocytic transport in HeLa cells: implications for viral uncoating and infection.* Journal of virology, 1998. 72(12): p. 9645-9655.

289. Parton, R.G., B. Joggerst, and K. Simons, *Regulated internalization of caveolae.* The Journal of cell biology, 1994. 127(5): p. 1199-1215.

290. Leung, Y.Y., L.L.Y. Hui, and V.B. Kraus. *Colchicine—Update on mechanisms of action and therapeutic uses*. in *Seminars in arthritis and rheumatism*. 2015. Elsevier.

291. Skoufias, D.A. and L. Wilson, *Mechanism of inhibition of microtubule polymerization by colchicine: inhibitory potencies of unliganded colchicine and tubulin-colchicine complexes.* Biochemistry, 1992. 31(3): p. 738-746.

292. Boisvert, M. and P. Tijssen, *Endocytosis of non-enveloped DNA viruses.* Molecular Regulation of Endocytosis, 2012.

293. Akiyama, T., et al., *Genistein, a specific inhibitor of tyrosine-specific protein kinases.* Journal of Biological Chemistry, 1987. 262(12): p. 5592-5595.

294. West, M.A., M.S. Bretscher, and C. Watts, *Distinct endocytotic pathways in epidermal growth factor-stimulated human carcinoma A431 cells.* The Journal of cell biology, 1989. 109(6): p. 2731-2739.

295. Meier, O. and U.F. Greber, *Adenovirus endocytosis.* The Journal of Gene Medicine: A cross-disciplinary journal for research on the science of gene transfer and its clinical applications, 2004. 6(S1): p. S152-S163.

296. Suomalainen, M., et al., *A direct and versatile assay measuring membrane penetration of adenovirus in single cells.* Journal of virology, 2013. 87(22): p. 12367-12379.

297. Crisostomo, L., et al., *Temporal dynamics of adenovirus 5 gene expression in normal human cells.* PloS one, 2019. 14(1).

298. Lyle, C. and F. McCormick, *Integrin $\alpha v\beta 5$ is a primary receptor for adenovirus in CAR-negative cells.* Virology journal, 2010. 7(1): p. 148.

299. Varki, A., et al., *Nematoda--Essentials of Glycobiology*. 2009: Cold Spring Harbor Laboratory Press.

300. Cagno, V., et al., *Heparan Sulfate Proteoglycans and Viral Attachment: True Receptors or Adaptation Bias?* Viruses, 2019. 11(7): p. 596.

301. Tyagi, M., et al., *Internalization of HIV-1 tat requires cell surface heparan sulfate proteoglycans.* Journal of Biological Chemistry, 2001. 276(5): p. 3254-3261.

302. Flatt, J.W. and S.J. Butcher, *Adenovirus flow in host cell networks.* Open biology, 2019. 9(2): p. 190012.

303. Mercer, J. and A. Helenius, *Virus entry by macropinocytosis.* Nature cell biology, 2009. 11(5): p. 510-520.

304. Meier, O., et al., *Adenovirus triggers macropinocytosis and endosomal leakage together with its clathrin-mediated uptake.* The Journal of cell biology, 2002. 158(6): p. 1119-1131.

305. Nemerow, G.R. and P.L. Stewart, *Insights into adenovirus uncoating from interactions with integrins and mediators of host immunity.* Viruses, 2016. 8(12): p. 337.

306. Gonçalves, C., et al., *Macropinocytosis of polyplexes and recycling of plasmid via the clathrin-dependent pathway impair the transfection efficiency of human hepatocarcinoma cells.* Molecular therapy, 2004. 10(2): p. 373-385.

307. Kremer, E.J. and G.R. Nemerow, *Adenovirus Tales: From the Cell Surface to the Nuclear Pore Complex.* PLOS Pathogens, 2015. 11(6): p. e1004821.

308. Burckhardt, C.J., et al., *Drifting motions of the adenovirus receptor CAR and immobile integrins initiate virus uncoating and membrane lytic protein exposure.* Cell host & microbe, 2011. 10(2): p. 105-117.

309. Lindert, S., et al., *Cryo-electron microscopy structure of an adenovirus-integrin complex indicates conformational changes in both penton base and integrin.* Journal of virology, 2009. 83(22): p. 11491-11501.

310. Mecke, A., et al., *Synthetic and natural polycationic polymer nanoparticles interact selectively with fluid-phase domains of DMPC lipid bilayers.* Langmuir, 2005. 21(19): p. 8588-8590.

311. Vaidyanathan, S., B.G. Orr, and M.M. Banaszak Holl, *Role of cell membrane–vector interactions in successful gene delivery.* Accounts of chemical research, 2016. 49(8): p. 1486-1493.

312. Fletcher, D.A. and R.D. Mullins, *Cell mechanics and the cytoskeleton.* Nature, 2010. 463(7280): p. 485-492.

313. Suomalainen, M., et al., *Microtubule-dependent plus-and minus end–directed motilities are competing processes for nuclear targeting of adenovirus.* The Journal of cell biology, 1999. 144(4): p. 657-672.

314. Pollard, T.D. and G.G. Borisy, *Cellular motility driven by assembly and disassembly of actin filaments.* Cell, 2003. 112(4): p. 453-465.

315. Fuchsova, B., L.A. Serebryannyy, and P. De Lanerolle, *Nuclear actin and myosins in adenovirus infection.* Experimental cell research, 2015. 338(2): p. 170-182.

316. Durrbach, A., D. Louvard, and E. Coudrier, *Actin filaments facilitate two steps of endocytosis.* Journal of cell science, 1996. 109(2): p. 457-465.

317. Salisbury, J.L., J.S. Condeelis, and P. Satir, *Role of coated vesicles, microfilaments, and calmodulin in receptor-mediated endocytosis by cultured B lymphoblastoid cells.* The Journal of cell biology, 1980. 87(1): p. 132-141.

318. Lamaze, C., et al., *Regulation of receptor-mediated endocytosis by Rho and Rac.* Nature, 1996. 382(6587): p. 177-179.

319. Maples, C.J., W.G. Ruiz, and G. Apodaca, *Both microtubules and actin filaments are required for efficient postendocytotic traffic of the polymeric immunoglobulin receptor in polarized Madin-Darby canine kidney cells.* Journal of Biological Chemistry, 1997. 272(10): p. 6741-6751.

320. Fujimoto, L.M., et al., *Actin assembly plays a variable, but not obligatory role in receptor-mediated endocytosis.* Traffic, 2000. 1(2): p. 161-171.

321. Bronner, F., *Cell shape: determinants, regulation, and regulatory role*. 2012: Elsevier.

322. Kuznetsov, S.A., G.M. Langford, and D.G. Weiss, *Actin-dependent organelle movement in squid axoplasm.* Nature, 1992. 356(6371): p. 722-725.

323. Glotzer, J.B., et al., *Microtubule-independent motility and nuclear targeting of adenoviruses with fluorescently labeled genomes.* Journal of virology, 2001. 75(5): p. 2421-2434.

324. Schnitzer, J.E., *Caveolae: from basic trafficking mechanisms to targeting transcytosis for tissue-specific drug and gene delivery in vivo.* Advanced drug delivery reviews, 2001. 49(3): p. 265-280.

325. Rogée, S., et al., *Intracellular Trafficking of a Fiber-modified Adenovirus Using Lipid Raft/Caveolae Endocytosis.* Molecular Therapy, 2007. 15(11): p. 1963-1972.

326. Kiss, A.L. and E. Botos, *Endocytosis via caveolae: alternative pathway with distinct cellular compartments to avoid lysosomal degradation?* Journal of cellular and molecular medicine, 2009. 13(7): p. 1228-1237.

327. Hong, S., et al., *Interaction of polycationic polymers with supported lipid bilayers and cells: nanoscale hole formation and enhanced membrane permeability.* Bioconjugate chemistry, 2006. 17(3): p. 728-734.

APPENDICES

I. Grafting ratio calculation and ^{1}HNMR

The grafting ratio of PEG onto PLL was determined using ^{1}H NMR spectroscopy. The number of PEG chains grafted onto the PLL was calculated by integrating the peaks in the PLL-g-PEG NMR spectrum that correspond to protons of the PLL (-CH- at 4.3 ppm) and PEG (-CH_2CH_2- at 3.7 ppm) portions of the copolymer. First, the number protons per mole of PEG were calculated by using the PEG molecular weight (5kDa) (Equation 1). Next, the average number of protons per mole of PLL was calculated by using the molecular weight of the PLL polymers (22,500 Da) (Equation 2). The relative number of moles of PEG and PLL were calculated by taking the quotient of the polymer peak area and the number of protons per mole of the polymer (Equations 3 and 4). Once the relative number of moles of each polymer was determined, the grafting ratio was calculated by taking the quotient of the relative number of moles of PEG and the relative number of moles of PLL (Equation 5). The calculation used to determine the grafting ratio and a sample ^{1}HNMR spectrum are included:

$$Number\ of\ H\ for\ PEG\ mixture\ (N_{PEG}) = \frac{(5000\ g)}{mole\ PEG} \times \frac{1\ PEG\ mer}{44\ g} \times \frac{4\ H}{PEG\ mer} \quad 1.$$

$$Number\ of\ H\ for\ PLL\ (N_{PLL}) = \frac{22500\ g}{mole\ PLL} \times \frac{1\ PLL\ mer}{146.17\ g} \times \frac{1\ H}{PLL\ mer\ (-CH-)} \quad 2.$$

$$Relative\ number\ of\ moles\ PEG = \frac{Area_{PEG}}{N_{PEG}} \quad 3.$$

$$Relative\ number\ of\ moles\ PLL = \frac{Area_{PLL}}{N_{PLL}} \quad 4.$$

$$Grafting\ Ratio = \frac{Relative\ number\ of\ moles\ of\ PEG}{Relative\ number\ of\ moles\ of\ PLL} \quad 5.$$

1H NMR spectrum example may be found below:

NMR Spectrum

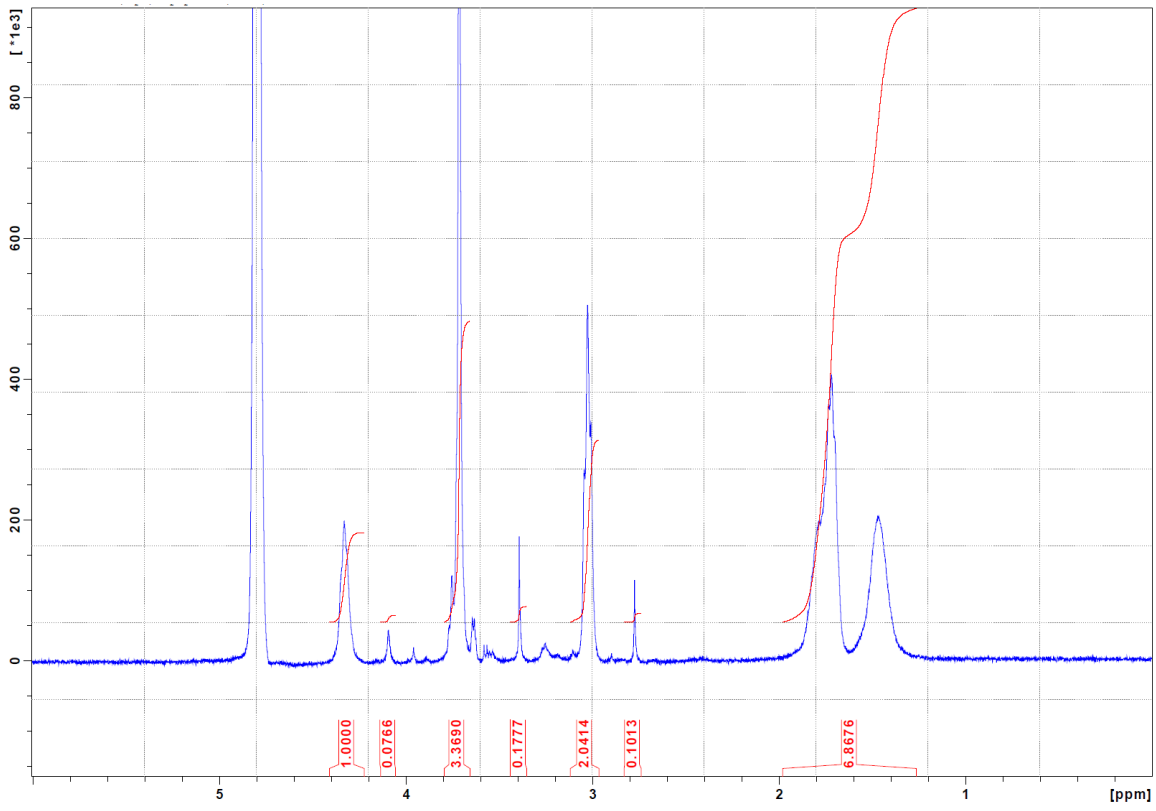

II. Determination of fold difference in cellular uptake of NtAd, FlAd or hybrid vectors after treatment with drug inhibitors using Livak method (ΔΔCt)

It is used as a relative quantitation method to compare the efficiency of expression of gene of a test compared to a control.

Steps:

Sample	**Gene**	
	Target	Reference
Control	C_t (Target, control)	C_t (reference, control)
Test	C_t (target, test)	C_t (reference, test)

1- Normalize C_t (target gene) to C_t (reference gene)
2- Normalize ΔC_t of test sample to ΔC_t of calibrator.
3- Calculate fold difference.

Example:

Sample	**Gene**	
	Target (*E2*)	Reference (*ACTB*)
Untreated	29.33	20.3
Drug treated (CPZ)	31.11	23.16

1- Normalize C_t (target gene) to C_t (reference gene)

ΔC_t (untreated) = 29.33 – 20.3 = 9.03

ΔC_t (treated) = 31.11 – 23.16 = 7.95

2- Normalize ΔC_t of test sample to ΔC_t of calibrator.
$\Delta\Delta C_t = \Delta C_t$ (untreated) - ΔC_t (treated) = 9.03 – 7.95 = 1.08

3- Calculate fold difference in gene expression.
$2^{-\Delta\Delta C_t}$ = Normalized gene expression
$2^{-(1.08)} = 0.47$

Treated cells express gene at 0.47-fold lower than control cells.

VITA

Yasmine Gabal

Candidate for the Degree of

Doctor of Philosophy

Dissertation: DESIGN AND INTRACELLULAR TRAFFICKING OF POLY(L-LYSINE)-GRAFTED-POLY(ETHYLENE GLYCOL) FIBERLESS ADENOVIRAL GENE DELIVERY VECTOR

Major Field: Chemical Engineering

Biographical:

Education:

Completed the requirements for the Doctor of Philosophy in Chemical Engineering at Oklahoma State University, Stillwater, Oklahoma in July 2020.

Completed the requirements for the Master of Science in Pharmaceutics at Ain Shams University, Cairo, Egypt in July 2014.

Completed the requirements for the Bachelor of Science in Pharmacy at Ain Shams University, Cairo, Egypt in 2006.

Experience:

Graduate Teaching and Research Assistant at the School of Chemical Engineering, Oklahoma State University, Stillwater, Oklahoma from August, 2015 through July 2020.

Assistant Lecturer and Graduate Research Assistant at the School of Pharmacy, Ain Shams University, Cairo, Egypt from 2007 through 2014.